# Fracture Healing Analysis:

## Creating a Micro-Displacement of Distal Radii to Diagnose Healing Defects

**Submitted to the Faculty of**

**WORCESTER POLYTECHNIC INSTITUTE**

In partial fulfillment of the requirements for the
Degree of Bachelor of Science


By:

Daniel Amirault, Biomedical Engineering
Maddison Caron, Biomedical Engineering
Julie McLarnon, Biomedical Engineering
Alex Witkin, Biomedical Engineering


Submitted to:

Project Advisor: Karen Troy, WPI Professor – Biomedical Engineering
In Association With: Ara Nazarian, Associate Professor


Date Submitted: April 25, 2018

## Abstract

The most prominent fracture to the distal radius is a Colles' fracture. The healing time for a Colles' fracture is approximately six to eight weeks. However, 5-10% of Colles' fractures experience non-unions, healing defects that hinder healing by preventing the two ends of the fracture from joining to form a callus. To monitor the progression of a fractured wrist, doctors use radiographs and other imaging techniques to measure the reduction of the fracture line. Currently, there is no way to quantify the extent of bone healing. We have a novel device that applies a non-damaging bending load to a healing distal radius fracture, while simultaneously recording the applied force. The prototype device utilized a drive-screw mechanism to apply a compressive force to the patient's wrist and a strain gauge attached to the screw to measure the applied force. Our project goals were to redesign the force application and sensing portions to improve ease of use, to displace a fractured bone 0.25-0.75mm, and increase the radiolucent window by an inch to maximize viewing of a wrist in a CT scanner. We fabricated a pneumatic applicator system with a digital pressure transducer to record data. The force:pressure relationship was calibrated using a materials testing machine and found to be 0.24 N/mmHg. To test our design, two cadaveric wrists with simulated distal radius fractures of varying severity were scanned with a High Resolution Peripheral Quantitative Computed Tomography Scanner (XtremeCT, Scanco, Switzerland), which has a resolution of 164 microns. By comparing these scans, the micro-displacement of the bone can be quantified. Displacement ranged from 0.18-0.51mm in the distal radius with an applied pressure of 100 mmHg, which correlated to 23.32N of force, ± 0.19N. We conclude that the device produces measurable displacements of bone in a simulated fracture model, and is quick and easy to use. The device will be the first to quantify the integrity of healing fractures for faster nonunion diagnosis, reducing potential extended treatment. This device also has potential applications in clinical trials to quantify the effects drugs have on bone healing.

## Acknowledgements

We would like to thank the following individuals that helped make this project successful:

- Professor Karen Troy for her continued support and guidance throughout this project
- Megan Mancuso, Joshua Johnson, and Ying Fang for their help with CT analysis and material gathering
- Ara Nazarian for his help in 3D printing the device and help with cadaver arm testing
- Mohammed Yousef and Jack Wixted for their help simulating fractures for cadaver arm testing
- Lisa Wall for her help in obtaining materials and designating usable laboratory space for the team.

# Table of Authorship

| Chapter/Section Numbers | Section Name | Primary Author(s) | Primary Editor(s) |
|---|---|---|---|
| | Title Page | Alex Witkin | Team |
| | Abstract | Team | Team |
| | Acknowledgements | Team | Team |
| | Table of Authorship | Alex Witkin | Team |
| | Table of Contents | Alex Witkin | Team |
| | List of Figures | Alex Witkin | Team |
| | List of Tables | Alex Witkin | Team |
| Chapter 1 | Introduction | Maddison Caron | Daniel Amirault |
| Chapter 2 | Literature Review | | |
| 2.1 | Bone Fracture | Julie McLarnon | Maddison Caron |
| 2.2 | Bone Healing | Julie McLarnon | Maddison Caron |
| 2.3 | Fracture Imaging | Daniel Amirault | Alex Witkin |
| 2.4 | Fracture Healing Devices | Daniel Amirault | Alex Witkin |
| 2.5 | Device Requirements | Maddison Caron | Alex Witkin |
| 2.6 | Data Acquisition Systems | Alex Witkin | Maddison Caron |
| 2.7 | Alternate Force Applicators | Alex Witkin | Maddison Caron |
| Chapter 3 | Project Strategy | | |

| | | | |
|---|---|---|---|
| 3.1 | Client Statement | Team | Team |
| 3.2 | Design Requirements: Technical | Alex Witkin | Daniel Amirault |
| 3.3 | Design Functions | Maddison Caron | Team |
| 3.4 | Design Specifications | Julie McLarnon<br>Daniel Amirault | Maddison Caron |
| 3.5 | Design Constraints | Julie McLarnon | Maddison Caron |
| 3.6 | Design Requirements: Standards | Julie McLarnon<br>Daniel Amirault | Alex Witkin |
| 3.7 | Revised Client Statement | Team | Team |
| 3.8 | Management Approach | Julie McLarnon | Alex Witkin |
| 3.9 | Financial Consideration | Alex Witkin | Maddison Caron |
| Chapter 4 | Alternative Design | | |
| 4.1 | Needs Analysis | Maddison Caron | Julie McLarnon |
| 4.2 | Concept Designs | Daniel Amirault | Alex Witkin |
| 4.3 | Design Modifications | Maddison Caron | Alex Witkin |
| Chapter 5 | Design Experiment | | |
| 5.1 | Force Application Piece | Alex Witkin | Julie McLarnon |
| 5.2 | Turkey Bone Testing | Julie McLarnon | Maddison Caron |
| 5.3 | Digital Pressure Gauge | Daniel Amirault<br>Alex Witkin | Julie McLarnon |
| 5.4 | Cadaver Arm Testing | Maddison Caron<br>Julie McLarnon | Alex Witkin |

| | | | |
|---|---|---|---|
| Chapter 6: | Final Design | | |
| 6.1 | Design Overview | Maddison Caron<br>Alex Witkin | Team |
| 6.2 | Device Operation | Maddison Caron | Alex Witkin |
| 6.3 | Recommendations | Maddison Caron | Julie McLarnon |
| Chapter 7: | Summary and Conclusion | | |
| 7.1 | Ethical Concerns | Maddison Caron | Alex Witkin |
| 7.2 | Health and Safety Issues | Maddison Caron | Alex Witkin |
| 7.3 | Economic Impact | Julie McLarnon | Daniel Amirault |
| 7.4 | Environmental Impact | Julie McLarnon | Daniel Amirault |
| 7.5 | Societal Impact | Julie McLarnon | Alex Witkin |
| 7.6 | Political Ramifications | Julie McLarnon | Daniel Amirault |
| 7.7 | Manufacturing and Sustainability | Daniel Amirault | Alex Witkin |
| Chapter 8: | Appendix | Maddison Caron | Team |

# Table of Contents

# Table of Figures

# Table of Tables

# Chapter 1: Introduction

Colles' fractures makeup 87% of all radial fractures, and occur in 25% of all pediatric fractures and 18% of all elderly fractures (Nellans 2012). For children, the Colles' fracture is most commonly due to high impact situations, such as during sports. For older adults with lower bone density, a simple fall commonly causes a distal radius fracture. Also, 70% of Colles' fractures occur in postmenopausal women due to their bone density decreasing after a loss of estrogen (Nellans 2012). Since this fracture is so close to the wrist joint (less than 1 inch) it is often referred to as a wrist fracture (Payne).

After a fracture of the distal radius, the main goals during treatment are reliable and rapid rejoining of the ends of the fractured bone, stable fixation and lastly, restoration of function (Lowth 2014). To keep fractures stable during healing, some are held together in a cast, while others are held through surgical fixation devices such as screws and plates. Cast immobilization is the most common treatment of distal radius fractures due to their minimal displacement (Lowth 2014). However, if healing defects occur during the healing process, surgery and internal fixation devices must be utilized in order to correct the problem, and further healing time is required.

For Colles' fractures, the bone is typically healed in 6-8 weeks (Wolfe 2009). Sometimes, however, Colles' fractures do not heal evenly or even at all during the treatment process, known as a nonunion, which occurs when the fracture lacks the proper stability and blood flow (Nunamake). Five to ten percent of all fractures proceed to nonunion (Mills 2013). Another healing defect that occurs in patients is a delayed union. A delayed union is when the bone is still not fully healed after the predicted healing time has elapsed due to a slow blood supply to the fracture site (Nunamake). In order to diagnose these defects, a doctor must be able to visibly see a gap in the bone, or the patient must express a constant pain at the "healed" fracture site. Early diagnosis is critical in order to decrease the chances of more serious complications, further injuries, and morbidity.

To assess how a fracture is healing and progressing, Doctors can use a novel approach that involves high resolution peripheral quantitative computed tomography (HR-pQCT) in combination with finite element analysis (Zhou, 2015). This method is superior to μCT imaging because it can be performed at only peripheral sites like the distal radius and distal tibia, rather

than the central skeletal sites. The results are less exposure to radiation in clinical studies, while also maintaining an excellent imaging resolution, with a voxel size of 82μm (Zhou, 2015). After conducting the scan, images can be converted into finite element models, which can be used to understand the mechanical properties of the bone and assess fracture healing, as well as drug and disease effects on human bone. While it is possible to use finite element models to show how a force could displace bone, it is also possible to apply a force on the bone while simultaneously imaging. While no patent exists on a device that applies a load on a distal radius as a diagnostic tool, it is within the realm of possibility.

A past Major Qualifying Project team was given this same problem and they came up with a device that applies a load to a fractured bone in order to quantify the strength of the distal radius during healing. This device applies a load and calculates the current elastic modulus of the bone and compares it to the normal projected elastic modulus of a bone at the same time of healing. An image with the applied load will then show the displacement of the bone and calculate the elastic modulus, where a doctor can then decide if the fracture is healing properly, or if it has early signs of a healing defect by comparing the actual modulus of the bone to the calculated modulus (Golden 2017). This team was able to design a device, but had little if any time to test and validate the process they came up with. The process they planned on using require a lot of user calculations and therefore a very complex system of data retrieval.

The goal of this project was to create an easy to use interface for the load-bearing device created for analysis of fracture healing. By first validating the device created for analysis of fracture healing, it ensured the database created was as accurate as possible when declaring proper or improper healing of a fracture. This data acquisition system is also able to help detect healing defects earlier and can therefore address the problem before the end of the estimated healing time has arrived. This is beneficial for distal radius patients to ensure they are getting the quickest healing time possible by identifying nonunions or delayed unions as early as possible while also making sure the fracture is completely healed upon removal of the cast. Not only is this beneficial for distal radius fracture patients, but this can create a framework for other fractures that are at risk for healing defects due to an inadequate vascular supply such as the tibia, fibula and femur.

The implementation of this device will also lower medical costs for the patient. With earlier detection of malunions and nonunions, the number of hospital visits and the number of doctors for the patient will decrease, which overall decreases medical costs related to this injury.

The device last year's Major Qualifying Project created was improved upon to make it more ergonomic as well as efficient. The major improvement our group did was enhance the force application of the device. By inserting a balloon pump it allowed the user to more efficiently and safely apply a load to the patient's arm. By relating the pressure applied to the bone to force, and the estimated range of Flexural Moduli of the healing fracture, we were able to calculate the displacement of the fracture with a certain load applied through the three point bending equation. We also created a program to provide and easy to use interface for doctors to quickly and accurately make diagnoses if the distal radius is healing correctly or not. The program analyzes CT images taken before and after a three point load is applied and the displacement is measured. Based on the calculations used in the program, the program then outputs whether or not the bone is properly healing based on the displacement of the fracture after a load is applied. Once this diagnosis is displayed for the doctor, the doctor can help treat the patient accordingly.

# Chapter 2: Literature Review

## 2.1 Bone Fractures

The radius is the larger of the two bones in the forearm, of which the distal is the end closer to the wrist. The distal radius fracture is the most common break in the arm. A fracture of the distal radius occurs where the radius bone breaks near the wrist, about 1 inch from the end of the bone (Liverneaux, 2017).

Distal radius fractures typically occur in postmenopausal women as a result from a low energy fracture such as a fall from a standing position. Adolescents who experience distal radius fractures are more likely to have high energy fractures from events such as motor vehicle crashes. Falling on an outstretched hand is the most common cause of injury to the distal radius (Hosseini, 2017). During this event, the wrist is hyperextended and the highest point of impact forces the energy through the distal radius causing the fracture. There are many things that impact the severity

if the wrist fracture, some of these include patient weight, degree of deviation of the radius and ulna, and degree of dorsiflexion during impact (Walsh 2013).

Distal radius fracture patients often experience complications early in the course of treatment. These can include malunions and stiffness/pain in the hand and wrist. Distal radius fracture patients have an excellent amount of blood supply to the affected area which aids bone regrowth (Walsh 2013).

Colles fracture is a fracture of the distal radius with dorsal angulation and displacement of the distal fragment. Although no two colles fractures are alike, Figure 2.1.2 displays a typical colles fracture. The wrist is bent upward, specifically the broken fragment tilts upward. Entrapment of the median nerve is common in colles fractures. Many surgeons opt to perform carpal tunnel releases over time (Walsh 2013). Some complications with the colles fracture is a dorsal tilt, the loss of normal inward tilt. The unaffected wrist has an inward tilt ranging from 13-30 degrees, with an average of 23 degrees (Hosseini, 2017). After injury the tilt is decreased to as low as 4 degrees (Hosseini, 2017).

Complications from colles fractures also include radial deviation and shortening. In many distal radius fractures, the fragment along the long axis is rotated in supination. "As the fracturing force strikes the pronated hand, he distal radius fragment is displaced backward. This backward displacement produces tension on the fibrocartilage, with the result that the lower fragment is pivoted around the head of the ulna in a direction of supination"(Hosseini, 2017). Shortening is another result from fracture. Shortening results from a combination of impact, loss of the normal tilt, and absorption of bone at the fracture site.

## 2.2 Bone Healing

Interventions for wrist fractures include aligning the fractures anatomically, accurately diagnosing the fracture type, immobilizing the fracture until healing occurs, and preserving function. Many fractures can be manually reduced and splinted by the surgeon without surgical intervention. Splints are fracture specific and are designed to facilitate proper anatomic support as the fracture heals. Others require surgery to correct and align the bone fracture. A wrist fracture typically takes 6 weeks to heal. During this time, many complications can occur. The most

common complication that needs correcting is a malunion. This is when the bone does not heal properly. Malunions can be seen through x-ray imaging. In this case, the bone would have to be rebroken and casted again. Non-unions can also occur, although uncommon. This is where little to no callus forms and the bone fragments do not connect. Healing problems from distal radius fractures occur from unstable periods of immobilization. Nonunions can be considered if there is persistent pain after remobilization of the wrist and visible deformity. Diagnosis is determined by showing movement under flexion and extension using lateral radiographs of the wrist (Prommersberger, 2004). Surgical treatment of wrist fractures can require plates and screws, percutaneous pins, cannulated screws, and external fixation. A cast would thus be applied to the wrist after this surgery to aid in immobilization of the wrist and thumb for best healing (Walsh 2013).

## 2.3 Fracture Imaging

Radiographs (X-rays) and Computed Tomography (CT) are imaging machines that are commonly used for observing distal radius fractures. Radiographs are the preferred method of imaging because they are universally available, inexpensive, and easy to perform (Metz & Gilula, 1993). Forearm radiographs are the gold standard used to determine the fracture pattern, location, displacement, angulation, and rotation of distal radius fractures (Noonan & Price, 1998). For x-rays that are inconclusive, a CT scan is the next step in the imaging process. CT scans are superior to radiographs in assessing fracture healing, as they create a detailed image of the distal radius, in addition to the size, shape, and location of surrounding fracture fragments (Metz & Gilula, 1993). However, there have been many cases where fractures were also missed using CT imaging due to the difficulty of assessing microfractures (Cho, 2012). With both radiographs and CT scans, doctors look for callus size and progressive loss of a fracture line to assess healing (Morshed, 2014).

In avascular nonunions, a common malunion in distal radius fractures, there is no or minimal callus formation as a result of poor blood supply to the fracture ends (Morshed, 2014). When a bone is healing, a callus is formed from the outside to the inside, making it difficult to determine the density of the callus through imaging alone (Morshed, 2014). Due to the difficulty

in determining the callus density with only imaging, scientists have explored other options for fracture healing assessment.

## 2.4 Fracture Healing Devices

Due to the difficulty of determining the mechanical properties of a bone with imaging alone, there is a possibility that the distal radius could not be fully healed when it is time to remove the cast.

Another promising approach to assess how a fracture is healing and progressing involves high resolution peripheral quantitative computed tomography (HR-pQCT) in combination with finite element analysis (Zhou, 2015). While it is possible to use finite element models to show how a force could displace bone, it is also possible to apply a real, non-damaging force on the bone while simultaneously imaging in the scanner. While it may sound unusual, it is not a novel concept, as a patent exists on a very similar device (Labarbera, 1999). In this device, a compressive force is applied indirectly to the thorax through the lower limbs, shoulders and head. This device is not considered a relevant competitor since it focuses primarily on the thorax and lower extremities and is a diagnostic tool, not used specifically to measure bone strength recovery in healing fractures. The device developed by a past MQP team and improved upon by our project team will be a novel contribution to the field of fracture healing measurement and diagnostics. With this device, it will be possible to apply a known force to create a distal radius micro-strain that will provide information about its stage of healing.

## 2.5 Device Requirements

Prior to our project, a team of four students were presented with the need for a device that can accurately measure the strength of a fracture during healing for their Major Qualifying Project. This team was able to successfully build a device, however they did not test or validate the device due to time constraints. The device additionally lacks an easy to use interface for users to quickly and efficiently measure bone strength and therefore recovery of distal radius fractures.

### 2.5.1 Device Needs

This device is to be used in a High Resolution Peripheral Quantitative Computed Tomography (HR-pQCT) machine. Because of this, the device had to be radiolucent to not cause artifacts in the CT image. Therefore, this device had to be created without the use of metal within the imaging zone in order to prevent the artifacts from skewing the CT image. The device was 3D printed in order to allow for faster production time, therefore increasing efficiency.

In order for this device to work, it must be:

- Radiolucent
- Compact
- Repeatable
- Able to apply enough force to displace a healing fracture 162 microns-2mm
- Able to apply a small enough force in order to not injure or hurt the patient

To meet all these specifications, the team created a device that applied a bending load to a fracture. The bending design used a mechanical advantage to apply higher internal bone forces and higher fracture displacement. By using a bending design, the repeatability of the device also increased. However, one distinct disadvantage with the application of a bending load is that the procedure is not compatible for patients wearing a cast. Yet, due to the recasting period being once every two weeks, this is not too detrimental because patients can get their bone strength tested in between recasting procedures.

The device as shown in Figure 1 was lightweight and compact. It measured 5.5 inches tall, 5.5 inches wide and 12 inches long. Their design consisted of a base, elbow support, padding, force application component, hole for imaging and screws. The base, elbow support and force application component were all made from PLA with carbon fiber reinforcement to ensure radiolucency. The screws were made of steel but were out of the imaging view of the CT, so the imaging area was a small region to decrease the amount of artifacts seen in the CT scans.

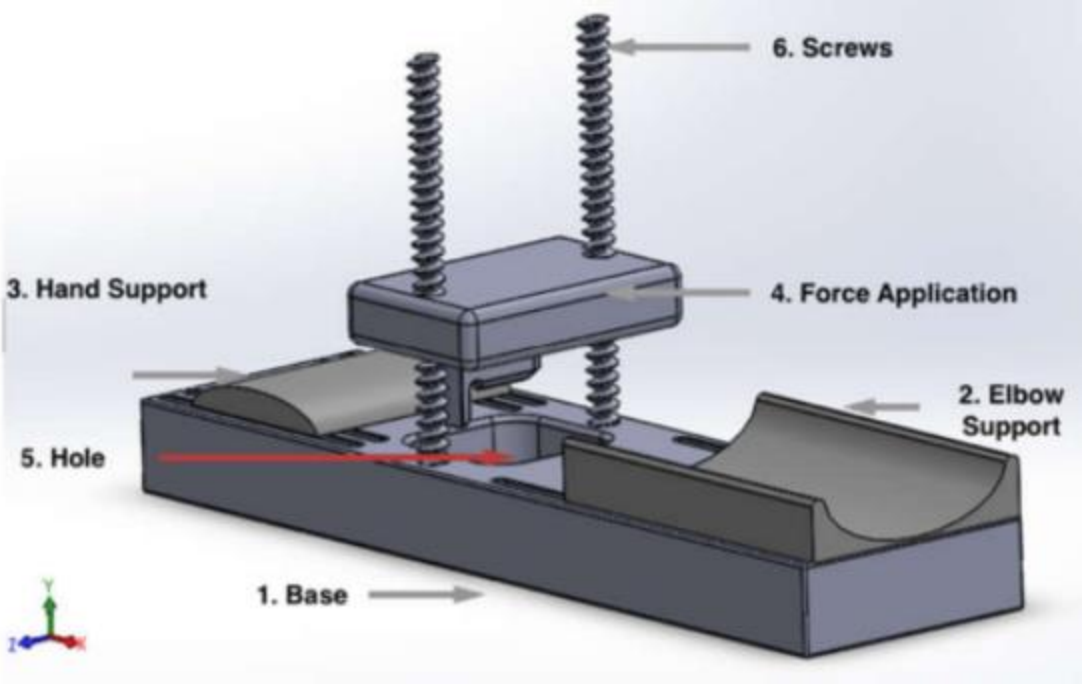


***Figure 1 – CAD Model of Past MQP Device. 1 shows the base of the device where the arm goes. 2 shows the elbow support where the patient's elbow rests comfortably. 3 shows the hand support where the patient's palm rests. 4 shows the force application piece that is driven down to apply a load to the distal radius. 6 shows the screw mechanism that is screwed from underneath the base to slowly lower the force application piece.***

The base is a platform that allowed support for both the arm and the elbow as well as the loading mechanism. To increase stability of the arm even more, the base included slots along the edges for a strap to be inserted into the device. There was a hole in the base at which the load was applied from above to create the 3-point bending force.

The elbow support padding consisted of a circular shape that allowed the patient to rest their forearm and elbow. The circular shape was meant to increase the comfort of the device for patient use.

The force application piece was a piece attached to the base via screws. The piece moved downwards onto a wrist by tightening the screws to increase the force on the arm. The rectangular applicator had the pressure point piece attached as shown in Figure 2. This pressure point piece concentrated the force being applied to the wrist so that it is only being applied to the distal radius and therefore increases the internal force on the bone. This piece was created to fit an average sized wrist and radius bone. On the side of the piece was a flat vertical piece for the distal radius

to be lined up with the styloid process on the side of the wrist. This ensured that the load is applied to the same location of the radius each time, therefore increasing repeatability.

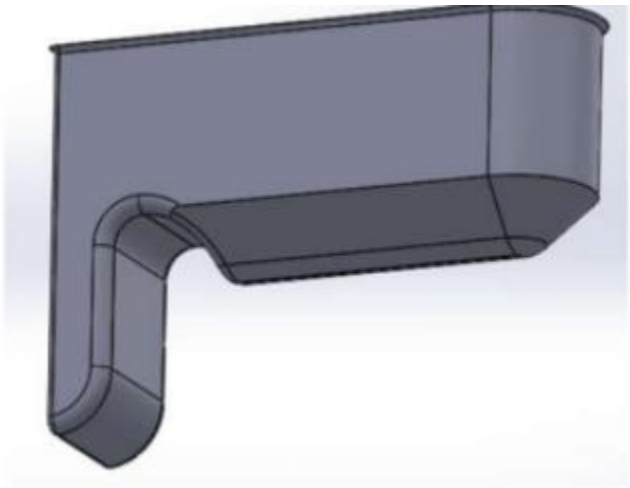

***Figure 2 - Pressure Point Piece Attached to the Force Applicator. This piece is used to localize the force being applied solely to the distal radius.***

This design allows the base to hold the elbow and hand supports while also allowing a 3 point bending moment to the patient's distal radius via the screws and the force application component to be applied. This design is advantageous due to the stability of the forearm while the force is applied to the radius, therefore improving the repeatability of the procedure. The device also included a clip on the front of the device in order for the device to clip into the CT in order to ensure the device does not move in the CT scanner.

## 2.5.2 Strain Gauge Load Cell

To measure the force that was being applied by the force application piece, a strain gauge-based load cell was used. A strain gauge load cell contains a strain gauge, which is a device that uses electrical conductivity to measure the strain that occurs. The strain gauge was attached to the device on the inside of screws via an adhesive. When the screws were deformed or twisted down to tighten the force application on the wrist, the foil in the strain gauge deformed which then causes the foil’s electrical resistance to change. A Wheatstone bridge was then utilized to measure the resistance change. From these values, a quantity known as the gauge factor then related the resistance change to strain. To calculate force from strain, a force was converted into a measurable electrical output. When a weight was applied to the strain gauges, the strain changed the electrical

resistance of the gauges in proportion to the load that was applied, thus relating voltage to strain which allows for a user to find the force being applied.

### 2.5.3 Three Point Bend System

Three point bend analysis is used in mechanical testing to measure the elastic modulus, stiffness, and other important properties of materials. Advantages of three point bending tests is the ease of preparation and testing. The disadvantages of this test is the sensitivity the test has to different geometries of specimens (Bower, 2009). Non-destructive bending tests can be done to predict the stiffness of a material. When a known force is applied to a material and displacement is measured, stiffness can be found (Wehner, 2014). When applying this knowledge to our project, the stiffness of a bone callus can be found at a specific point in time when a non-damaging three point bend is applied. When the force being applied is known, and the displacement of the fracture is measured, the stiffness of the callus can be found as shown in Figure 3. Knowing the stiffness of a callus is important to understand the integrity of a callus in a more quantifiable way than imaging to help diagnose healing defect faster and more accurately. Additionally, being able to quantify callus stiffness at a specific point in time can help understand effects of bone density over time due to the use of certain drugs and medications. Giving quantifiable data to researchers on the effects of drugs on bone healing and bone density can help produce viable data to prove the effects new medicine has in the medical industry.

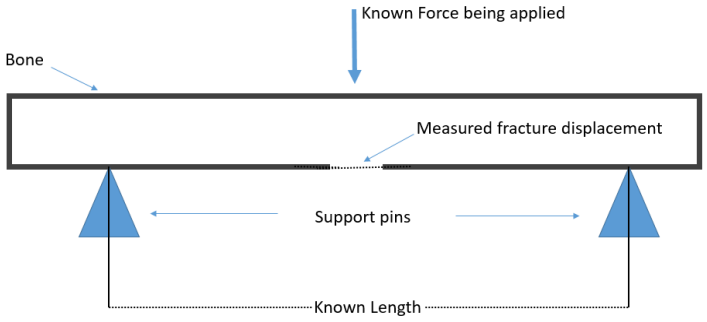


**Figure 3 – Three Point Bend Schematic.**

### 2.5.4 Drawbacks

The device's strength, though satisfactory, was not as rigid and strong as it could be. The team recommended to instead use Polycarbonate and Carbon fiber to provide maximum strength while still allowing the device to be radiolucent. They recommended having a material with a higher flexural modulus than the current device to decrease the amount of bending deformation when a load is applied in the middle of the device. Another drawback was that the fingers of the patients overhang from the device. By inserting a handgrip mechanism this allows for the patient's arm to be concentrated on the device, increasing the repeatability of the device.

The force application process was not as efficient as it could be. The screws took some time to pull the force applicator down and did not provide a quick release system to unload the patient's arm quickly. Also, the process required the doctor to tighten the force applicator from underneath, which is not very efficient and could not be done within a CT machine which caused more moving and twisting on the patient's arm. Once the force applicator was down, it was hard to get it back up to loosen the force application from the patient's wrist. The team suggested a quick release system to increase the efficiency of the device. If the device had a mechanism that allowed the loading to immediately be released instead of having to slowly turn the screws to decrease the load this would make the procedure much quicker. Also, the bottom of the screws had two spools of fishing line that were tied together to twist the screws simultaneously and keep the force applicator piece moving down uniformly to create an equal force being loaded onto the bone to increase repeatability. This design, though innovative, could be enhanced and be made so the piece moves down uniformly without having to worry about the fishing line constantly tangling when having to reset the device. Lastly, the device design currently has no way of digitally recording force application data. By creating a simple and easy interface, this would increase the efficiency of the device, and increase the desire for use of the device on patients.

## 2.6 Data Acquisition Systems

To make data collection less complex and more automated, a data acquisition (DAQ) system can be used. A DAQ system measures various mechanical or electrical events with the aid of a computer. The three main components of this system are physical sensors, a DAQ hardware device, and a computer with a customizable software that can be programmed to the user's needs.

These components work together to collect valuable data as an input, and create a comprehensive, organized output that the developer and client can both interpret and understand. (National Instruments, 2017)

A functional DAQ system converts information from the physical device and converts it into data that can be analyzed by a program. This is performed by converting electrical signals into digital information. Major parts of the system include sensors to convert the physical phenomena into an electrical signal, an analog-to-digital converter, a multiplexer and amplifier to switch and amplify the input analog signals, and a display monitor (computer) to visualize and manage the data. Transducers can be used to detect a wide range of physical phenomena such as movement, electrical signals, radiant energy, and thermal, magnetic, or mechanical energy (Emilio, 2013).

### 2.6.1 DAQ Requirements:

Data Acquisition Systems require transducers, hardware, and a programming software. Transducers are mechanisms that convert a physical phenomenon into a measurable electrical signal. In order to collect vital data, transducers such as a strain gage, thermocouple, photo sensor, microphone, piezoelectric transducer, potentiometer, accelerometer, and others based on the application can be installed onto a device. In this application, a strain gage will be connected to the device in order to measure the exact force being applied to the distal radius. The chosen transducers are wired to a DAQ hardware instrument in order to digitize the incoming analog signals. The hardware device is then connected to a PC via USB in order to receive and interpret the digitized signals through the WinDAQ software.

### 2.6.2 Software Programs

Once the DAQ has digitized the inputs, a LabVIEW can be used to further organize the data into an interface using spreadsheets, charts, and graphs. LabVIEW is a graphical programming software which simplifies hardware integration, allowing rapid acquisition and visualization of data sets. LabVIEW is more practical to use over other programming software because it is a visual language and is easy to understand and visualize from a developer standpoint. A LabVIEW program can initiate the collection of data, organize the data through while loops until all necessary data is received, and then export the raw data while creating visual tools such

as graphs and charts. This is beneficial for fracture healing analysis since LabVIEW can interpret data such as the load applied on the fracture and the displacement of the device and create visuals to assist doctors in making a diagnosis. (National Instruments, 2017)

Additionally, other programs such as MATLAB and ImageJ can be used together to further analyze the data and even interpret other data sets. MATLAB (Matrix Laboratory) is a high-performance language which specializes in computation, visualization, and programming. Typical uses of MATLAB include math and computation, algorithm development, modeling and simulation, data analysis and visualization, engineering graphics, and graphical user interface development. (Mathworks, 2017)

ImageJ is an open source image processing program for multidimensional image data was a focus on scientific imaging. ImageJ provides a user interface with functions to load, display and save images while allowing image processing, localization, deconvolution, registration, segmentation, and tracking techniques. Plugins and scripts can be easily added to create an automated and reproducible processing sequence. (ImageJ, 2017)

ImageJ-MATLAB is an extension in MatLab that translates data between ImageJ images and MATLAB matrices. It enables execution of MATLAB scripts from inside ImageJ's script editor. This allows ImageJ to be launched and interacted with while inside of MATLAB. This is extremely valuable since a CT image of the fractured bone can be opened in MATLAB and then analyzed visually using automated code. The code will be able to analyze CT images and calculate the displacement of the bone after a load has been applied. This creates a repeatable process of analyzing fracture displacements and will assist doctors in making a diagnosis while minimizing bias between users.

## 2.7 Alternate Force Applicators

Expanding from the threaded mechanical force applicator on the original device, we considered pneumatic and hydraulic force applicators as a powerful and consistent option. Pneumatic and hydraulic systems use compression properties to create a force, thus performing an action. Pneumatic systems compress gas, while hydraulic systems use the non-compressive properties of liquid to move a joint. Pneumatic systems tend to be slower but more accurate due to

the need to build up pressure by compressing gas. Hydraulic systems are immediate and more powerful due to liquid immediately forcing a joint to move and therefore are used more in heavy machinery.

Due to the device being imaged under HR-pQCT, all parts of the system including the force applicator must be MRI compatible. Ningbo Yu et al. performed studies on hydraulic and pneumatic actuators in limited space with strong magnetic fields. After testing, both systems were MRI compatible and yielded no artifacts in the images. With the hydraulic system they achieved smoother movements, higher accuracy, and improved robustness against force disturbances. In contrast, the pneumatic system was back-drivable, showed faster dynamics with lower pressures, and allowed force control than the hydraulic system. (Yu et al.,2008) For the device, both hydraulic and pneumatic force applicators would work in our system on a small scale and would be an extremely consistent and accurate option.

# Chapter 3: Project Strategy

## 3.1 Client Statement

The goal of this project is to improve upon an initial prototype that assesses fracture healing by measuring force and displacement with high resolution CT imaging. However, the prototype requires testing, validation, and refinement. Furthermore, the prototype needs improved force measurement capabilities, better adjustment, and an easy to use user-interface so that precise forces (+/- 5 N) can be applied.

## 3.2 Design Requirements: Technical

The existing design needed to be improved to ensure the system was performing to the best of its ability. To do this, the system had to go through thorough design validation. Design validation tests were used to evaluate the device's performance to ensure the product requirements were met. For the device to be validated and the program to be developed, seven technical objectives were established to guide our project.

**I. The Device**

*1. The use of the device must be repeatable.*

Repeatability of the device allows doctors to be able to make a prognosis more efficiently. By designing the procedure to be repeatable, all patients will get a consistent and appropriate prognosis since user bias and error are diminished. We would like a standard deviation of precise application of force to be under one Newton of force. This is because we are applying a small load to displace the patient's fracture a small amount so by keeping the variation under one Newton increases the precision and repeatability of our device.

## II. The Program

*2. The program must be intuitive and provide an ease of use for all users*

A basic interface must be setup in order to allow the operator to use the program to measure the displacement of the bone and make a prognosis. A simple start button will decrease the amount of user input and possible user error. This helps ensure all patients are getting consistent and valid measurements to determine whether or not the patient's distal radius is healing properly.

*3. The output of the program must be displayed in a simple and informative way*

By displaying results in a simple and informative way, users can make a quick and efficient prognosis for the patient. Additionally, this contributes to the ease of use for the interface and increases the user's desire to use it.

## III. The Entire System

*4. The system must be CT compatible*

The entire system need to be compatible with CT machines in the imaging area so that the device can collect image data. If the device is within the CT spatial parameters and is not radiolucent, images will not be taken or will be distorted due to artifacts.

*5. The system must be portable and compact*

Designing the device to be portable and compact allows for easier transportation and setup, also contributing to the device's ease of use. By keeping our device under five pounds, and under a foot in length and height, this allows our device to be easily transported and moved.

*6. The system must be cost effective*

The device should be cost effective so that hospitals and clinics are more likely to implement them as a diagnostic tool for their patients. Additionally, a lower cost allows the product to be a viable solution in third world countries.

*7. The entire system must be accurate.*

Accurate measurements and calculations will ensure that the results from the test appropriately represent the condition of the fracture site. Designing the device to be as accurate as possible will allow the doctor to provide a respectable and consistent healing analysis to the patient. This will also save time and money by allowing fewer hospital visits since chances of premature cast removal and further complications decrease.

***Table 1 - Project Objectives and Related Importance***

| Objectives | Importance |
|---|---|
| The use of the device should be repeatable | • Trustworthy results<br>• Able to address variability in patients<br>• Decrease user bias<br>• Decrease potential user error |
| The entire system should be accurate | • Calculations should be correct<br>• Amount of force applied should be exact<br>• Precise placement of patient's arm |

| | |
|---|---|
| The program should provide an ease of use for all users | • Minimal user input<br>• Less human error or bias |
| The output of the program should be displayed in a simple and informative way | • Minimizes hand-written math<br>• Increases repeatability<br>• Decreases chance of user error |
| The system should be CT compatible | • Radiolucent/Should not distort CT images<br>• Artifacts in images if metal is in imaging zone |
| The system should be portable and compact | • Easy to transport and setup<br>• Increases feasibility |
| The system should be cost effective | • Not too expensive for clinics and hospitals to implement<br>• Increase desire for product |

## 3.3 Design Functions

To outline the design requirements of the device to make sure the objectives are achieved, a list of functions that our program and device must do was created. These functions and their means are additionally outlined in Table 1.

**I. The Program**

*1. The program must collect data with minimal input*

The program should require minimal input from the user, and run calculations autonomously. By minimizing the input, it increases the ease of use while decreasing potential user variability or error. To do this, all of the constants normally used should be pre-programmed into the software and device. Another way to minimize user error is by utilizing ImageJ and MATLAB in order to determine the displacement of the bone.

*2. The program must calculate the modulus of the bone*

By having the program automatically calculate the elastic modulus of the bone increases the repeatability of the procedure by minimizing the chance of user error. In order to do this the program will have different functions and equations programmed into it in order to correctly calculate the displacement based on force applied and elastic modulus of the bone. By adding the Three Point bend equation into the program this allows for the predicted displacement to be calculated and a proper diagnosis to be made without the risk of user error.

*3. The program must measure the displacement of the bone after a load is applied*

An ImageJ-MATLAB extension in the program will automatically measure the displacement of the fractured bone when a load is applied. This will help ensure repeatability since the program will use the images to exactly calculate displacement, reducing user bias.. For this to work effectively, the program should be able to read the before and after CT images. The MATLAB code will convert the CT files into a PDF file for it to be run and analyzed through ImageJ.

*4. The program must generate tables of elastic modulus and displacement collected and the diagnosis*

The goal of our design is to have an easy to use interface for physicians to quickly and efficiently measure whether a fracture is healing correctly. To do that the program must output easy to read analysis of the data measured. The program should output comparison charts to effectively see whether the patient's distal radius is healing. An easy to read visual analysis will help doctors make effective prognoses. To have a nice visual presentation of data, LabVIEW will be used to output data in an appealing way to help doctors as quickly as possible.

*5. The program must be able to handle errors*

The program must be capable of error handling to ensure the procedure is quick and efficient. If an error occurs, there will be an integrated troubleshooting guide within the system that will solve the error. This is paramount since if an error occurs and cannot be solved, the user

must go through each element of the program to try and figure out what the problem is, thus decreasing the efficiency of the device.

## II. The Device

*6. The device must be comfortable for the patient.*

The device applies a small load to a patient's fractured wrist, which can sometimes be painful. The device should be as comfortable as possible to minimize patient pain. The device should restrict the patient's arm from hanging off the device when the arm prepared for application. With the arm restricted, the patient is in a more comfortable position and every patient's arm would be in the exact same position for testing, which increases repeatability of the device. On the Mosby pain scale, we do not want to exceed a threshold of five.

*7. The force applicator must be able to apply and release a force quickly*

The force application process is the part of the procedure that can endure the most pain on the patient. The device should have a smooth and efficient way of applying a load to the patient's distal radius. Additionally, by utilizing a quick release system this can reduce the risk of pain inflicted onto the patient. By improving on the efficiency of the force application process this can not only increase repeatability, efficiency and ease of use, but it can also minimize patient pain.

***Table 2 - Function-Means Table***

| Functions | Means |
|---|---|
| The program must collect data with minimal input | • Input constants<br>• Program an ImageJ extension<br>• Automatically calculate displacement of bone after load is applied<br>• Have a known force that is applied based on the input of the Flexural Modulus<br>• Increases efficiency while also decreasing user bias |
| The program must calculate the modulus of the bone | • Program Three Point Bending formula |

| | |
|---|---|
| | • Input all known constants<br>  ○ Force based on Flexural Modulus<br>  ○ Length of support spans<br>  ○ Moment of Inertia<br>• Increases repeatability<br>• Decreases potential for user error |
| The program must measure the displacement of the bone after a load is applied | • ImageJ extension<br>  ○ BoneJ plugin<br>  ○ Automatically analyze image taken in CT after load applied<br>• Decreases user bias |
| The program should display charts of analysis such as force applied, elastic modulus of the bone and the displacement that occurred | • An easy to use interface<br>  ○ Program such as LabVIEW or MATLAB<br>  ○ Display all information in a simplified way<br>• Increases productivity<br>• Decreases time needed to analyze data<br>• Can make quick diagnosis based on data displayed |
| The program must be able to handle errors | • Display what parameter is wrong and why<br>• Increases efficiency of procedure<br>• Allows Doctors to quickly fix problem by themselves<br>• Increases productivity |
| The device must be comfortable for the patient | • Adding a grip mechanism for patient to comfortably rest fingers on device without hanging off device<br>• Smooth and efficient force application process<br>• Decreases risk of pain for patient |

| | |
|---|---|
| The force applicator must apply a point force to the distal radius efficiently | • Smooth application<br>• Concentrated force to create accurate calculation results<br>• Decreases patient pain<br>• Increases efficiency |

After analyzing the functions and objectives, a pairwise comparison chart was made as shown below in order to prioritize our device needs as shown in Table 2. The needs in the rows are compared to the needs in the columns using 1s and 0s. A 1 means that the need is more important.

***Table 3 – Pairwise Comparison Chart***

| | Min. input | CT compatible | Simple output | Easy use | Accurate | Cost Effective | CPU comp | Portable | Error Handle | Total |
|---|---|---|---|---|---|---|---|---|---|---|
| Minimal input | | 0 | 0 | 0 | 0 | 1 | 0 | 1 | 0 | 1 |
| CT compatible | 1 | | 1 | 1 | 1 | 1 | 0 | 1 | 0 | 6 |
| Simplified output | 1 | 0 | | 1 | 0 | 1 | 0 | 1 | 1 | 6 |
| Easy setup/use | 1 | 0 | 0 | | 0 | 1 | 0 | 1 | 0 | 3 |
| Accuracy | 1 | 0 | 1 | 1 | | 1 | 1 | 1 | 1 | 7 |
| Cost Effective | 0 | 0 | 0 | 0 | 0 | | 1 | 1 | 0 | 2 |
| Computer Compatible | 1 | 1 | 1 | 1 | 0 | 0 | | 1 | 1 | 6 |
| Portability | 0 | 0 | 0 | 0 | 0 | 1 | 0 | | 0 | 1 |
| Error Handling | 1 | 1 | 0 | 1 | 0 | 1 | 0 | 1 | | 5 |

The results of this comparison shows that the accuracy of the device is the most important need, followed by compatibility with the CT scanner and computer, as well as a simple output. Additionally error handling was ranked as very important. These five needs are essential to the success of our project, and should not be compromised. The other characteristics that would be desirable, such as portability, cost effectiveness, minimal user input and easy setup would be nice to have and are important, but they are not essential to our project's success.

## 3.4 Design Specifications

To quantify the parameters for our project, a list of specifications was created:

1. *The minimal setup time should be no more than 15 minutes*

The process should be quick and efficient. By only allotting 15 minutes for setup of the device, it will reduce the total amount of time to 30 minutes. This will ensure a rapid and effective procedure.

2. *The device needs to be kept within the constraints of the CT*

The size of the CT is 5.5 x 13 x 5.5''. The device itself is 5.5 x 12 x 5.5''. This allows 1 inch lengthwise for any additions if necessary. Any additions we make must be added lengthwise and must still fit in the CT machine to ensure accurate analysis of the distal radius.

3. *The force should be kept under a certain threshold*

The force needs to be large enough to displace a fracture 164 microns, the minimum displacement accurately detectable by a CT. Likewise, the force should not exceed the force required to displace a fracture 2 mm, which is the maximum displacement a bone can withstand before soft tissue is damaged. The maximum and minimum forces will vary depending on the fracture healing stage, due to the changing flexural modulus. Through calculations, it was calculated that to displace a healthy bone, it would take a very large amount of force. Though this force is not attainable on our device, we still need to be aware of the amount of displacement of the bone as the flexural modulus decreases at earlier stages of healing to make sure we do not damage the soft tissue.

## 3.5 Design Constraints

A list of constraints was created and documented in Table 3. These constraints are the parameters of this project that need to be addressed when beginning the design of our program and the validation of the device.

1. *The current process used to quantify the strength of fracture healing*

The process used to quantify strength was unclear in the past MQP because of time limitations. Determining the process was inferred from reading the past MQP Paper and researching through literature. It was determined that through using 3-point bending and the strain analysis, we could get the stiffness.

*2. The minimum displacement detectable on a CT machine*

The minimum displacement detectable on a CT machine is 82 microns. However, to get an accurate enough reading to produce the desired results, 164 microns is the minimum displacement detectable on a CT. This is due to the Nyquist Theorem, which states that the sampling rate must be at least two times the force applied, or twice the highest analog frequency to correctly represent the digitized output. If the sampling rate is less than two times the force, this could cause distortion in the image, also known as aliasing.

3. *The maximum displacement a bone can undergo*

The maximum displacement a bone can undergo is 2mm. Displacement beyond this value would cause soft tissue damage (Littlewood 2010). Our goal is to displace a fracture 0.25-0.75 mm.

4. *The maximum force a bone can undergo before pain or damage*

The maximum force a bone can undergo before pain or damage due to the displacement of the bone depends on the stage of bone healing. As the bone is earlier in healing, the flexural modulus decreases and the amount of force the bone can withstand before the displacement reaches the point at which damage begins to occur to soft tissue also decreases.

5. *The compatibility of the device with the CT scanner*

The device has to be compatible with a CT scanner. The device is 5’’x 12’’x 5’’, which is CT compatible because the space allotted for inserts is 5.5’’x 13’’x 5.5’’. Physically fitting is only one aspect to being CT compatible. Software compatibility is an important component. The CT scanner outputs voxel files. These must be converted to PDF files for BoneJ, the ImageJ extension, to be able to analyze. In addition, there must be no metal in the 2’’x 4’’ imaging area as it will interrupt the image processing.

*6. The amount of time allotted to complete*

A total of 30 minutes is allotted for the whole appointment. Four minutes is allotted for the initial CT image with unloaded bone. Fifteen minutes is allotted for device setup and application of the load. Eleven minutes is allotted for the final CT scan and collection of data. This will increase efficiency and ease of use of the device. Additionally, the entire project must be completed by April 2018 which gives our group a 10-month span to create our device and interface.

*7. The amount of money allotted to complete*

$1000.00 was allotted for the project budget. Of this money, $300 for general supplies such as modeling clay to model design pieces, blood pressure pumps, turkey bones for testing, etc. Another $250 will be put aside for our final design production. The last $400 will be for further expenses that could arise as we continue our design validation and testing. Table 4 further outlines the constraints discussed and the parameters of each constraint below.

***Table 4 – Project Constraints and Parameters***

| Constraints | Parameters |
|---|---|
| Current calculation procedure | • Past MQP did not outline, assumptions made to determine process using 3-point bending, strain analysis, and elastic modulus |
| Minimum displacement detectable on CT is 1 voxel (82 microns) | • 164 micron displacement would allow accurate analysis of bone |

| | |
|---|---|
| Maximum displacement a bone can undergo | • 2 mm before damages to soft tissue |
| Maximum force a bone can undergo before pain or damage | • ~1278 N for full union<br>• ~34 N for very early fracture<br>  ○ Based on 3-point bending |
| No metal in the CT (CT compatible) | • Metal causes artifacts, must be outside of the imaging zone (2 in. x 4 in.) |
| Time | • Approximately 8 months (April 2018)<br>• 30 minutes for total imaging process: 4 minutes initial scan, 6 minutes device setup and loading, 5 minutes final scan and data collection. |
| Money | • $1000: $300 supplies, $250 final device, $400 other materials |

## 3.6 Design Requirements: Standards

This device is categorized as a class II medical device. There are many regulations under which this device will be designed and operated due to its interactions with human patients. Standards for this device can be found in Title 21, Volume 8 of the Food and Drug Administration's Code of Federal Regulation. In this process, the design undergoes many levels of clearance. Specifically, our device would be a diagnostic tool for orthopedic applications in the distal radius.

The scope of the design must be classified for human use, identified as accurately described for its usage, and it must be stated why the device is subsequently equivalent to other devices. This device is not "Substantially Equivalent" to any other devices currently or previously available and thus is a "New" device. To avoid duplications, all orthopedic devices must have two or more types of uses, for example it can be used for both diagnostic and surgical procedures.

An additional standard that pertains to this device is ISO 13485. ISO 13485 is a quality management system for medical devices which allows for the device to maintain regulatory

compliance. Certification of this regulation creates an effective solution to stay within the comprehensive means of the QMS. It also provides a foundation for manufacturers to address directives, responsibilities, and regulations which commit to the safety and quality of the medical device. Premarket testing and validation should be guided by the appropriate FDA guidance document: Center for Devices and Radiological Health Standard Operating Procedure (SOP) Level 1, immediately in Effect Guidance Documents on Premarket Data Issues. After clinical trials and before clinical use, the device needs to file for a 510(K)).

## 3.7 Revised Client Statement

The goal of this project is to further develop and validate a fracture healing device which applies a mechanical load to displace the distal radius to determine if the fracture is healing correctly through CT imaging. The current force application design requires two screws to be simultaneously twisted underneath the device while the patient's arm is inside, making the force application process tedious and inefficient. Our project goals were to redesign the force application and sensing portions to improve ease of use, to displace a fractured bone 0.25-0.75mm, and to create a user interface that records real-time pressure to measure the force that is being applied at any given moment.

## 3.8 Management Approach

| TASK TITLE | START DATE | DUE DATE | % OF TASK COMPLETE |
|---|---|---|---|
| Paper | | | |
| Research | 8/30/17 | 11/20/17 | 100% |
| Introduction | 9/11/17 | 10/14/17 | 100% |
| Literature Review | 9/11/17 | 10/14/17 | 100% |
| Project Strategy | 9/11/17 | 10/14/17 | 100% |
| Alternative Designs | 10/1/2017 | 11/20/17 | 100% |
| Design Verification | 11/15/17 | 12/20/17 | 100% |
| Final Design and Validation | 1/16/18 | 2/24/18 | 100% |
| Conclusion and Recommendations | 2/18/18 | 3/3/18 | 100% |
| Device | | | |
| Obtain Device | 8/30/17 | 9/18/17 | 100% |
| Pressure gauge setup | 10/12/17 | 11/15/17 | 100% |
| Pressure gauge coding | 11/15/17 | 12/15/17 | 100% |
| Changing force application process | 1/11/18 | 2/15/17 | 100% |
| Testing | 11/20/17 | 2/20/17 | |
| Reprinting final device | 2/27/18 | 3/15/18 | 100% |
| Iteration | 2/5/18 | 2/23/18 | 100% |
| Validate Device | 10/9/17 | 11/15/17 | 100% |



**Figure 4 – Gantt Chart. This figure shows our tasks that were to be completed throughout the year. Each task has a start and end date as well as a visual layout of the tasks that will be done in parallel to one another throughout the year.**

The Gantt chart above displays a timeline for the work being completed for the project over 2017-2018 academic calendar. Within the paper section, we have time frames in which each chapter of the paper will be written. The first four chapters of our paper will be completed in A term and will serve as a guide for us in the actual design of the project. The remaining chapters will be written while the device is being designed and finished during B and C term. Within the device section, we have split it into three main goals, obtain the device, improve upon the device, and validate that the device works properly. Obtaining the device was our first objective, as there was some confusion as to where the device was located, and we needed to have the device to start working on it. We improved the device by adding comfort features as well as parts that will update the ergonomics and device function such as a hand grip to keep the patient's hand in the correct position, changing the force application to air pressure, and adding a pressure point onto the balloon to apply a concentrated force to the fracture site. To validate that the device works

properly, the device was tested on turkey bones and cadaver arms. This took place in B and C term. C term heavily focused on design experiments to validate our device and iterate changes accordingly. C term also included testing our device on a cadaver wrist to ensure efficiency and functionality of the device. Along with a visual calendar for events, we have the start and end dates included, as well as a color progression bar that indicates what percent of the task has been completed. Our biggest due date is the last week of C term (2/26/18-3/2/18) when we are completing the writing, concluding work on the device and have our working code. Our goal is to be completed with all tasks indicated above by the last week of C term to allow ourselves time flexibility towards the end of the school year in case of unaccounted for events. The final 3D print of the device was completed at the end of C term after all testing and design experiments have been completed and the design had been finalized. This Gantt chart was a resource for keeping the project progressing in a timely manner.

An additional measure of organization is weekly meetings with our advisor, Professor Troy. During these half hour meetings once a week, we go over our accomplishments for the past week, discuss our work, ask questions, and plan out next week. In addition to these meetings, we have end of term reports due on the last day of each term. These reports outline what was accomplished in the previous term and outline week by week what will be accomplished in the following term. These schedules keep the timeline progressing as planned and make the group aware of any lagging behind work that needs to be caught up on.

## 3.9 Financial Consideration

With an overall budget of $1000 ($250 for each team member), financial restraints have been taken into consideration. The budget is dedicated to the supplies and tools needed to research and test various options for the enhancement of our device. These enhancements include ways to increase the ergonomics of the device, as well as all aspects of the force application mechanism. For prototyping, supplies were purchased such as modeling clay, turkey bones to test device function, cinch straps to further constrain the arm, a blood pressure pump to act as a force applicator, and accessories to help develop the applicator such as a dowel or pinpoint. Moving into validation efforts, additional turkey bones were purchased to further test device function, and load cells to prove that the force applicator was accurate and consistent. By allocating our budget to

range from prototyping to design validation, we can ensure that the improvement of the device is the main priority, while still saving money for building and production costs. We also took into consideration additional costs could occur during our project as we may run into unexpected changes during validation and decide pieces need to be altered or removed on the device. By keeping the budget flexible, the team will be able to adapt easily to issues at any stage of the project. An estimated $500 was allocated for testing and building materials. $350 was allocated for the group to attend the Northeast Bioengineering Conference (NEBEC) at Drexel University in Philadelphia to present our project. A summary of our spending can be found in Appendix A.

# Chapter 4: Alternative Designs:

## 4.1 Needs Analysis

To create an optimal and efficient device, certain needs and specifications are outlined in this section. The following are the needs of the device:

*1. Easy to Setup and Use*

It's important for the device to be intuitive for the user. It should be obvious where the patient should put their arm, and it should also be easy for a physician to strap the patient into the device. Additionally, the device should be simple enough for a physician to perform tests without having to go through extensive training. Our goal is to require a maximum of 30 minutes for the doctor to take a CT image of the patient's distal radius, set the patient's arm in the device, apply a load to the arm and take another CT image, and finally analyze the output data from the program and develop a prognosis.

*2. Minimal User Input*

In addition to being easy to setup, the device should require minimal input from the user, and run calculations autonomously. The program should have constants defined such as Stiffness of bone at different stages (not healed, partially healed and completely healed), radius of bone and. By minimizing the input, it will allow physicians to use the device with greater ease.

*3. Simple Output*

The device must also be able to produce results that are easy to read and interpret. Using the applied force, the stiffness of the bone, the area of inertia of the bone. After running those calculations, our device should visually display these results in a way that is easy for physicians or doctors to understand.

*4. Accurate*

If the device cannot produce accurate results repeatedly, it would not be able to detect if a bone is healing properly, and it would serve no purpose as a diagnostic tool. Our team believes that the calculated displacement should be within 100 um to ensure proper accuracy for our

device and diagnosis. To make sure we are accurate we will develop a standard operating procedure to provide the same image analysis for all images to ensure accuracy and repeatability. Additionally, we will add filters and scan edits to the images to make the borders of the fracture as clear as possible to increase accuracy.

*5. Capable of Error Handling*

If the device is used improperly, or if there was a type of calculation error, the output should tell the user that an error has occurred and should instruct them to try again. It should tell the user exactly what the problem is and why it's a problem. This would ensure that the program is being used properly and can further minimize the amount of time the patient has to spend at the appointment.

*6. Compatible with a CT Machine*

The device also needs to be compatible with the CT machine that will be imaging the bone. This means that the device must be radiolucent and not obstruct the fracture site that needs to be imaged, and it also needs to be a small enough device to fit within the parameters of the CT machine's imaging space.

*7. Portable and Compact*

It would be preferable for the device to be lightweight if it needs to be transported from one location to another. It would also be beneficial for the device to not appear over-engineered or too clunky, but rather sleek and simple. The whole system should be able to be carried by one person easily and be lightweight. The target is to make the whole system less than 5 pounds. This would allow one person to easily transfer the device around without any problems or constraints.

*8. Cost Effective*

The device should preferably be cost effective, since clinics and hospitals would not want to pay a lot of money for a device that predicts the healing of bone. While it may save time and effort during the healing process, it really shouldn't be too expensive. The production of the device should not exceed $400 to both fit our budget and be a cost-effective tool for physicians.

*9. The maximum force a bone can undergo before pain or damage*

As a bone is slowly separated, once it reaches 2 mm of displacement the soft tissue

begins to undergo damage which slows the healing process. Our team must be extremely careful when applying load to the fractured bone. We will be aiming to apply the force on the lower end to get a small displacement, but still large enough to pass the minimum threshold for the CT machine (164 microns). Our targeted displacement is 0.25-0.75 mm.

## 4.2 Concept Designs

Once our functions and objectives were outlined, we began thinking of ways to apply these needs to our system to create a repeatable and efficient device for patients with distal radius fractures. Our three main tasks for this project are to enhance the ergonomics of the device, improve the force application process, and create a program from the device to display data efficiently for the doctor to make a quick prognosis. We began to brainstorm possible designs for all three of these components of our project and tested them to determine which designs were the best for our goals.

### 4.2.1 Ergonomics of Device

It is important that the device is as comfortable as possible for the patient. The patient will have their fractured wrist in the device without a cast. This can cause the patient to feel scared and uncomfortable, so providing a comfortable fit for the device could help ease the patient. There are two factors for the device that we believe need to be improved. We believe inserting a gripping mechanism for the hand as well as improving the way the arm is strapped into the device could improve the ergonomics of the device. Through talking aloud, drawing design plans, modeling with clay and 3D printing, we were able to come up with a few different ideas for the enhancement of the ergonomics for the system.

### 4.2.2 Gripping Mechanism

The device itself is made of plastic and is overall comfortable. However, every section of the arm has a place in the device except for the hand. The hand hangs off the end of the device which causes the fingers to be free in the CT machine. In order to ensure comfort, as well as making sure every image taken comes out the same, we thought it was necessary for some kind of

gripping mechanism to be added to the device. We discussed and tested several designs and then furthered testing with a 3D printed model.

### 4.2.2.1 Ball Gripping Mechanism

Our first concept we progressed with was using a ball to grab at the end of the device. We began by taking a rubber stress ball and taping it to the end of the device as shown in Figure 5. However, once we began testing the comfort of this we realized that the ball was too high up and caused our wrists to be overextended to flex upwards to reach the ball. This was not comfortable, and we decided that the ball had to be smaller.

***Figure 5 – Stress Ball Experimentation. This test was done to see how comfortable the patient's hand was during testing, as well as the amount of restriction the patient had while holding the grip.***

We then took the stress ball and cut it in half using a saw in the lab and then placed it on the device again using tape as shown in Figure 6. After testing out the new design, we noticed that though our wrists were in a more comfortable position, our fingers still hung over the device and allowed movement, which is what we were trying to avoid. We then decided that to restrict patients

from moving around they needed something they could wrap their fingers around to lock their hand in place.

***Figure 6 – Cut Stress Ball Experimentation. This test was done to see if the cut stress ball provided more comfort to the patient than the full stress ball.***

## 4.2.2.2 Rod Gripping Mechanism

After concluding that we needed a gripping mechanism that allowed patients to wrap their whole hand around to ensure their hand would not move, we decided that a bar was a more ergonomic choice for our device. We first drew out a bar that was fixed on one side and hung over the end of the device for the patient to grab. However, we realized that if it wasn't fixed on both ends then the patient could easily break the bar off, so we changed our design to have a bar that was fixed at both ends.

Our process for the fixed bar began with a drawing. Once we finalized our drawing and decided the shape we wanted, we began modeling our design with clay as shown in Figure 7. Once

we made the model with clay we realized that we did not consider where the thumb would rest comfortably on the device. We then decided that instead of straight fixed sides, we were going to add a slight curve to the sides for the thumb to rest comfortably. Once we got something that felt comfortable we redrew our design and measured the dimensions of the modeling clay and designed the piece in Solidworks, so we could 3D print the piece as shown in Figure 8.

***Figure 7 – Clay Modeled Grip. This grip was first modeled in clay to test the comfort of the grip before 3D printing.***

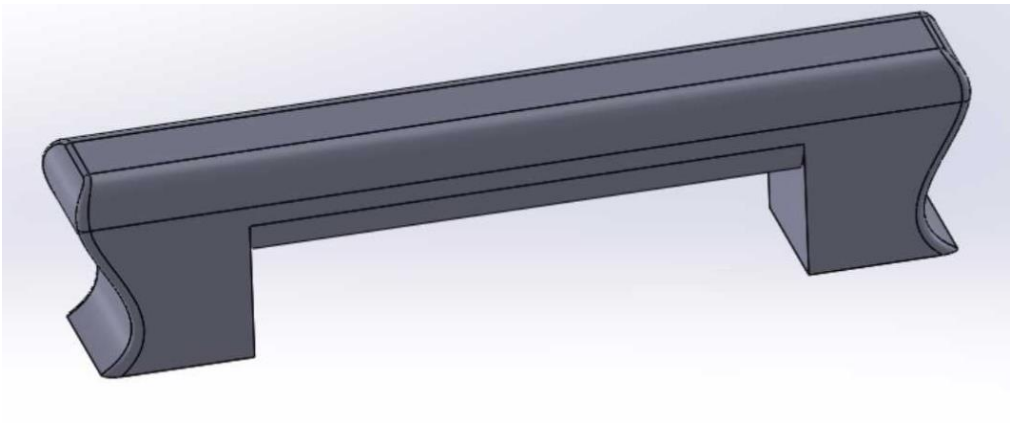

***Figure 8 – SolidWorks Model Grip***

Once the piece was 3D printed we attached it to the device using duct tape in order to test it in the system before permanently attaching. To decide if the piece was comfortable and worth adding to our device, all four group members tried it out to make sure it fit the needs of many people and not just one as shown in Figure 9. After all of us agreed that the piece was comfortable, we decided to print the piece again and permanently attach using hot glue.

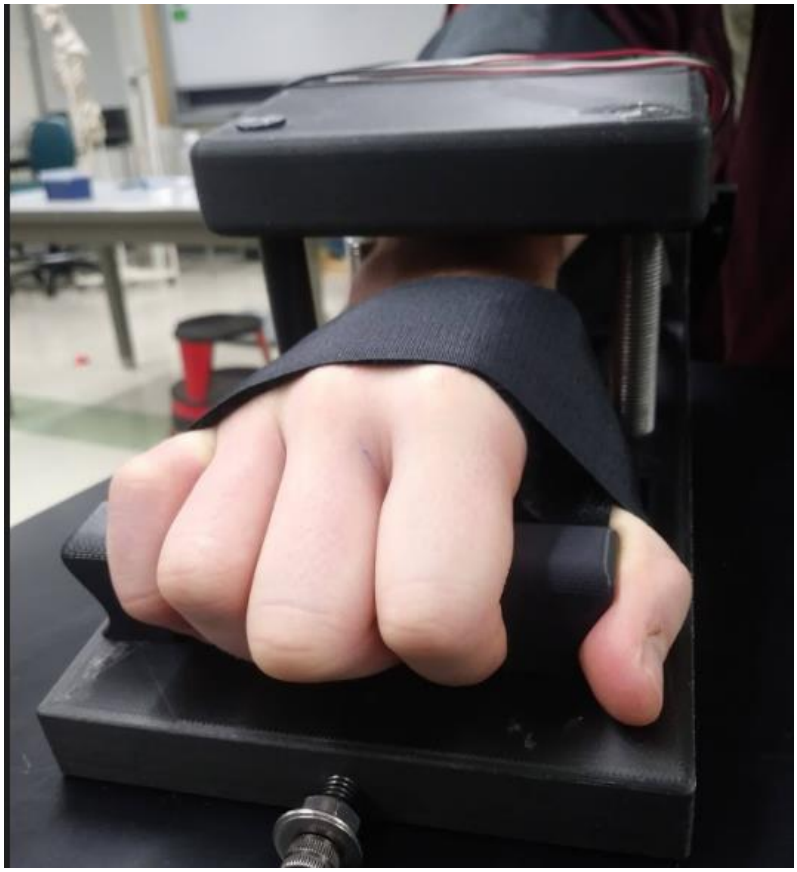

***Figure 9 – 3D Printed Grip Testing. This test was done to ensure proper size and comfort of the grip during testing with the device.***

***Table 5 – Comparison of Gripping Mechanisms***

| Material | Advantages | Disadvantages |
|---|---|---|
| Stress ball whole | ● Comfortable material<br>● Cheap and easy to obtain | ● Hand flexes up to hold ball<br>● Causes unnecessary flexion on wrist/fracture<br>● Hard to attach due to limited contact point |
| Stress ball half | ● Comfortable material<br>● Cheap and easy to obtain<br>● Easier to attach due to its flat surface | ● Fingers still overhang off device<br>● Defeats the purpose of having a grip |

| | | |
|---|---|---|
| 3D Printed rod | • Allows fingers to wrap around rod so fingers stay in one spot<br>• Fingers don't hang off device<br>• All fingers fit nicely and securely<br>• Left/right hand compatible | • Custom print job- cheap but still more expensive than a stress ball |

We decided to choose the 3D printed rod. It can be seen in Table 5 that the 3D printed rod allows for the patient's fingers to not only be restricted to only the device and not allow overhang, but the patients fingers will rest in one place and not move due to the ability to wrap their fingers around the piece. This ensures the patient's hand will not move during scanning. Though the 3D printed rod is a custom printed design, it is still a cost-effective method for providing patients with something to grab ahold of during testing.

### 4.2.3 Strap Mechanism

When we first received the device everyone in our group tested out the device and explained what wasn't as efficient as it should be and what needed to be changed. It didn't take long for all of us to agree the strapping method should be improved. The forearm is held into place using 2 straps at the end of the device. It is currently not as efficient as it could be because the straps are two separate pieces and requires both doctor's hands to strap the patient in correctly. However, our group believes that if the device had a Velcro cinch straps instead, the doctor could strap the patient in using one hand while the other hand makes sure the patient's arm is staying in place and the exposed fracture is safe.

A cinch Velcro strap as shown in Figure 10 are Velcro straps that attach back on themselves using a small piece or buckle that allows the straps to efficiently tighten on itself. Using this mechanism allows the process to be more efficient while still ensuring the arm is still safely secured into place. To test the cinched Velcro strap, we purchased one from Amazon and first looped it around the device and tested it out before attaching it. Once we all agreed that it was a

more efficient way of strapping in the patient's arm, the initial straps were removed, and the new straps were glued on.


***Figure 10 – Addition of Cinch Strap***

The cinch strap was able to be tightened with one hand instead of two, unlike the original design. This increased the efficiency and the overall ease of use for our device.

## 4.2.4 Force Application of the Device

The critical component of the device we believe needed the most improvement was the force application of the device. The force application process lacked validity and efficiency. The previous process required the doctor to tighten screws from underneath the device simultaneously while trying to minimize patient pain. The force was then measured through a strain gauge attached to the device. We decided that we needed a way to apply a point load to the distal radius easily and

efficiently, while also making sure the procedure accurately measures the force that is being applied to the wrist.

#### 4.2.4.1 Screwing Mechanism

We first believed that the best way to apply a force more efficiently was to reduce the amount of time the doctor must spend under the device tightening the screws. So, we began looking into ways that we could screw the device automatically and simultaneously. We began to research a robotic force application system that would ensure that the force would be repeatable. Using an Arduino as a base system, we would design a robotic gear mechanism that would move the force applicator up and down using a Bluetooth connection to a mobile device. While this would ensure an even force that could be applied automatically, it was ultimately declared unfeasible because of the amount of wires and hardware that was needed. The system we design should be as simple as possible, and wires that connect an Arduino to motors would be ungainly sitting on top of our device.

However, we believed there was a simpler way to go about this small problem. After a meeting with our advisor, she suggested that we investigate hydraulics. We believed that hydraulics could have been a simpler solution than creating a robot that could turn the screws simultaneously, and instead create a whole new system that could apply a force a different way.

When we began researching hydraulics we believed having a hydraulic pump of some sort to push down on the fracture. We believed our system could benefit from this kind of pump because it was:

- Radiolucent
- Efficient
- Easy to reverse the force application
- A more automatic way to apply a force

We knew we needed a small enough force application point so that when calculating displacement of the fracture, so we began looking into small hydraulic pumps. However, during our research we found that fluid and air compressors were often related. That's when we thought of the idea of filling a balloon with air instead. We then realized that a blood pressure pump could

possibly give us what we want because the balloon is small, and it is easy to pump air into the balloon.

### 4.2.4.2 Balloon force application

Once we decided we wanted to pursue the balloon pump idea, we purchased a standard blood pressure pump. We then cut the balloon from the blood pressure cuff and placed it under the force applicator from the device. Once we began pumping we noticed the bag was much too big and was applying a force across the whole wrist rather than just on the distal radius. We had to somehow make the balloon much smaller to create more of a point load on the fracture, rather than a distributed load. We also realized we must lock the force applicator in place so that it doesn't rise as the balloon pumps. We locked the force applicator into place using the screw nuts provided. To make the balloon smaller, we tried to use an iron to melt the plastic into each other and then cool it down to create a more contained balloon. However, when the iron was applied the plastic quickly melted away and off the balloon because it was far too hot for the plastic. We needed something that could apply enough heat to melt into each other but not hot enough to melt the plastic away. We then decided to use a flat iron for hair due to the ability to lower and higher the temperature as well as the ability to clamp down easily on the balloon as shown in Figure 11. We found that it was more efficient to have the temperature low (about 200 degrees Fahrenheit) and slowly melt the plastic as this reduces the risk of the plastic melting onto the flat iron. Once we finished melting the balloon we let it cool back to room temperature to harden and solidify the smaller balloon. We then pumped the balloon as much as it could go to test if it would pop and if the smaller balloon would rip open at the seams. The balloon did not pop at maximum pressure (300 mmHg) nor did it rip back open, so we continued testing with the small balloon.

***Figure 11 – Blood Pressure Modification. The balloon was sealed using a hair straightener at a low temperature to melt the balloon smaller to better fit onto a patient's wrist.***

We then placed the small balloon under the force application device and began to pump on one of our group members arms. It appeared to generate a high amount of force on healthy bone, so we decided to gather more data. For the blood pressure balloon to be a viable force applicator, there must be a linear relationship between the internal pressure of the balloon and the force it exerts on a point. To prove this, the Instron was utilized to perform an initial 3 point flexural test as shown in Figure 12. The deflated balloon was loaded onto the support pins and the loading pin was brought down until it contacted the balloon and a small force was shown. The balloon was then inflated at intervals of 20 psi and the corresponding force was recorded. Just as we hypothesized, as the internal pressure of the balloon increased, the applied force increased in a consistent and linear manner as seen below in Figure 13.

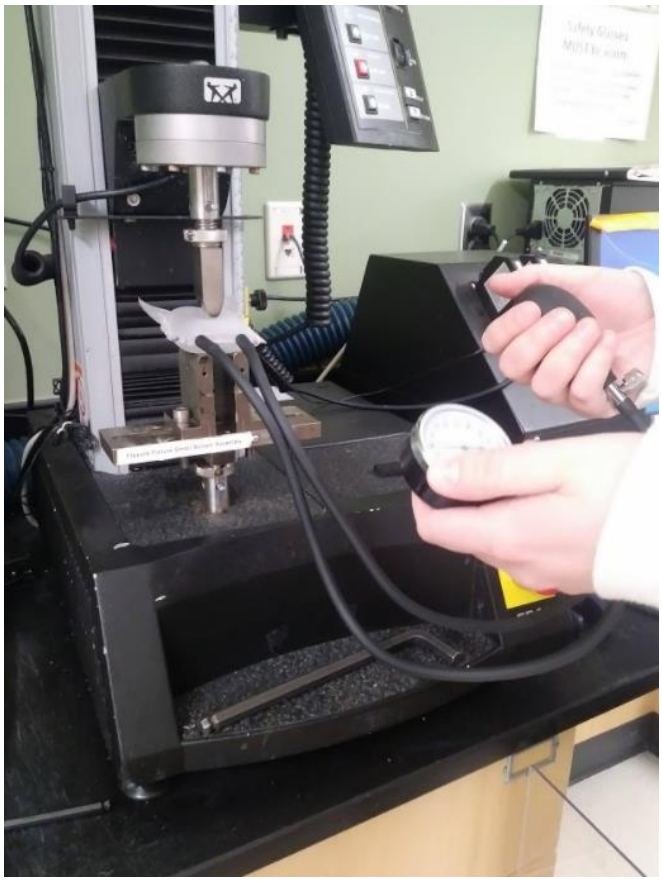

***Figure 12 – Balloon Instron Testing. This test was done by pacing the balloon on the Instron and testing the force measured at each 20 mmHg interval.***

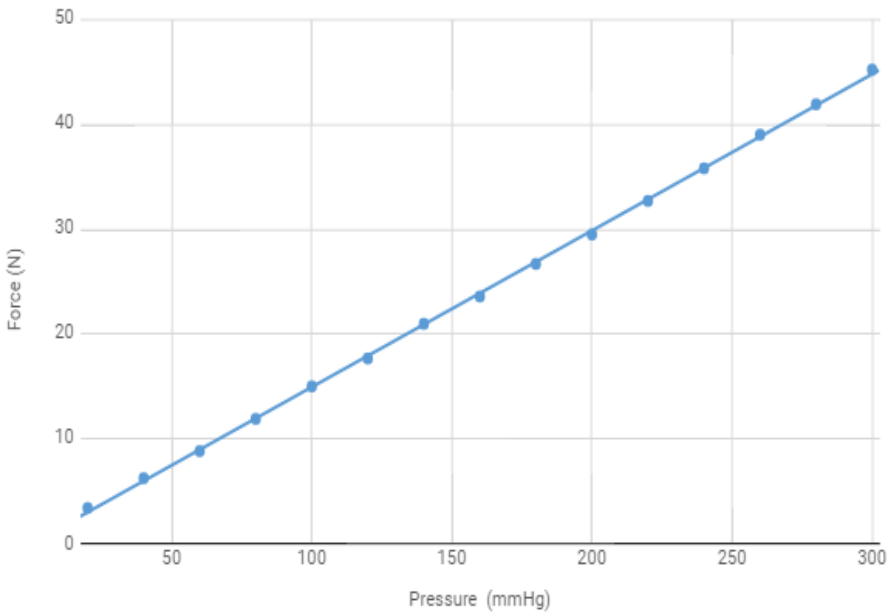


***Figure 13 – Linear Instron Data: $R^2$=.99. Standard deviation .19 mmHg***

The $R^2$ value is .99, which shows a linear relationship between pressure reading on our gauge and the amount of force being measured on the Instron. This linear relationship and high R2 value shows that the pressure force relationship is constant and repeatable, proving that our calculated values are accurate. Once we proved that the balloon could be a consistent and accurate force applicator, we put it back on our device to observe how it interacted with the existing threaded applicator. After trials using both our arms and turkey bones as shown in Figure 14, we concluded that the balloon was not applying a force straight down at a specific point. Instead, the balloon was expanding in different directions due to it not being fully constrained and was applying force over a varied area due to the shape of the balloon. For a 3 point flexural test to be accurate, the bone must be fixed by two support pins, and then the force must be applied vertically at one point by a precise loading pin. In Chapter 5, Design Experiments, different loading pins and a modification to constrain the balloon to vertical movement will be tested to ensure an accurate 3-point flexure force is being applied to the bone.

***Figure 14 – Turkey Bone Instron Testing Prep. This picture shows Alex prepping turkey bones for testing with our device to see how the force applied affects a cut turkey bone.***

### 4.2.5 Programming Languages

While exploring options for the Graphical User Interface (GUI) with the strain gauge in place to measure the mechanical force applicator, multiple programming software was investigated such as LabVIEW, Python, Java, and C++. Python, Java, and C++ are all commonly used general purpose programming languages, while LabVIEW is a system engineering software utilizing a graphical programming syntax that is both easy to use and reduces programming time. To use a general programming language to create a GUI, the user must be experienced in the language and create it from scratch. However, in LabVIEW, the graphical language allows the user to plug in the inputs and the sought-after outputs and a GUI is generated on the front panel. The advantages LabVIEW offers over general programming software makes it a clear choice for the programming language to use while creating a GUI for the strain gauge.

The same approach was used while exploring quantitative image analysis programs to measure the displacement of the fractured bone from a before and after image. Programs that were investigated were ImagePro, ImageJ, and Olympus imaging software. Image-Pro image analysis software allows the user to acquire images, count, and measure and classify objects. ImageJ is an image processing software that is programmed in Java that can display, edit, analyze, process, and save images while running in a multithreaded fashion, allowing multiple functions to be performed in parallel. Olympus imaging software is a program which acquires, filters, measures, documents

and archives images. ImageJ was chosen as the quantitative image analysis program over the other two competitors due to its free cost, ease of use, and all members of the team have experience with and feel comfortable using it.

## 4.3 Design Modifications

After doing all of the above experiments we proposed our first design. To achieve our first objective of making a more efficient force application system, we decided this was the criteria our new system needed to meet to achieve our first objective:

- Radiolucent
- Efficient
- Easy to reverse the force application
- A quicker way to apply a force

When comparing these criteria to the current screw mechanism design to our balloon pump system it can be seen in Table 6 that our balloon design achieves more of these criteria, making it a better system to apply a load to a patient's wrist.

***Table 6 – Comparison of Force Application Systems***

| | Screw Mechanism | Balloon Pump System |
|---|---|---|
| **Radiolucent** | 0 | +1 |
| **Efficient** | 0 | +1 |
| **Easy to reverse force application** | 0 | +1 |
| **Quick application of force** | 0 | +1 |
| **Total** | 0 | 4 |

Along with the pump system, we also added a finger support to restrict the patient's fingers from moving freely within the scanner, a cinch strap to improve ease of use and decrease setup time. These modifications help achieve our first of three objectives. However, during testing of the balloon on our arms we noticed that instead of applying a load directly to the distal radius, it was applying a load to the entire wrist as seen in Figure 15.

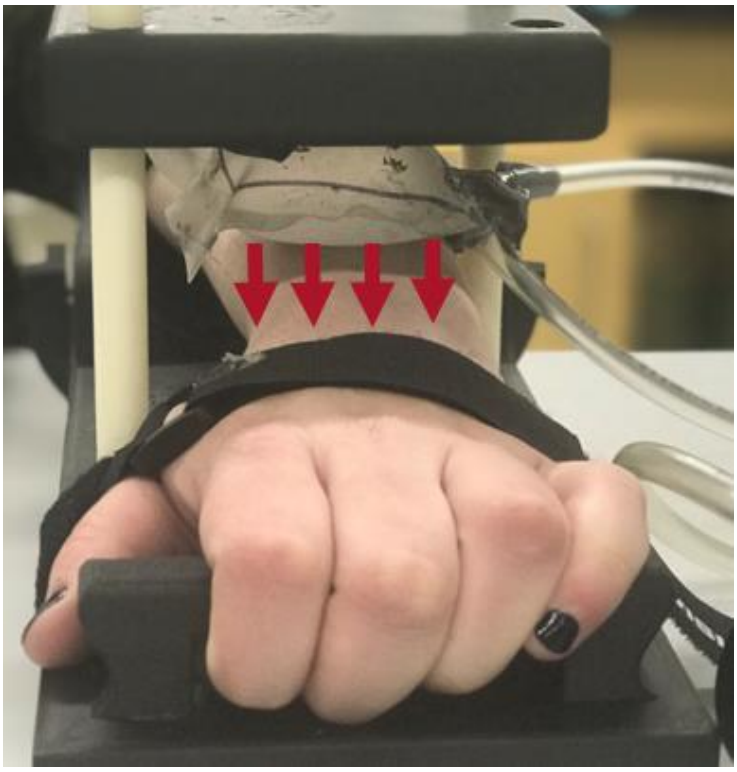

***Figure 15 – Balloon Force Dispersion. This figure shows the force of the balloon and how it is exerted onto the wrist. The balloon exerts force equally across wrist. However, this is a problem because to ensure accurate results during three point bend analysis the load should be localized only to the distal radius.***

This is not ideal because when analyzing data using the three point bend formula, the load being applied must solely be applied to the bending material, or in this case the distal radius. So though we chose to pursue the balloon system as our first prototype, we had to further modify the system by adding a piece to the balloon that can localize the pressure across the distal radius to produce more accurate and repeatable.

# Chapter 5: Design Experiments

## 5.1 Design Experiment #1 Force Application Piece

**Purpose:** This design experiment was conducted to test which force application piece is best suited to apply a point force to the distal radius as the balloon inflates. The force application pieces focused on this this study include just the balloon, the legacy 3D printed piece, a marble, and a 6 mm and 12.5 mm diameter wooden dowel. This study considers force, pressure, comfort, and shape to select the optimal force application piece.

### 5.1.1 Force Measurement Test

**Method:** Force application pieces were connected to the balloon in the device and then mounted onto the Instron. The Instron was configured to run a three point bending compression test. The balloon was then inflated in increments of 20 mmHg up to 300 mmHg and the force in Newtons was recorded. This test was repeated three times for each material.

**Results:** Despite having different material properties and shapes, while applying a point force, all force application pieces produced roughly the same average max force of ~70N when the balloon was inflated to 300 mmHg. From this experiment we were able to conclude that all five force application pieces were capable of applying a reasonable point force in an ideal three point bending scenario as shown in Table 6.

***Table 7 – Instron Force Testing***

| **Force Application Piece** | **Average Max Force (300 mmHg)** |
|---|---|
| Balloon | 71.57 N |
| Legacy 3D Printed Piece | 75.53 N |
| Marble | 70.11 N |
| 6mm Diameter Wooden Dowel | 73.71 N |
| 12.5mm Diameter Wooden Dowel | 71.93 N |

For all the force application pieces, the resulting force vs the pressure in the balloon was linear with constant increments. Using the data, we were able to create a graph and produce a linear equation, allowing us to compare balloon inflation (mmHg) and force applied (N). Below is an example of the average Force vs Pressure graph for the 12.5mm diameter wooden dowel with a linear equation of y = .2434x-0.3449. With this force application piece, each mmHg of inflation in the balloon is equal to roughly 0.24 Newtons of force.

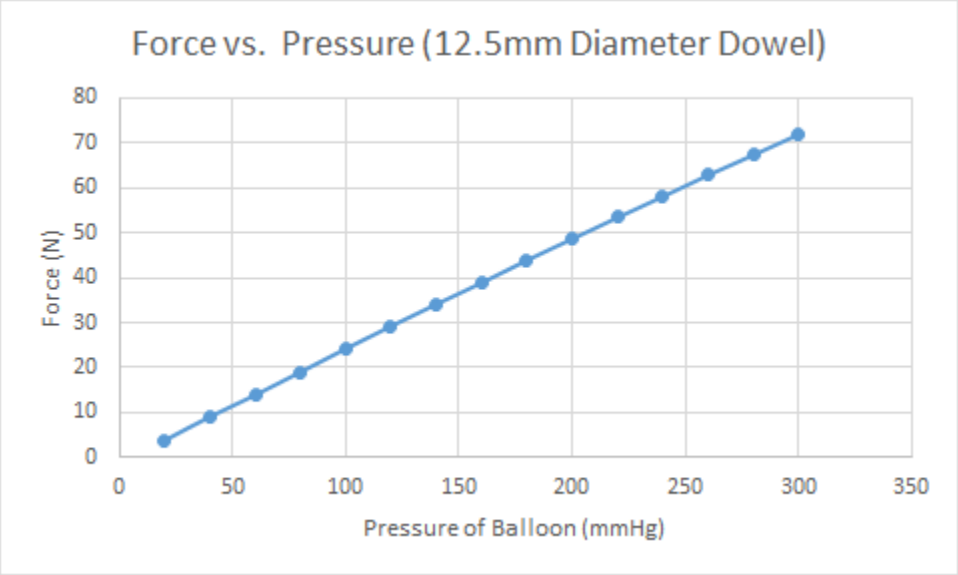


***Figure 16 – Instron Testing: 12.5mm Wooden Dowel***

## 5.1.2 FujiFilm Pressure Test

**Method:** Fuji Film pressure paper was prepped and then applied on top of Julie's skin directly above her distal radius. Her arm was then inserted into the device and the balloon was inflated at increments of 50 mmHg up to 300 mmHg. The area and intensity of the pressure was recorded on the Fuji Film paper and then was analyzed and interpreted using ImageJ. This test was completed for each of the force application options separately.

**Results:** Histograms were made to relatively understand how concentrated the pressures were based on the intensity of the red that was recorded on the Fuji Films (Appendix B). The marble in Figure 16C that it created the highest pressure in a single location, due to the single peak that is taller than all the other peaks. Though it created a large peak, during testing it was observed that the balloon was encasing the marble and the balloon was also exerting a pressure on the wrist.

Also, the marble did not provide a force along the entire radius, rather just a small surface of the radius, proving that the marble would not be a good choice for the force application piece. The legacy piece shown in 15B shows the highest number of peaks at the same level, proving that this piece provided a constant pressure throughout the whole radius. This is an ideal force applicator for this reason, however, as shown in the Section 5.1.3., the legacy piece was far too painful to use on patients. The last two histograms are of the 6mm dowel (15D) and the 12 mm dowel (15A). These dowels both had high peaks, however the larger dowel had more peaks at the same height, providing a more constant pressure throughout the whole radius.

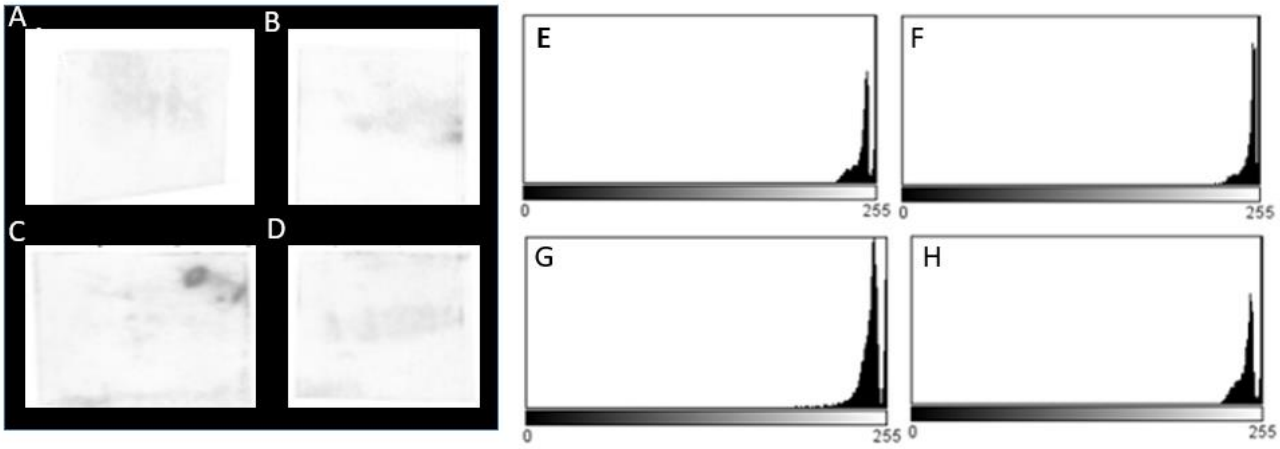


**Figure 17 – FujiFilm Analysis Histograms. A-D: Pressure film raw data. We placed the film on our distal radius and used the device as we would use it on a patient. A: 12.5mm dowel. B: legacy piece. C: marble. D: 6mm dowel. E-F: Histograms of the pressure film data. The histograms were created to compare the intensity of the color resulting from the pressure each piece applied onto a wrist when loaded in the device. E: 12.5mm dowel. Mean: 247.685, StdDev: 6.580, Min: 223, Max: 255. F: legacy piece. Mean: 248.968, StdDev: 7.449, Min: 177, Max: 255. G: marble. Mean: 242.067, StdDev: 13.908, Min: 142, Max: 255. H: 6mm dowel Mean: 245.583, StdDev: 6.873, Min: 206, Max: 255.**

## 5.1.3 Comfort and Pain Test

**Method:** Julie's arm was inserted into the device and the balloon was inflated at increments of 50 mmHg up to 300 mmHg (0N-72N). Relative pain was recorded at each increment on a scale of 1-10 as seen in Figure E1. To measure relative pain, the Mosby Pain Scale was utilized as

described in Appendix E. This test was completed for each of the force application options separately.

**Results:** The balloon by itself and the 6mm diameter wooden dowel were consistently painless and comfortable throughout the entire test. The marble, legacy piece, and 12.5mm diameter wooden dowel built up and caused extreme pain during higher pressures (150-300 mmHg). Pain readings of 7 and above are not bearable for procedures that could last as long as 10 minutes. Therefore, the marble, legacy piece, and 12.5mm diameter wooden dowel are not viable for force application unless they are modified to cause less pain.

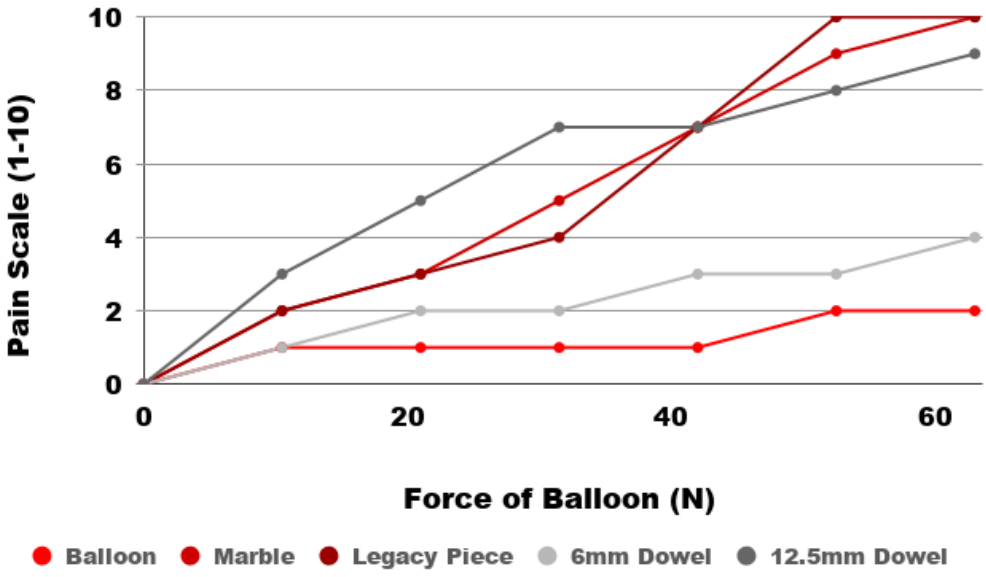


***Figure 18 – Pain Scale Testing. This test was done to ensure our pain threshold stayed under five and to test which pieces caused the least amount of pain. We asked our patient to rate the pain 1-10 based on the Mosby Pain Scale every 10 mmHg.***

## 5.1.4 Additional Experimentation Discussion

**Shape:** As discussed previously, the force application piece must can apply a constant three-point bending force to the distal radius in order to accurately calculate displacement of the distal radius. From this design experiment we were able to conclude that the balloon, marble and 6mm wooden dowel were not suitable for our needs. The balloon would press on a large area of the lower arm and then reform around it, causing the pressure to be applied on a larger area, thus applying less force to the distal radius. On the other hand, the marble and 6mm wooden dowel

were too small and applied an extremely concentrated pressure to the arm causing extreme pain at lower forces.

**Comfort:** In order decrease the pain caused by the force application piece while imaging and collecting displacement data, we explored modifying the 12.5mm wooden dowel since we had many dowels to test with and only one legacy piece. We wrapped one dowel with leather strips, and another dowel with a layer of neoprene to absorb some of the impact against the skin. We repeated parts #1-3 of this design experiment with both dowels to determine if either successfully reduced pain while still applying an appropriate force. Both alternatives applied an appropriate force, however to successfully dampen pain, the leather alternative had to be wrapped multiple times around the dowel. This caused the 12.5mm dowel to be too large for use. Below are the pain scale improvements resulting from modifying the 12.5mm wooden dowel.

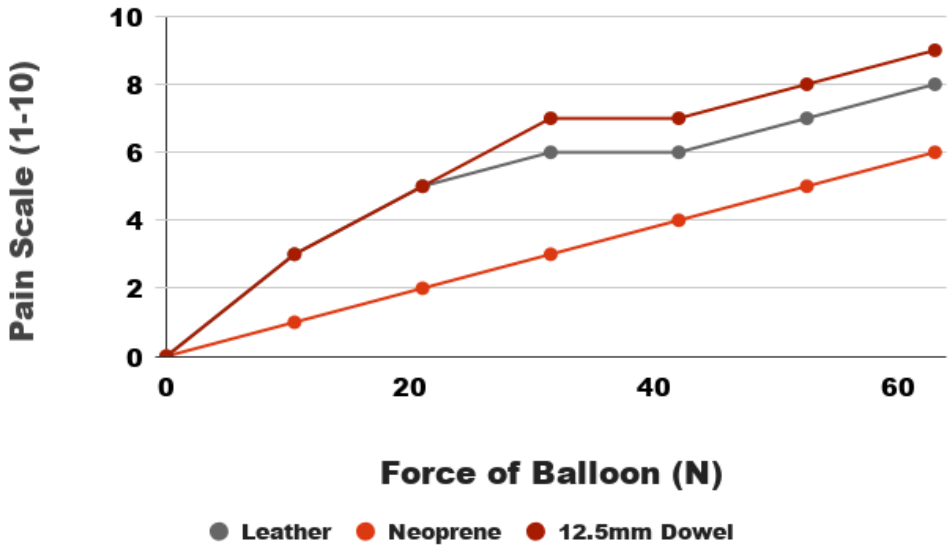


***Figure 19 – Pain Scale Testing – Dowel Modifications. The same pain scale test was done at the same pressure intervals but with different materials wrapped around a 12.5 mm dowel.***

The neoprene wrapped dowel provided ideal absorbance while still applying an appropriate force to displace the distal radius. From this design experiment, we can conclude that the neoprene wrapped 12.5mm wooden dowel is the best design choice for the force application piece due to its force, pressure, comfort, and shape.

## 5.1.5 Pressure Piece Verification and Validation

After exploring the pressure and pain characteristics of the 12.5mm wooden dowel covered in neoprene, we had to ensure that it would be able to provide a force that was repeatable and accurate. This was done through calibration of the entire force application system on the Instron 5544 in order to find an accurate pressure to force relationship. With three trials, this relationship was mapped out and resulted in 1 mmHg being equivalent to 0.24 Newtons of force (y=0.2407x-1.0211). As seen in Figure 19, the force application setup with the 12.5mm wooden dowel covered in neoprene allowed the system to output 0-72 Newtons, which is more than acceptable for the nominal 25 Newtons required for a procedure. This relationship was utilized for the Arduino live force reading which is discussed further in section 5.3.1.

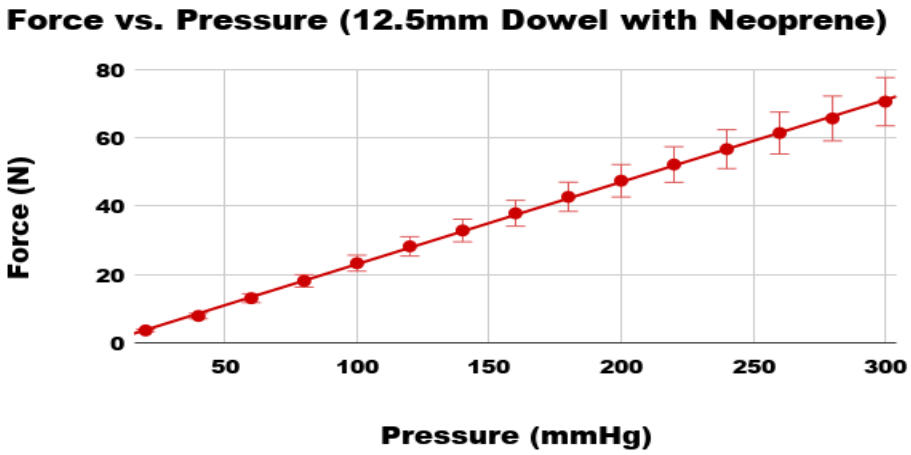


***Figure 20 – Instron Pressure to Force Calibration. Y=0.2407x-1.0211. 0.24N=1mmHg***

## 5.2 Turkey Bone Testing

**Purpose:** The turkey bone experiment was conducted to test the functionality of the device as well as obtain a predictable range of force needed to displace a human cadaver bone.

**Method:** Three turkey bones were dissected from the skin and flesh to reveal just the exposed bone. This bone was then cut using a hand saw specified for specimen cutting. Three arbitrary cuts were made to the turkey bones to test their displacement values: a small nick, a 25% cut and a 50% cut. The turkey bones were then bagged and loaded into our device where they were tested at 50 mmHg intervals and observations were taken at each.

**Results:** The first part of this experiment was to ensure the device worked as intended and exerts enough force to be able to displace a human cadaver bone. The device was able to break a 50% cut into the turkey bone which is, when correlated, more than enough force to displace a human cadaver bone. The next stage of this experiment was intended to give estimated values at which displacement would occur in human cadaver bones by relating force to modulus of the different bones. Because the modulus of turkey bone is less than that of a human cadaver bone, the experiment was designed to determine the force needed to displace a turkey bone with a synthetic fracture 50% through the bone. We used half of this force as the recommended value that cadaver testing be started at for the intended 2 mm displacement. With a small nick in the bone, displacement was visible at 240 mmHg (56.74N). With a quarter cut through the bone, displacement was visible at 220 mmHg (52.23N). Finally, with a cut halfway through the turkey bone, it took only 100 mmHg (23.3N) to completely snap the bone. Because the turkey bone has a lower modulus than human bone, it will snap at a lower value. We used half of this value to recommend testing on the cadaver bone be started at 50 mmHg to ensure only displacement, not breakage, of the bone occurs.

## 5.3 Digital Pressure Gauge Air Leakage Test

**Purpose:** The leakage experiment was conducted to test if the force applicator piece could apply a consistent force over a five-minute period, which is the typical duration of a CT scan. After initial testing, it was decided an air sealant was necessary to reduce the amount of air leakage in the tubing. This leakage was due to the change in tubing of the device and additional elbows added such as the y-valve for the digital pressure gauge.

Method: A digital pressure gauge was purchased to measure force in real time and store the data in excel. This pressure gauge was attached to the balloon pressure applicator via a y-valve to accurately detect the internal pressure of the balloon to determine the force exerted on the bone. The leads of the pressure gauge were connected to an Arduino which was connected to a computer through a USB.

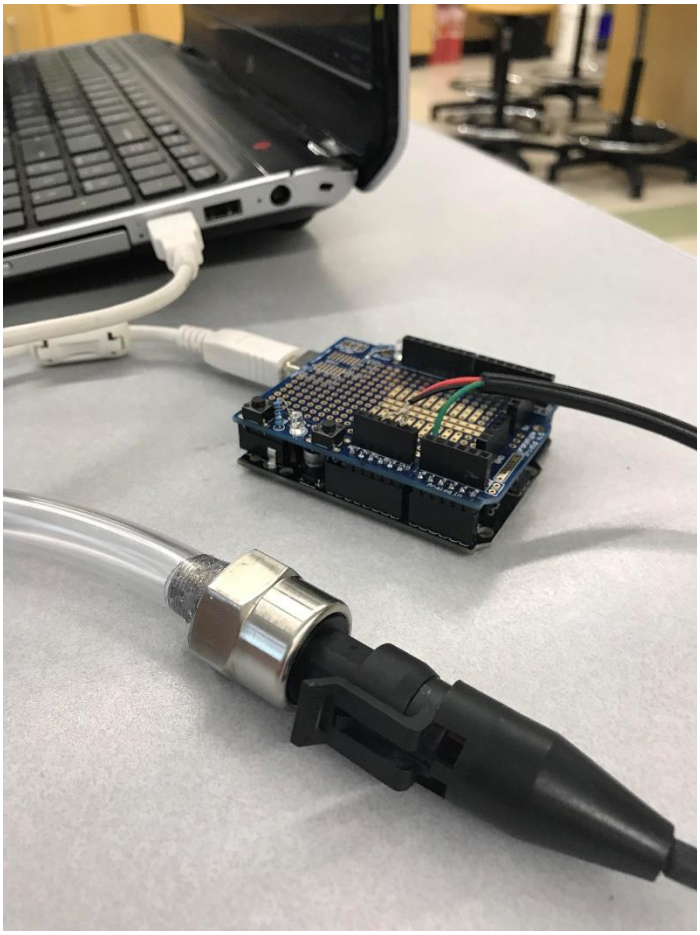

***Figure 21 – Wired Arduino Assembly. This figure shows the pressure transducer which is connected to the Arduino which is then connected to a laptop. The Arduino was coded so that the data being transmitted to the laptop was instantaneous force application.***

Initially when testing the pressure gauge, there was a substantial amount of air that was leaking. A test was developed to see how much pressure dropped over a five-minute span. This test involved filling the balloon up to a set pressure (50, 100, 150, and 200 mmHg), and then recording the change in pressure after a five-minute time interval.

**Results:** After filling the balloon to a pressure of 200 mmHg, the pressure was found to drop 24 mmHg in a five-minute span with the pressure transducer, and only 10 mmHg in a five-minute span with an initial pressure of 100 mmHg (Table 7). This leakage was significant, as the device needs to hold a steady and reliable pressure while placing a load on a bone in the CT scanner. To fix this problem, silicone Loctite sealant was purchased and used on the tubing at all the connection points, including where the pressure gauge connected to the rest of the balloon system. After using the sealant, leakage was reduced to around two mmHg per five minutes with an initial pressure of

100 mmHg (Table 8). While the pressure leakage was not eliminated, the smaller drop in pressure was considered suitable for the device's application. This data can be seen in the tables below:

***Table 8 – Leakage Test***

| Pressure (mmHg) | Pressure lost (mmHg) |
|---|---|
| **50** | **5.75** |
| **100** | **10.00** |
| **150** | **16.25** |
| **200** | **24.00** |

***Table 9 – Air Sealant Leakage Test***

| Pressure (mmHg) | Pressure lost (mmHg) |
|---|---|
| **50** | **1.25** |
| **100** | **1.75** |
| **150** | **3.75** |
| **200** | **4.5** |

The data summarized in Tables 7 and 8 were then compared as shown in Figure 21.

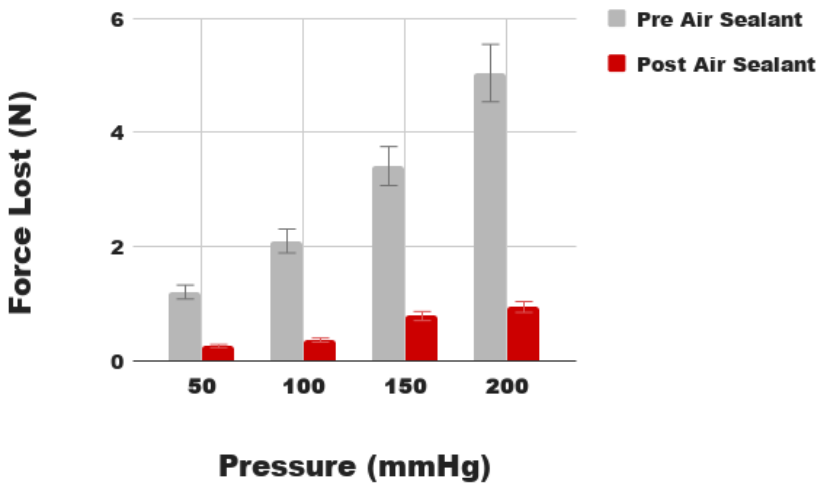

***Figure 22 – Air Leakage Test. The pump system was pumped up to various pressure intervals and left for five minutes. At the end of the five minutes the final pressure was reported. This was done before and after adding air sealant to the system.***

As it can be seen in Figure 21, the error bar shows the dispersion of pressure because of three different trials when using the dowel with the neoprene. The standard deviation at this pressure is ±.191, which is minimal. This translates to about ±1 Newton. So, losing about 5 Newtons of force during the CT scanning is not ideal because the load needs to remain as constant as possible to produce an accurate displacement measurement. With the sealant, at 100 mmHg which is our testing pressure, we lose on average 1.75 mmHg which translates to .35 Newtons in five minutes. This falls within our standard deviation for 100 mmHg and allows the CT scan to capture a constant load for 5 minutes.

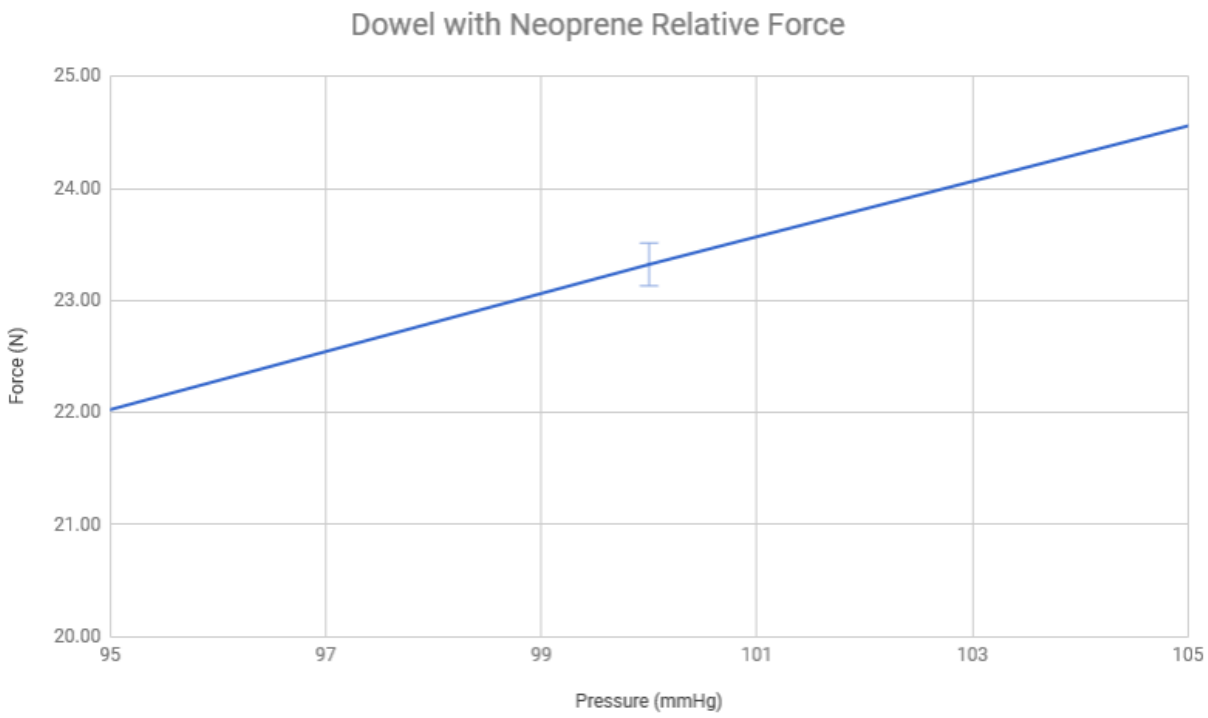


***Figure 23 – Dowel with Neoprene Relative Force. Standard deviation 0.19 mmHg.***

Once the leakage was minimized, the electronic output of the pressure gauge needed to be verified.

### 5.3.1 Arduino Code

To correctly and accurately measure the reading on the pressure transducer, the voltage must be converted into pressure. This is necessary since the SKU237545 Pressure Sensor is measuring a DC voltage difference between 0.5 and 4.5 V. The output voltage corresponds to the internal pressure in Pascals with the conversion factor specific to the pressure sensor. After converting from voltage to Pascals, the reading was further converted to mmHg to be consistent and relatable to the manual pressure gauge. This reading is then converted to the force applied on the distal radius as found. This is extremely helpful in a clinical setting since it allows the physician to monitor the force being applied in a live setting, while giving them the option to store and save the data for post procedure analysis. The Arduino code used can be found in Appendix H.

To verify that the code was working adequately, we pumped the balloon to a sustained pressure reading of 100mmHg on the analog pressure gauge, and ensured that the digital readout was around 24 Newtons (1mmHg=0.24N). After conducting this verification process at multiple pressures, we verified that our code was accurate at digitally determining the force, with an accuracy of +/-2N.

## 5.4 Cadaver Arm Testing

**Purpose:** The purpose of this experiment was to use our device on a simulated fracture from a cadaver arm. Cadaver testing was designed to ensure the functionality of the device in its final stages of development. The ultimate purpose of the device is to displace a distal radius by about 2mm and have that displacement be measurable through a CT image analysis. This would give us insight on:

1. The functionality of the device
2. The efficiency of the device
3. If the force application provides enough force to displace a fractured bone enough for a CT image to capture it
4. Patient/Physician feasibility

## 5.4.1 Testing: Round One

**Methods:** Testing the device with a cadaver arm was done with a team of surgeons. Ara Nazarian, Jack Wixted, and Mohammed Yousef were able to join to help perform simulated fractures on a distal radius.The cadaver arms were brought up the specimen prep room where 7mm cuts were made to simulate a fracture to the distal radius using a bone saw. The bone saw was used to cut the palmar side of the distal radius as shown in Figure 23A. Once the fracture was simulated on the specimen, the specimen was loaded into the device as it would a patient. The unloaded device and the specimen were placed in the CT machine and the first scan of the unloaded bone was done as shown in Figure 23B. The cadaver arm was then loaded with 100 mmHg (about 25 Newtons) and scanned using the CT machine while loaded. The final image was of the bone cut and loaded. This was done for 10mm cuts as well as fully fractured cuts. Imaging before and after being cut and loaded allows, through image analysis, for evidence that the device can displace the distal radius.

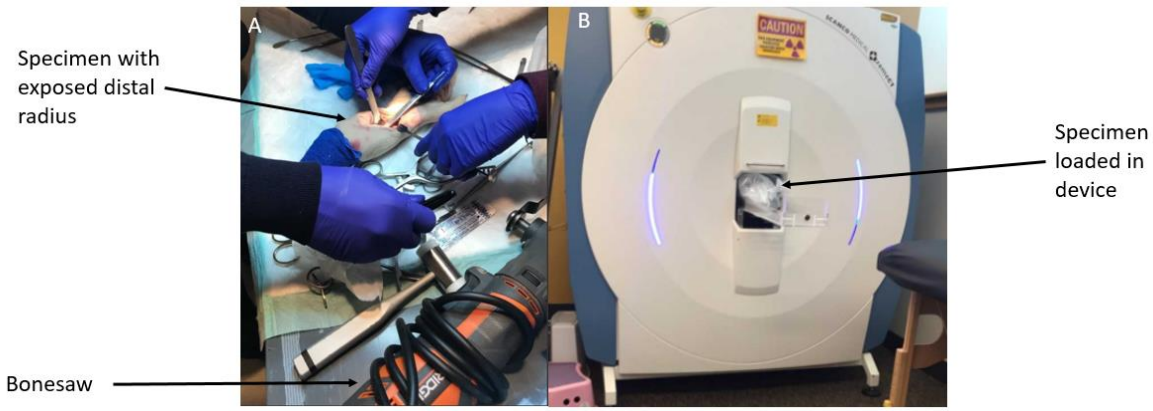


***Figure 24 – Cadaver Arm Testing Layout. The specimen (A) was first prepped in a specific prep room using a bonesaw to cut the palmar side of the distal radius. Once prepped the specimen was then taken into the CT room where it was loaded into the device and then the device was loaded into the CT scanner (B).***

**Results:** Once the cadaver arm testing with the device was completed, we were able to analyze these scans in an image analysis software (Materialise v.18). We used this program to measure the fracture width of the fractures both unloaded and loaded. An example of one of the measurements taken can be seen in Figure 24. We measured ten fracture widths across the fracture to find the average width as shown in Figure 25. Table 9 shows the measurements for the CT scans.

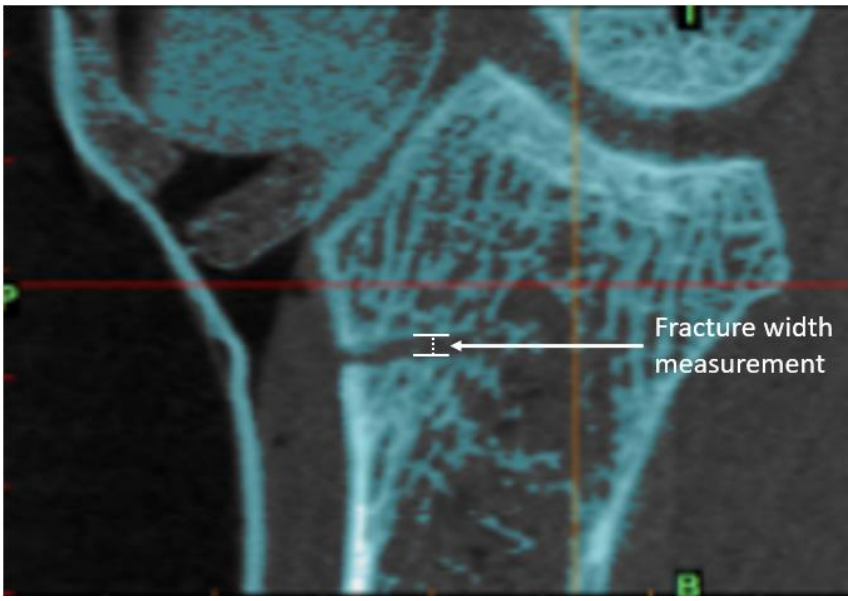


*Figure 25 – Fracture Width Measurement Example. The width was measured from the proximal side of the fracture to the distal side.*

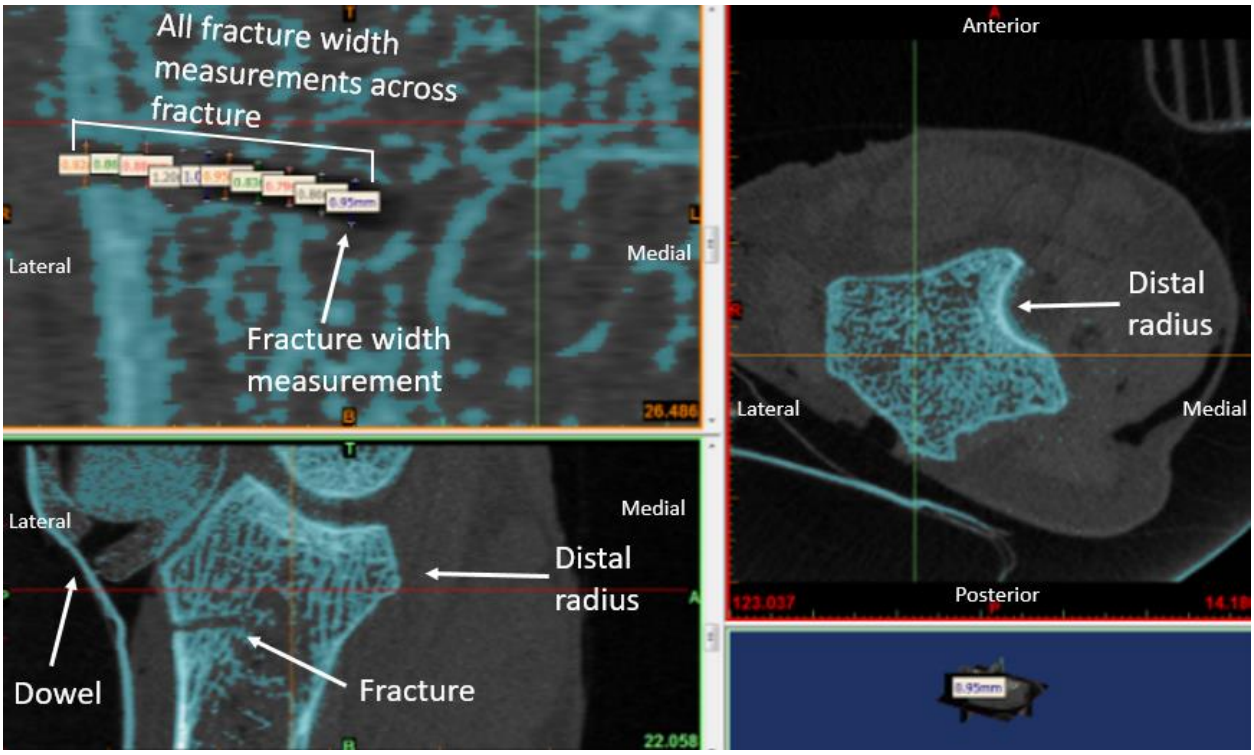


*Figure 26 – Mimic Software Grey Scale Analysis: Bone Fracture Length. Top Left shows an example of the ten fracture width measurements. Top right shows the cross section of the patient's distal radius. The Bottom Right shows the distal radius, the fracture and the dowel that was used to apply a load to the bone.*

*Table 10 – Mimics Analysis of Cadaver Wrist*

| Image | Average width (mm) | Displacement from 7mm unloaded bone (mm) |
|---|---|---|
| 7 mm wrist - unloaded | 0.839 | 0 |
| 7 mm wrist - loaded | 0.967 | 0.128 |
| 10 mm wrist - loaded | 1.309 | 0.47 |
| Full fractured wrist - loaded | 1.514 | 0.675 |

The wrist did experience a small displacement while under a load in the CT scanner. The wrist in total experience .675 mm of displacement. It was more beneficial to compare the 7mm cut because this simulated fracture had scans for both the loaded and unloaded wrist, so the displacement that was directly caused by the load that our device applied was able to be quantified. However, the overall procedure took a long time due to the difficult positioning of the wrist, as well as the need to flip over the device once the wrist was in and screw from the bottom until it was tight enough, costing us much needed time.

**Outcome:** Our device had to go through many iterations to reduce the difficulty of use. The dowel could not be seen at all during scanning due to the dowel being completely radiolucent as shown in Figure 26A. This caused setting up to be timely because it was difficult to see if the dowel was resting on the bone aligned with the fracture site. This costs us a lot of extra scans and time and reduced the efficiency of our device. To fix this problem, we added a small strip of aluminum foil to our dowel to see where it was located in the scanner more clearly as shown in Figure 26B. This allowed our setup time to decrease and less initial scanning had to be done.

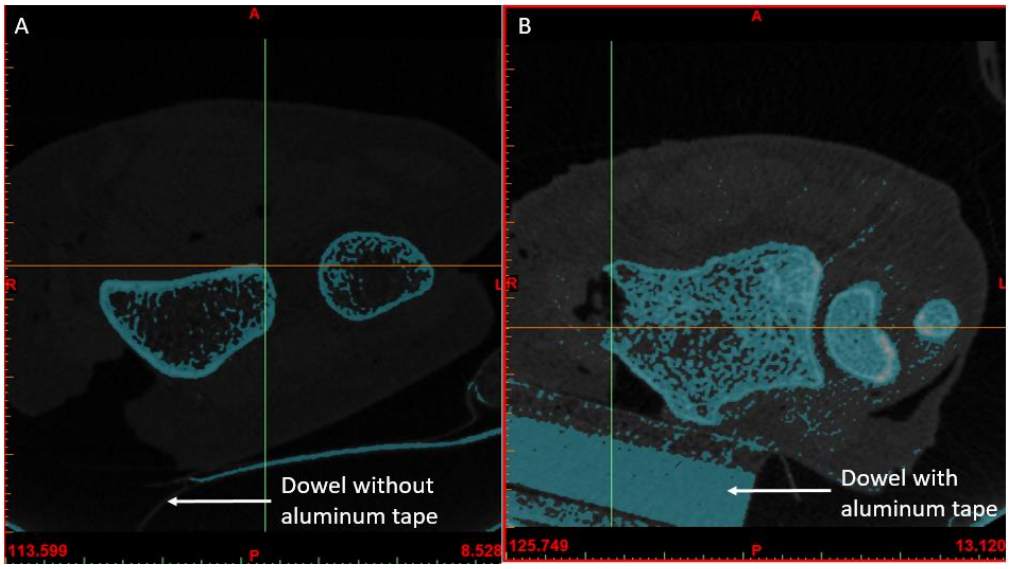


***Figure 27 – Dowel Imaging Modifications. A shows the scan of the distal radius with just the dowel. B shows the modified dowel with the addition of aluminum tape.***

Another change we made after this experiment was to eliminate the screwing mechanism. The past MQP had screws to measure the amount of force that was being applied to a wrist through a strain gauge. However, because we eliminated the strain gauge there was no purpose for the screws anymore. Eliminating the screwing mechanism reduces the amount of time it takes to lock the wrist in place, as well as increases the radiolucency of the device. We replaced the screws with dowels. However, we still wanted to eliminate the need to turn the device over while the wrist is in the device because this is particularly uncomfortable for the patient and isn't necessary to do from underneath the device. Due to these reasons, we attached four dowels permanently to the base of the device and detached the dowels from the force application piece as shown in Figure 27. This allows the force application piece to easily slide on and off the device and speeds up the set-up time drastically while also keeping the patient's arm flat rather than moving and twisted during application.

To clamp the dowels down and prevent the force application piece from being pushed up during the application of the load we bought 2 tripod quick release clamps as shown in Figure 27. These clamps slide onto the dowel and then screws tightly onto the dowel to ensure the force application piece will not move, however, they do contain metal screws which can interfere with the scans.

Lastly, during testing it was observed that the pressure gauge was decreasing while the CT was scanning the wrist. This caused us to have to restrict the tubing so that the air would not leak out as fast and cause the pressure to drop. To fix this problem, we changed the old tubing that was included with the blood pressure pump we bought to a Versilon C-210-A Polyurethane tubing. Besides changing the tubing, we also applied Loctite Clear Silicone Waterproof Sealant around all openings and attachments to decrease the amount of leaking. These improvements were made in time for our second round of cadaver arm testing and can be summarized as seen in Table 10.

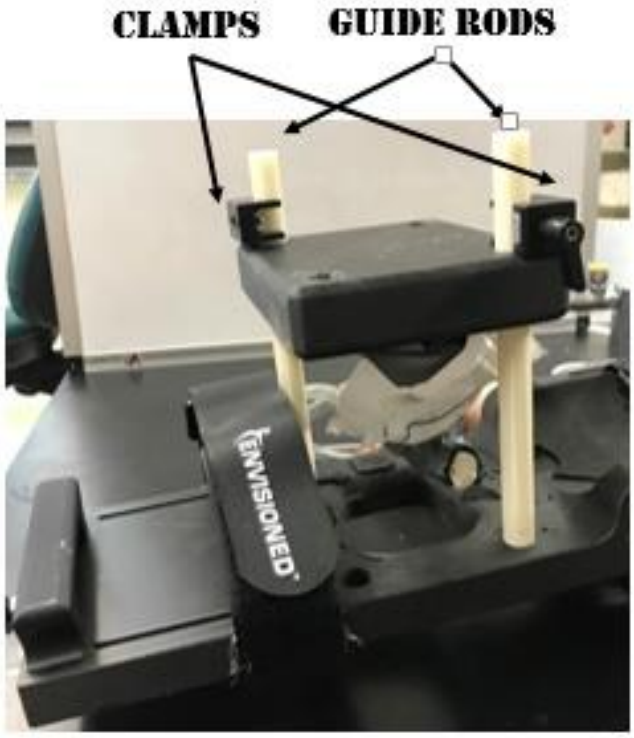


***Figure 28 – Clamps and Rods on Device. The rods were fixed to the base so that only the force application system is able to move vertically. The clamps were added to keep the force application piece from moving upwards during loading.***

***Table 11 – Mimics Analysis of Cadaver Wrist***

| **Change made to device** | **Effect** |
|---|---|
| Added aluminum tape to dowel | • Easier to see exact force application to wrist<br>• Decreased setup time<br>• Decreased amount of initial scans needed |

| | |
|---|---|
| Removed screw mechanism and replaced with fixed dowels | • Decreased setup time<br>• Allows for force application to be done from the top<br>• Allows for force to be applied within CT scanner<br>• Reduces amount of movement needed from patient |
| Added tripod clamps | • Keeps force application locked in place against patient's wrist |
| Replaced tubing and added sealant around ends of tubing | • Reduced amount of leaking during force application<br>• Allows for consistent force applied to patient's wrist during scanning |

### 5.4.2 Testing: Round Two

**Purpose:** The purpose of this experiment was to use our device and its new improvements on a simulated fracture from a cadaver arm.

**Methods:** For the second round of testing we followed the same procedure. However, we increased the number of scans we took so that we were able to compare an unloaded to a loaded scan of the same fracture size. This would allow us to measure the difference in displacement due solely to the loading of our device.

**Results:** During the second round of testing the time it took to set up each wrist into the device decreased drastically. However, there were still some complications. The blood pressure pump continued to leak, even after testing with the application of air sealant showed minimal leaking. This could be due to the wrist pushing against the balloon forcing air out faster. Another complication was that even though we took the screws out, the threads, which are also made of metal skewed the scans and made them extremely dark due to the auto-contrast. Though there were complications, the entire process took a lot less time due to the new design that applies the piece from the top without screws. Once we had all the scans, they were analyzed again in Mimics as shown in Table 10. The length and the average width of 10 widths measured across the span of

the fracture were found. The loaded widths were compared to the unloaded widths to find the displacement of the fracture. The measured displacements can also be seen in Figure 28.

***Table 12 – Mimics Analysis of CT Images Second Round of Testing***

| Name of cut | Average Displacement (mm) | Difference of displacement from unloaded to loaded (mm) |
|---|---|---|
| 7mm - unloaded | .751 | N/A |
| 7mm - loaded | .929 | .178 |
| 10 mm - unloaded | 1.577 | N/A |
| 10 mm - loaded | 1.773 | .196 |
| Full cut - unloaded | 1.183 | N/A |
| Full cut - loaded | 1.697 | .514 |

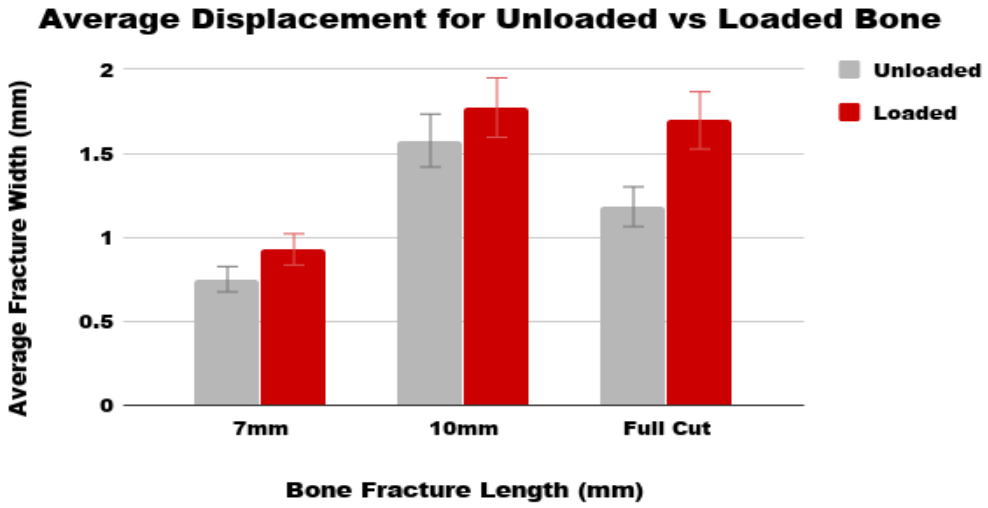


***Figure 29 – Mimic Analysis: Unloaded vs Loaded Bone***

# Chapter 6: Final Design

## 6.1 Design Overview

Our final design was 3D printed. Our design has a base with four 0.5in diameter dowels fixed and protruding upwards 7in. The device has a small rod at the front for the patient to grab ahold to and curves along the side to rest their thumbs. The design also includes two slits on both the front and the back where two cinch straps slide into to strap the patient's arm in to minimize movement within the CT machine. At the very front of the device is a screw to quickly lock the device into place in the scanner and a lip on the back to allow the device to rest at the edge of the scanner to keep it in place.

Once the patient places their hand on the base of the device, a force application piece that has a deflated balloon and a large Delrin dowel attached is then slid down the four dowels until it gently rests on the patient's wrist, with the dowel being placed right at the fracture site of the patient. The piece is then locked into place to prevent movement by using 2 small tripod clamps that slide onto the dowels until they reach the force application piece where they are then screwed into place. The wrist is then loaded by an air pumping system that slowly inflates a balloon which pushes a dowel onto the fracture site, displacing the bone a small amount. Figure 29 shows a diagram of our device with all the major components labeled.

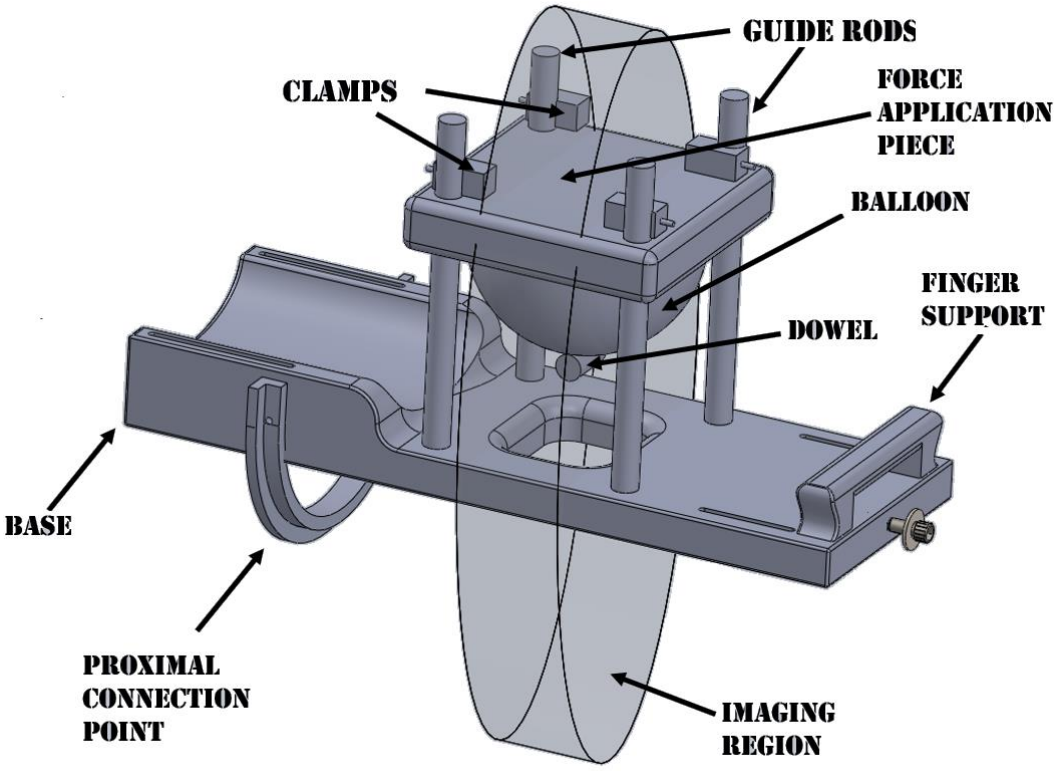


***Figure 30 – Labeled Device Draft***

**Base:** The base is where the arm rests. The base is flat towards the front where the hand but as it gets closer to the back where the forearm is placed the base curves upwards to provide comfort for the patient's arm. This forearm support is also covered in padding to keep for patient comfortable. Also included on the base is a clip on the front end of the device to clip into the CT scanner with ease. On the back end is a lip which allows the device to lock into the scanner to keep in place. In the middle of the base is the imaging center. This aids the doctor to have an idea of where the arm should be since this is the area where the imaging will take place. This hole also provides contact points to apply a three-point bend to the wrist. The base also has slits on both ends where cinch straps slide through to lock the patient's arm into place. We changed last year's design slightly to get a better image of the wrist by shortening the device one inch in the front from the end to the guide rods and adding one inch to the back from the guide rods to the back. By shifting everything forward an inch it allows the patient's wrist to be further in the scanner which gives the physician a larger range of the patient's arm.

**Finger support:** At the top end of the base is a small rod that helps restrict patient's fingers from hanging off the device. This keeps the procedure as repeatable as possible while also providing the patient with something to grip onto during the imaging procedure.

**Guide Rods:** Four 12mm inch plastic rods are fixed into the base and protrude upwards 7 inches. These rods are used to guide the force application system down onto the patient's arm. By taking out the screwing system from the last design, this creates a much larger radiolucent region which means more of the patient's wrist can be seen without obstruction. The guide rods were moved ¾ of an inch each way to increase the imaging region 1.5 inches. This gives the physician a larger view of the wrist.

**Force application system:** The force application system consists of three parts: The force applicator, the balloon, and the dowel. The force applicator is the piece that holds everything together. It has the balloon and the dowel attached to it. The applicator keeps the balloon and the dowel from being pushed upwards as the load is being applied. The balloon is the smaller version of a blood pressure pump balloon which was made to apply a load to a patient's wrist. By pumping up the balloon the applicator stays put so the balloon begins to push the dowel into the fracture site of the patient's wrist, causing a three-point bend. The dowel is the piece that applies the force onto the fracture site. It is a 12.5 mm Delrin dowel that is wrapped in neoprene for extra comfort. The dowel also has aluminum tape around it to see it in a CT scanner to aid the doctor in aligning the dowel with the fracture site. The dowel is attached to the balloon with a rubber casing that was made with silicone to attach the dowel to the balloon while also being flexible enough to bend as the balloon changes shape during inflation.

**Clamps:** Two quick release tripod clamps were used to hold the force application system in place. The clamps slide onto the rods and once in place screw on to tighten onto the rod well enough that when the balloon was inflated the force application system did not move.

## 6.2 Device Operation

Our force application device uses an air pump system to apply a force onto a patient's wrist. During a patient's biweekly check up to the doctor during healing time, the Doctors change the patient's cast. When the patient's cast has been removed this is when the Doctor can check healing quantifiably and determine if the patient has any healing defects. The patient places their fractured wrist onto the base of the device and grabs on to the finger rod. The doctor the slides the force application onto the patient's hand with the force piece aligning with the radius. Once the force piece is properly aligned with the fracture site, the doctor then locks the piece in place with the two clamps and straps the patient's arm into the device. The doctor then places their arm and the device into the CT and takes an initial scan. Once the initial scan is taken and the dowel is in the right place, the doctor then applies 100 mmHg of pressure (~23N) to the patient's wrist slowly. The pressure transducer will be providing a real-time reading of the pressure for the doctor to monitor. Once the gauge reads 100 mmHg the doctor then locks the load and takes a high-resolution scan of the patient's wrist. The scans are then exported, and the two scans are analyzed to detect the amount of displacement. Through three-point bend calculations, the doctor can then compare the measured displacement of the patient's bone to the predicted displacement of a bone with a specific stiffness of a distal radius callus at that point of healing. The doctor will then be able to determine if the patient's bone is healing as expected or if a healing delay is occurring.

## 6.3 Recommendations

We have four recommendations for future modifications and improvements for our project.

1. Make the clamps completely radiolucent: The metal screw in the clamp can be seen in the imaging area unless it is positioned a certain way. However, if the physician wants to scan a larger area of the wrist he/she can't unless the screws were radiolucent. To counteract this problem, we printed the device with the guide rods further apart, creating a 1.5-inch increase in space in the imaging area. This gives the physician the ability to see a larger area of the arm. If the metal screw was eliminated completely the whole device would be radiolucent and the physician would have no limits as to the area of the arm he/she could see due to the device.

2. Improve the balloon/device attachment method: Our team struggled to find an adhesive that was flexible to bend to fit the shape of the balloon as it inflated, while also creating a strong adhesive on both the 3D printed plastic and the plastic of the balloon. We ended up choosing the DOW CORNING 3145 Silicone RTV since it was the only adhesive we tried that allowed the balloon to fully inflate without falling off while also remaining flexible, however the bond between the Silicon and the force applicator was not as strong. It was strong enough for the balloon to stay on the device however it could easily be removed and peeled off. By finding an adhesive that bonds to both types of plastics but is also flexible will increase the durability of the device tremendously.

3. Finalize the calculations needed for healing bone: The three-point bend formula is:

F = (48*E*I*D)/(L^3)

Where F is force, E is stiffness, I am moment of inertia, D is displacement and L is length of support span. However, for a healing fracture, the Stiffness is changing as the soft callus changes to a hard callus which then changes to regular bone. Due to this constantly changing Stiffness, we recommend that research be found on stiffness at these different stages of healing to calculate predicted displacement.

4. Create a program in LabVIEW to have a more aesthetically pleasing visual for the real time pressure data: If there was a system where a physician can input the week of healing the patient is at and the program can automatically calculate the predicted displacement of the patient's bone. Also, if the system was programmed to analyze CT scans and automatically measure the displacement of the bone this would drastically decrease user error and bias. Having these major improvements would drastically increase the effectiveness of this device.

# Chapter 7: Discussion

## 7.1 Ethical Concerns

There are some ethical concerns that we dealt with throughout our project. The first concern was with cadaver testing. Though testing on humans is imperative to completely understand how new devices affect our bodies, there are many concerns in both religious and civilized society. Using cadavers in the research field has been debated as a breach of privacy and disrespectful to the deceased. To evade the ethical concerns during cadaver testing, we were sensitive and respectful during our procedures. Being professional during these tests was important in giving the donor the appreciation and respect they deserve. We also kept the identity of the donor anonymous to not risk breaching their privacy in any way.

Another ethical concern our device could have is the testing of our device on fractured wrists. We are unsure how much pain our device will cause to a patient with a fractured wrist during cast removal. Though we did not have the proper approval to test on people, we did obtain pain data for different pressure point pieces with our device by testing on ourselves. We were able to test the pain of our device with the person on our team with the lowest pain tolerance to have a better understanding of the pain a patient could endure. We also were sure to keep the pain threshold under five, and were able to obtain a pain threshold of two for our testing pressure, to make the patient as comfortable as possible.

## 7.2 Health and Safety Issues

There are a few health and safety issues we encountered during the course of our project. The first problem was with the potential damage to a patient's bone. If a bone is displaced too much (>2mm) the healing process can be damage. To make sure the bone was not damaged we pursued cadaver arm testing to test the effects and displacement the human bone underwent using our device. Our device aimed to displace a bone less than .75mm and the highest displacement it ever achieved was .56, proving that our device has minimal risk of injury. This test was done on adult bones, however, and should be tested on children bones as well, as children are also shown to frequently fracture their distal radius. Additional testing should also be done to further understand the amount of pain a patient with a fractured wrist would endure during testing.

Another safety concern was using cadaver arms during testing. Cadaver specimens can cause a moderate health hazard, making it biosafety level two material. We reduced risk and safely worked with cadaver arms by making sure the lab doors were shut while the specimen was exposed, worked with gloves and also bagged the specimen when not being prepped. We also did not have food or drink in the laboratory. We also properly cleaned the lab and disposed of all specimens in biohazard areas once testing was completed.

The last safety hazard we encountered was the exposure to radiation during testing. CT imaging causes exposure to radiation which can have harmful health effects. However, HR-pQCT emits a very low amount of radiation and only the patient being scanned would have potential radiation exposure. To counteract this for patients who will have to be close to the CT machine they will wear a radiation blocking vest to reduce the effects and minimize risk.

## 7.3 Economic Impact

This device can diagnose healing defects early on and overall reduce cast time. With the reduction of cast time come a decrease in patient visits. Casts are removed every 2 weeks to check on the fracture. Each visit costs the patient, so decreasing casting time and ultimately patient visits will decrease cost of treatment overall. Early diagnosis of fracture defects also improves patient outcomes and healing time. More accurate treatment plans decrease the cost to the patient as well.

Additionally, when finalized, this device could forever change the way the pharmaceutical industry researches drugs that impact bone health. By providing a method of quantifying how well a bone is healing, this device can serve as a framework for studies that will provide economic opportunity for companies that develop drugs that influence how bone heals.

The device was not expensive to manufacture as it was 3D printed with recycled plastic. It is valuable in the medical market to have devices that are inexpensive to manufacture and use. Although this device requires the use of an expensive high resolution CT machine, this device would be used in settings that already have a high resolution CT machine available. 3D printing of this device was relatively inexpensive and could be continued for small scale production. If this device is produced on a large scale, it would be financially beneficial to manufacture using fillable molds.

## 7.4 Environmental Impact

This device has an insignificant impact on the environment. The device was designed and 3D printed using recycled plastic. Using Recycled plastics allows for less negative impacts to the environment. Using recycled plastic not only gives meaning to already processed plastic, but also restricts the need for any new plastics to be made. All materials used on this project were disposed of using institutional protocol as to have minimal impact on the environment.

## 7.5 Societal Impact

There are many positive impacts as a result of this device. The first being ease of use. The device was modified to be as easy as possible while still functional. Easy and intuitive operation was essential when the device was being designed. It was also made to not be painful for the patient. Being easy to use and not painful improves the patient experience at the doctors overall. Many patients are hesitant to go to the doctors because of bad past experiences. If people are less hesitant about going to the doctors, they will go earlier on and early diagnosis will improve overall patient outcomes. This device also improves knowledge of bone density, and how callus strength changes through specific weeks of fracture healing. This has medical applications not only for our device but for the entire bone health industry. For example, if a pharmaceutical company wishes to develop a drug that will quicken the rate at which a bone heals, our device could be used in studies to quantifiably prove that their drug works. Bone health drugs have not been extensively researched because companies cannot quantify bone healing. Our device hopes to change that in the future.

## 7.6 Political Ramifications

Our device has little to no direct political ramifications. Politicians who push for better healthcare would be in favor of a device like this, which reduces health costs on average to patients. This device would first be manufactured and used in the United States. If clinical applications of this device go well in the US, it would be feasible to believe it would go into the global market.

## 7.7 Manufacturing and Sustainability

Additive manufacturing (3D printing) was selected as the most appropriate manufacturing method for this project. 3D printing allows for easier reproduction of the device due to the accessibility of CAD models. The CAD models can be seen featured throughout the paper, and can be easily reproduced using Solidworks. Injection molding was another manufacturing option that was considered when developing the proof-of-concept device, but it was ultimately decided against due to the fact that 3D printing has a quicker manufacturing time and lower production costs. The previous developers suggested that the finalized version of the device be manufactured using injection molding with carbon reinforcement, as it would offer a good balance between rigidity, material toughness and ease of processing. It would also remain relatively cost effective.

Furthermore, the sustainability of the device was evaluated by examining the material, financial, and usage considerations. The glass-fiber reinforced onyx that was used for the 3D printing is significantly better for the environment than many other petroleum-based plastics. The neoprene that was used is not the most environmentally friendly, so it may be better to look into other material alternatives in future iterations. The silicone adhesive and sealant that we used have minimal environmental impact, as they completely degrade and do not contribute to any greenhouse gases. Finally, the material and design considerations ensure that the device is safe for users and easy to use

# Chapter 8: Summary and Conclusion

Through final validation testing, it was found that the final device design can produce enough force to displace a human distal radius to create a micro strain. The final device also provides a real-time display of the pressure being applied. This can further be developed to find the extent of strength recovery in distal radius fractures. Validation testing proved that the new

force application process was able to apply enough force on the radius to create a three-point bend and to obtain a visible and safe displacement in the CT scanner. The new force applicator piece, the dowel, also proved was comfortable enough to not cause the patient serious pain while still applying enough pressure to produce a three-point bend. However, further clinical trials are needed to assess the amount of pain patients with Colles' fractures experience since our test subject had a healthy bone. Additionally, clinical trials need to be done to test the displacement on a currently healing bone that has a callus to test if displacement occurs when a load is applied.

Despite not being able to calculate the stiffness of a bone due to limitations in current available research, the device has much more room for advancement and was validated to prove that a fracture strength can indeed be quantified. Future steps for this device include the design changes such as further programming and automation for further ease of use a decrease in user error. A program that process images automatically would decrease user bias and increase the device efficiency by rapidly measuring the displacement of a patient's fracture. This would greatly reduce the time and labor required to analyze the CT images.

After these improvements and further validations testing are made, the device should move into the clinical trials stage. This will allow for testing on current patients with healing distal radius fractures in order to continue to validate the device and the strength recovery quantification process. After clinical trials and final validations, the device can move into hospitals and other medical centers to help quantify the strength of fracture healing and identify any possible healing defects. This can not only test other fracture site strengths throughout the body but can also provide insight to possible osteoporosis and bone strength decrease due to different drugs and medicine quantifiably rather than qualitatively through imaging.

# Appendix

## A. Summary of Spending

***Table 13 – Summary of Spending***

| Material | Cost |
|---|---|
| Smooth-On Silicone Mold Making, Liquid Rubber OOMOO 30, Easy to Use - Trial Size 2.8 lb | $23.90 |
| Sureflex Multi-Purpose Adhesive-29 ml | $8.91 |
| Loctite Marine Epoxy 0.85-Fluid Ounce Syringe (1405604) | $4.99 |
| It's Academic Premium Edition Super Stretch Book Cover: Black - Fits 10" X 15" Textbooks Guaranteed! | $4.40 |
| SmallRig Quick Release 12mm Rod Clamp Railblock for 12mm Rod System, Wingnut - 1403 | $7.96 |
| SmallRig Quick Release 12mm Rod Clamp Railblock for 12mm Rod System, Wingnut - 1403 | $20.00 |
| Eyourlife Universal 30PSI Pressure Transducer Sender Solenoid for Oil Fuel Gas Air Water G7 | $17.98 |
| Reusable Cinch Straps 1.5"x20" - 6 Pack - Hook and Loop Straps | $14.87 |
| Clay | $4.74 |
| Turkey Bones | $7.90 |
| Cinch Straps | $14.87 |
| Lab Notebook | 5.00 |
| Blood Pressure Pump | $19.11 |

| | |
|---|---|
| Wheatstone Bridge Phidget | $42.02 |
| Plexiglass Dowel | $12.37 |
| Loctite Clear Silicone Waterproof Sealant | $4.55 |
| Teflon Thread Tape | $2.56 |
| NEBEC Conference Registration | $320.00 |
| NEBEC Conference Travel/Stay | $497.49 |
| | |
| **Total** | **$1,033.62** |

## B. FujiFilm Procedure

**Purpose:** This test was to determine how the different force application pieces applied pressure relative to the distal radius and how concentrated the pressure was

1. Cut out 6 rectangles of Fuji Film (about 1 inch long and ½ inch thick) Shiny side to dull side to limit the amount of activation
2. Carefully put one rectangle dull side to dull side and gently tape to person's wrist where the force applicator will be applying pressure
3. Place the wrist with the Fuji film in the device and set up the device to apply a load
4. Inflate the balloon to 150 mmHg of pressure and then deflate
5. Carefully take wrist out of device and take the Fuji Film off wrist
6. Tape into lab notebook. Label which force applicator was used and where the radius and ulna were with respect to the film
7. Repeat with different force applicators (just the balloon, different sized dowels, a marble and the Legacy piece)

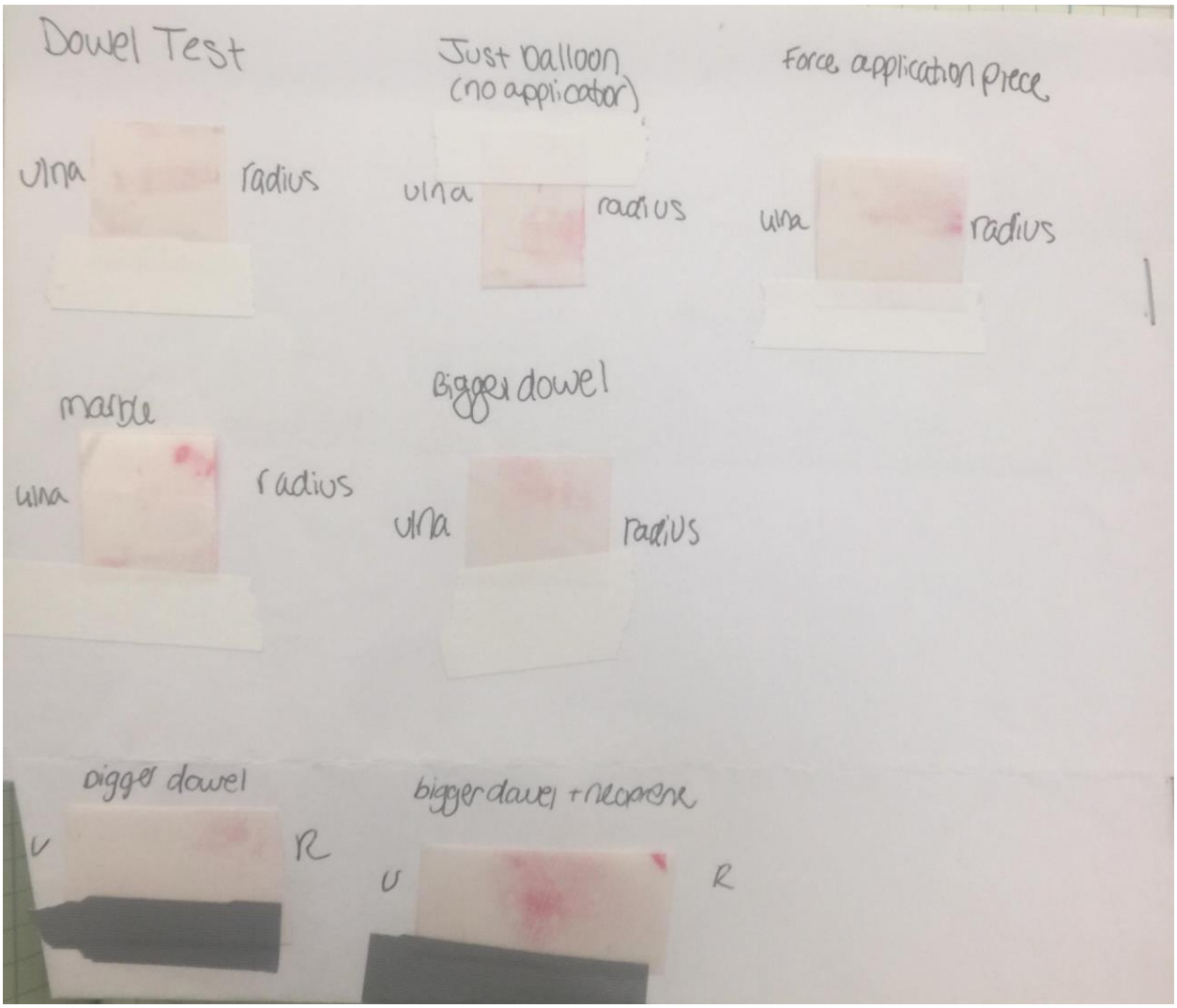


***Figure 31 – FujiFilm Results***

## C. Cadaver Arm Procedure:

**Purpose:** test feasibility of device on human wrists and to make sure the device can apply enough force to displace a fractured bone

1. Defrost cadaver arm until thawed
2. Place bagged cadaver arm into device and place into the CT scanner (unloaded)
3. Take a low resolution image of a the cadaver wrist to make sure the wrist and dowel are aligned
4. Once the wrist is in the right location, lock the wrist in place with the cinch straps and take a high resolution image of the wrist in the device unloaded

5. Apply a pressure of 100 mmHg (~23N) and lock the blood pressure pump to keep a constant load
6. Take a low resolution image to make sure the wrist did not shift when the dowel was applied
7. Once the wrist is in the right location, take a high resolution image
8. Bring the cadaver wrist to the specimen room to create a simulated fracture (~7mm cut)
9. Repeat steps 2-7 for each cut (7mm cut, 10mm cut and full fracture)
10. Export scans to be analyzed in Mimics

***Figure 32 – Cadaver Wrist Specimen Preparation***

## D. Mimics Analysis Procedure

**Purpose:** to analyze scans that were taken in regards to the displacement of the fracture after load

1. Open scans for unloaded and loaded wrist for one fracture (7mm cut)
2. Find the fracture site on the unloaded bone scan and rotate to find a good scan that can easily measure the fracture site

3. Locate any landmarks on the bone in order to find the same location in the loaded bone scan
4. Once you have both scans open measure both lengths of the fracture and record
5. Going across the fracture measure the width in 10 different places along the fracture line, record and take the average
6. Repeat for the loaded bone
7. Compare the difference in width averages in order to find the displacement
8. Repeat steps 1-7 for each fracture (7mm, 10mm and full cut)

## Mimics Analysis and Raw Data- Testing Round 2:

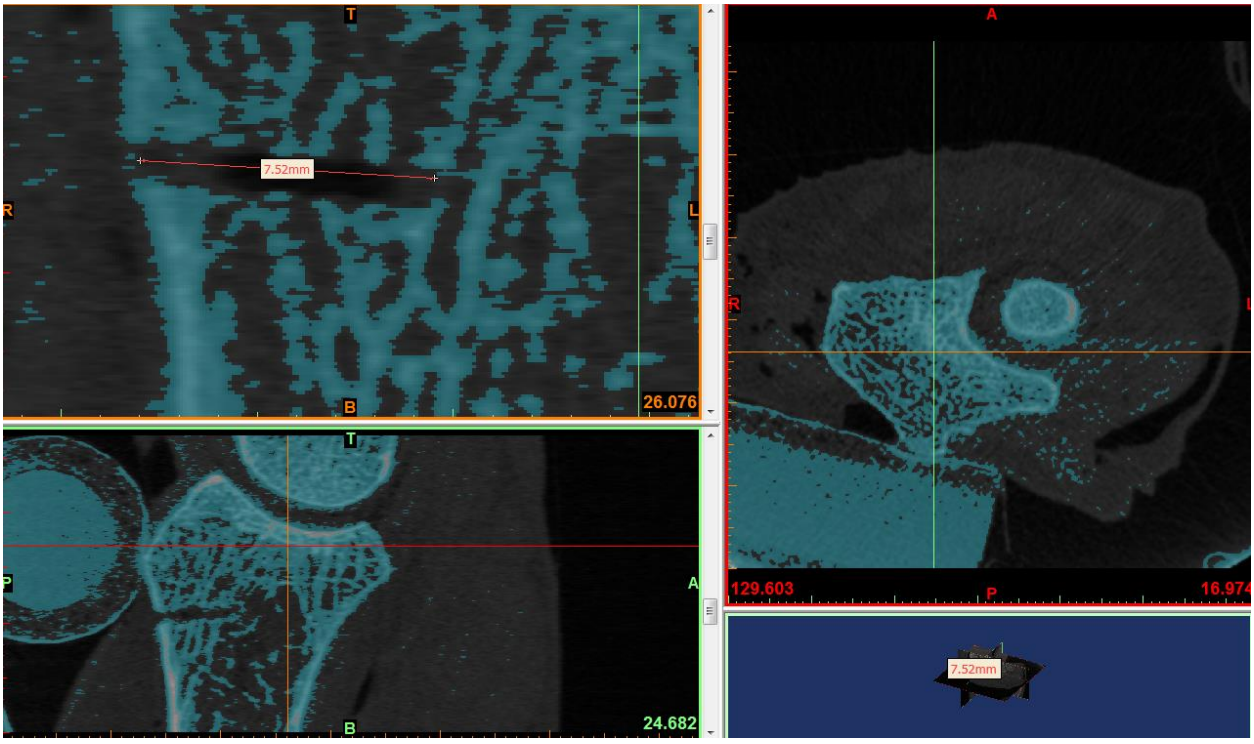


***Figure 33 – Length of 7mm Bone Unloaded***

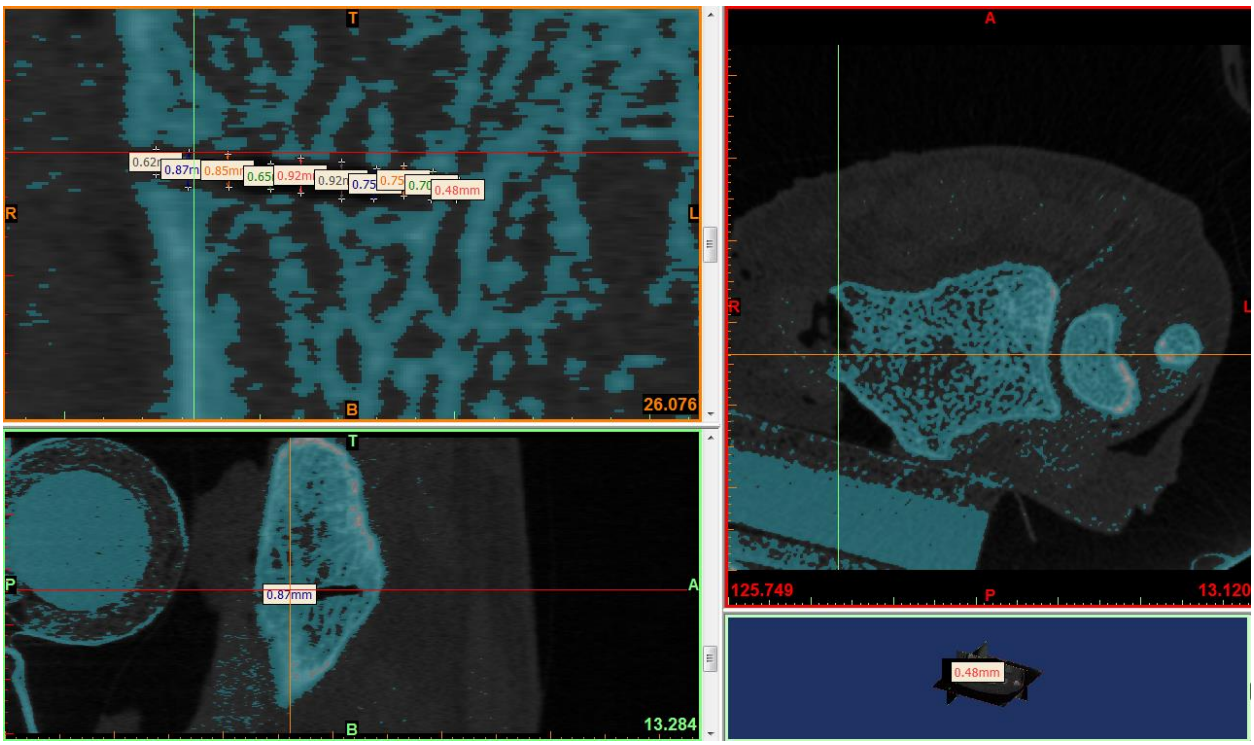


*Figure 34 – Displacement Measurements: 7mm Bone Unloaded*

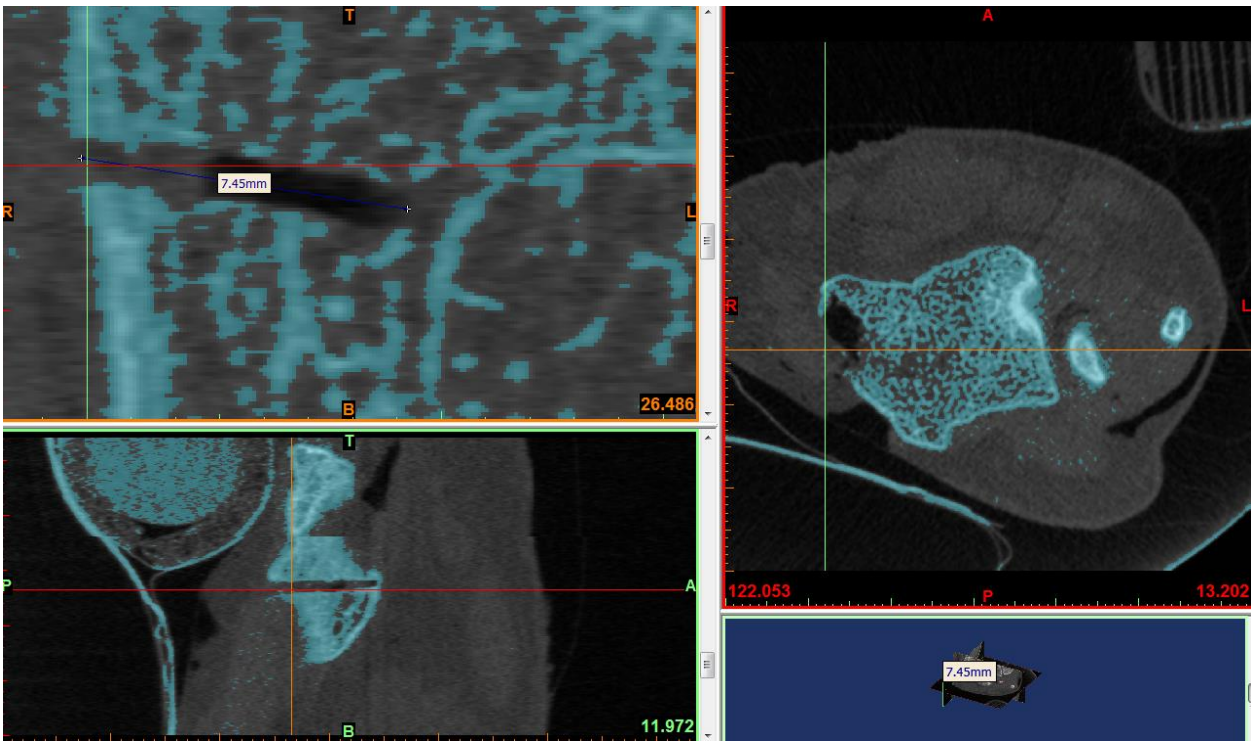


*Figure 35 – Length of 7mm Bone Loaded*

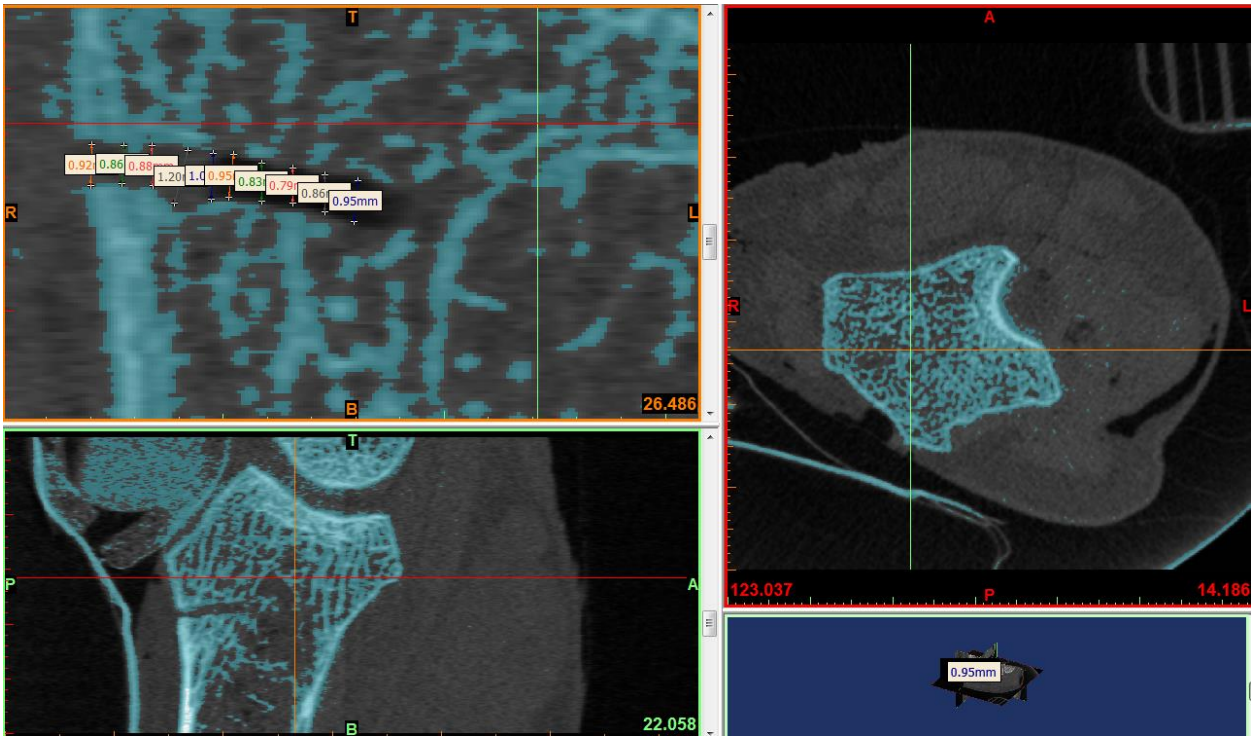


*Figure 36 – Displacement Measurements: 7mm Bone Loaded*

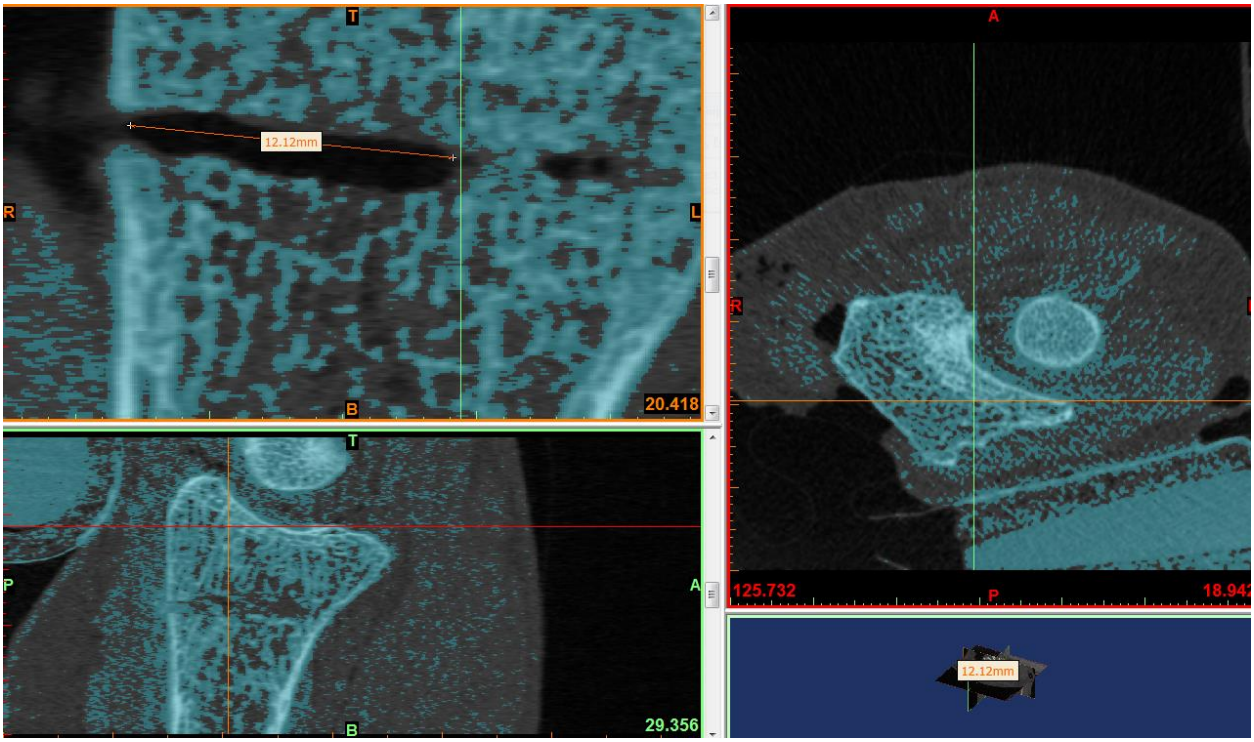


*Figure 37 – Length of 11m Bone Unloaded*

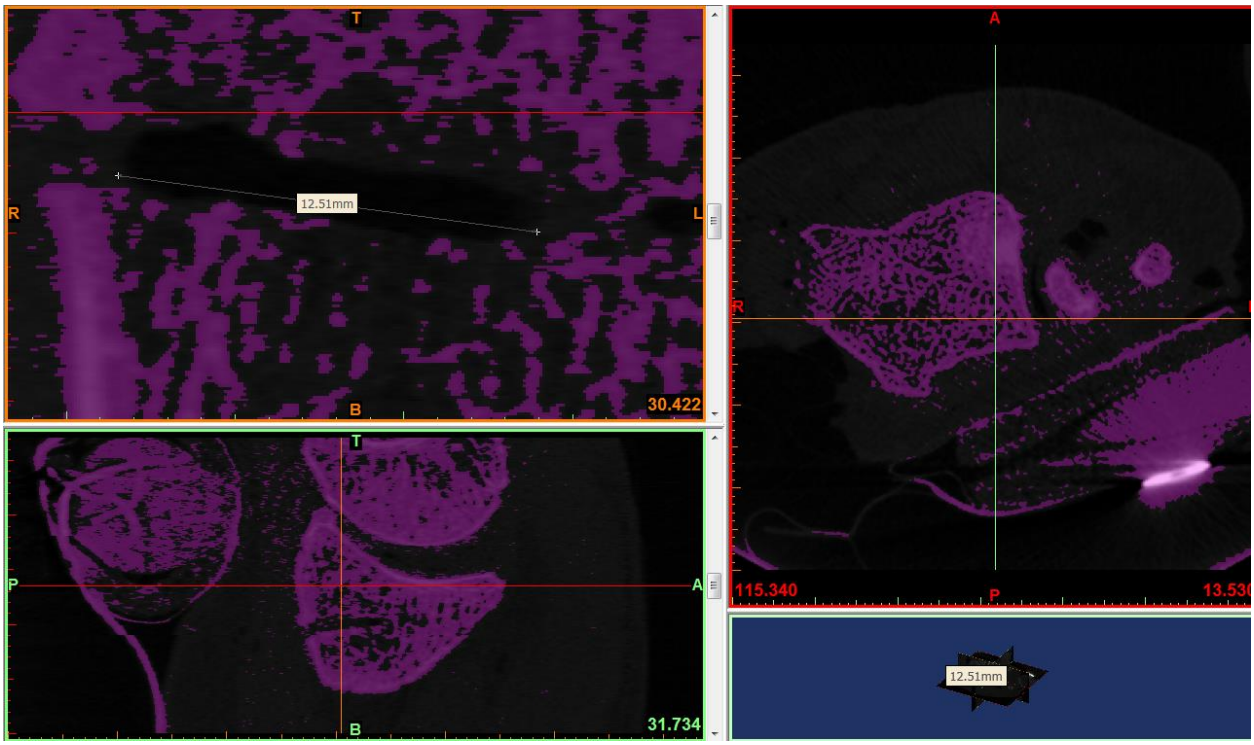


*Figure 38 – Length of 11m Bone Loaded*

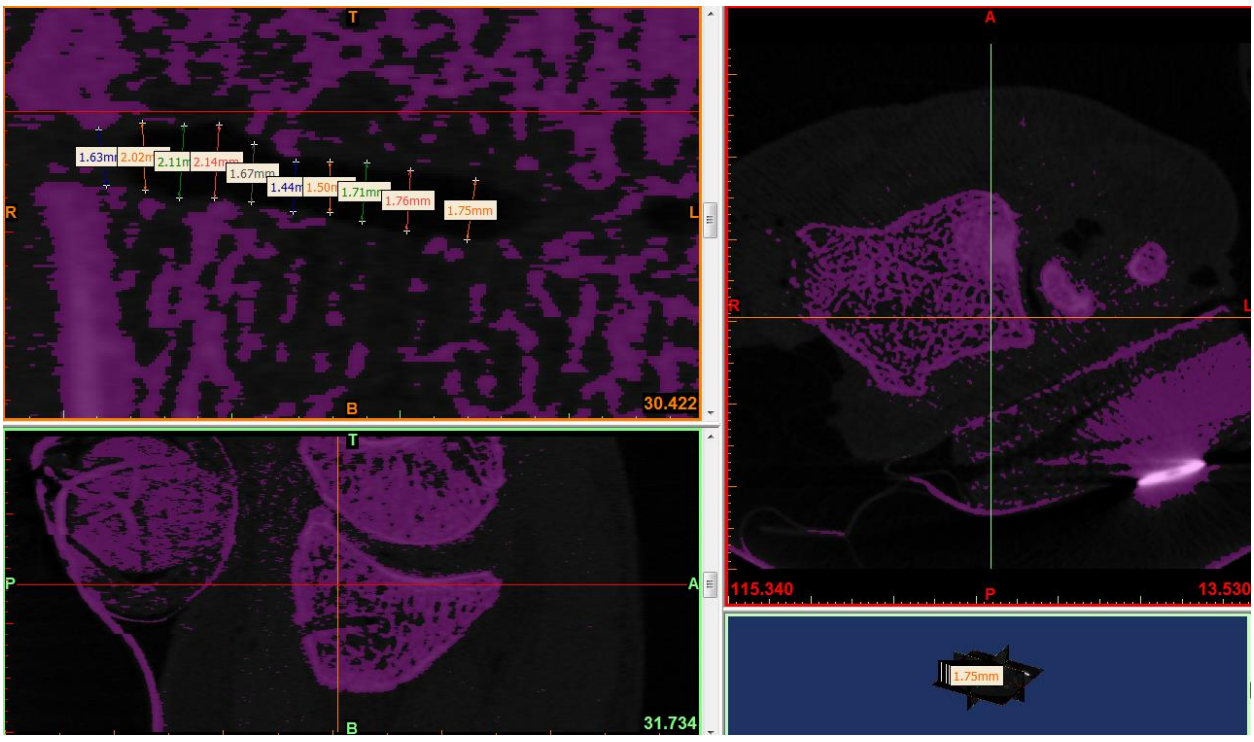


*Figure 39 – Displacement Measurements: 11mm Bone Loaded*

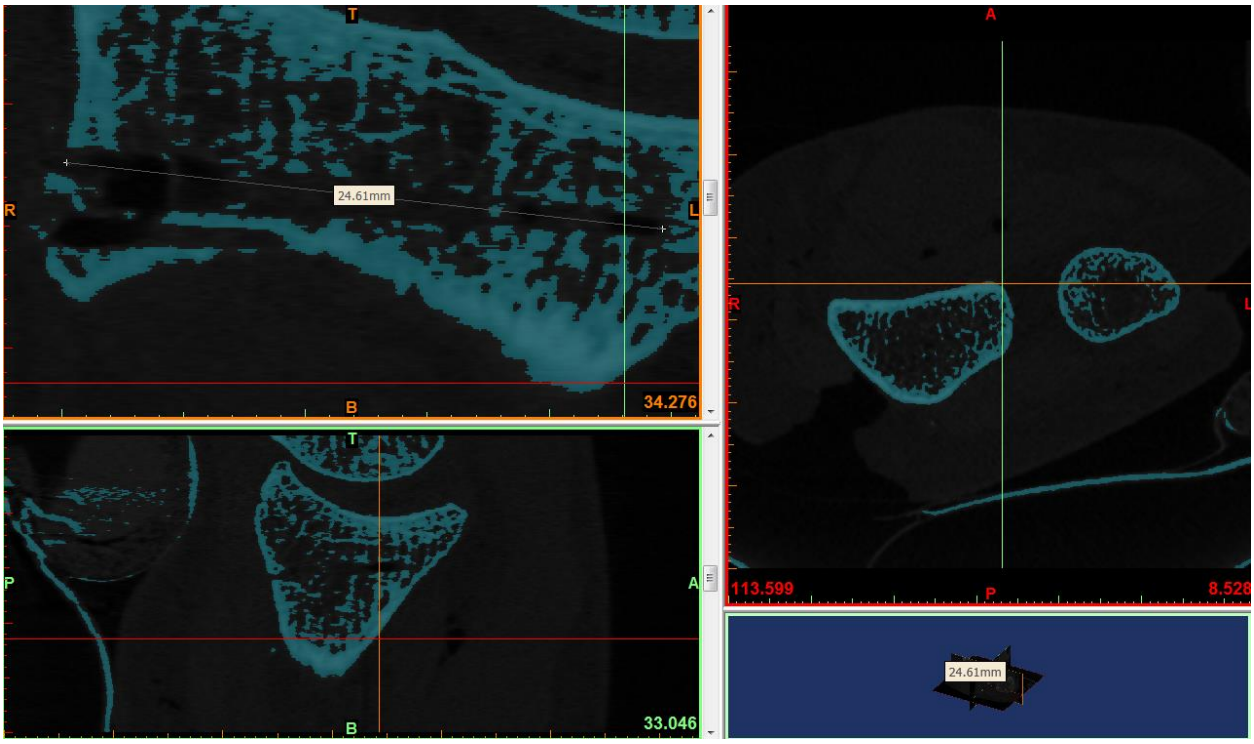


*Figure 40 – Length of Full Fracture Loaded*

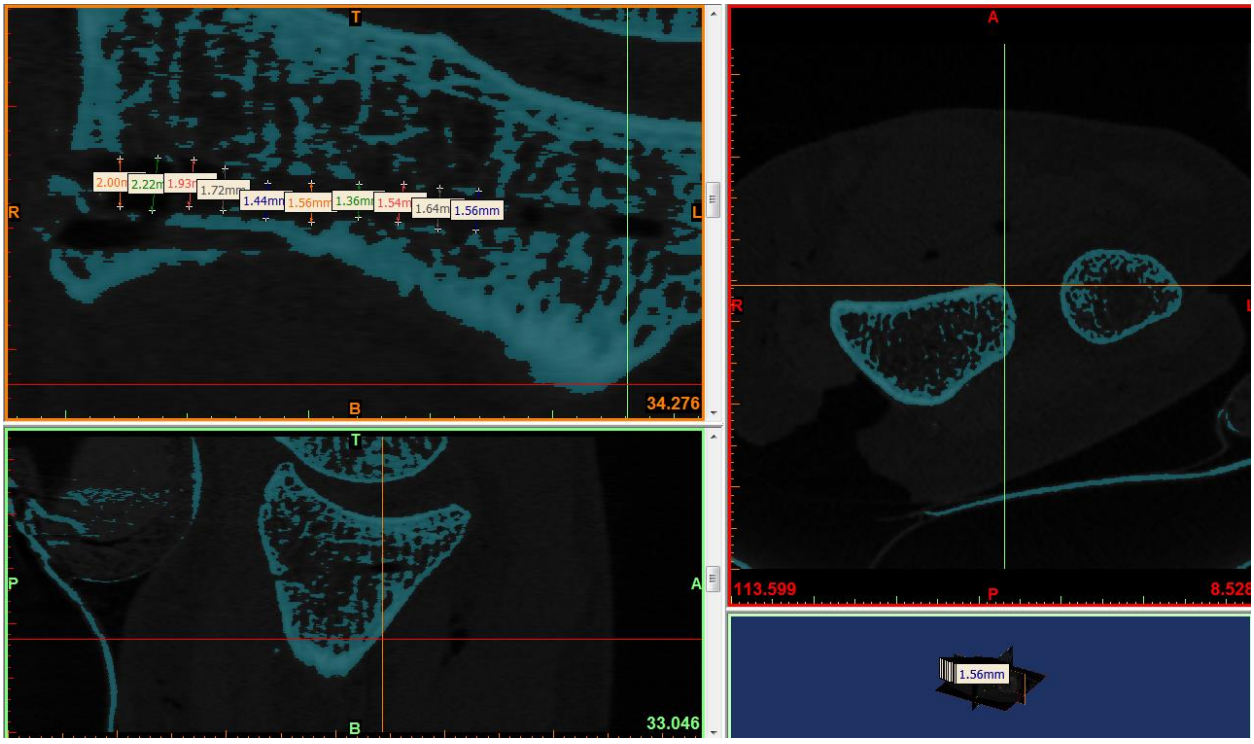


*Figure 41 – Displacement Measurements: Full Bone Fracture Loaded*

## E. Pain Test Procedure

**Purpose:** To identify which force application piece applies the most and least amount of pain to the patient's wrist

1. Have one person do all pain tests to decrease the amount of changing variables
2. Begin with just the balloon as the force application piece
3. Apply 50 mmHg of pressure, hold for 10 seconds and record pain rating in terms of the chart below

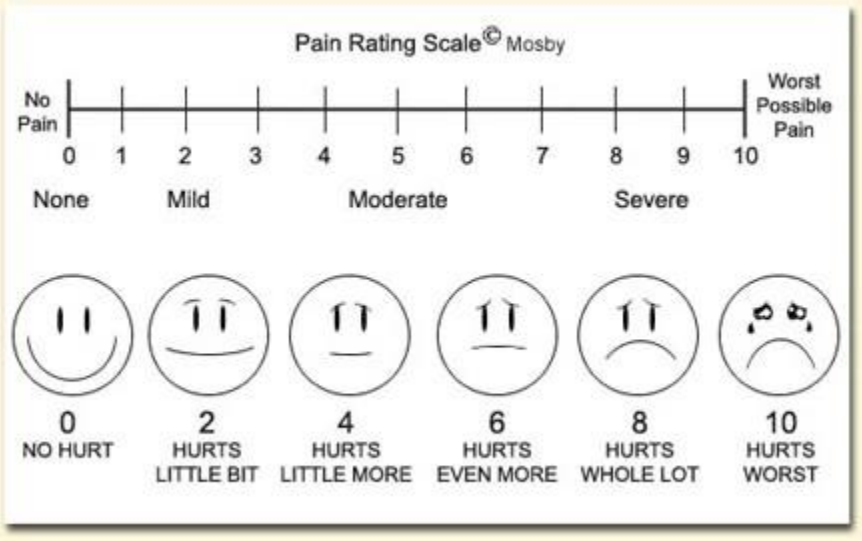


***Figure 42 – Pain Rating Scale***

4. Continue to apply 50 mmHg of pressure holding for 10 seconds and recording pain rating until the pressure is 300 mmHg
5. Repeat process for different force applications (balloon, different dowels, marble, legacy piece

## F. Instron Procedure

Purpose: To find the relationship between the pressure reading on the blood pressure pump and the force being applied, and to also see the difference in force with different application piece

1. Turn on the Instron and log into Bluehill

2. Place the force applicator piece and the balloon facing upwards so the compression piece and the balloon are touching each other
3. Begin inflating the balloon until the pressure reads 20 mmHg
4. Once it reaches 20mmHg take a record the force that is being displayed
5. Repeat this in intervals of 20 mmHg and record results
6. Repeat for each different application piece

***Table 14 – Marble Force Test***

| **Trial 1** | mmHg | Newtons | **Trial 2** | mmHg | Newtons | **Trial 3** | mmHg | Newtons | **Avg.** | mmHg | Newtons |
|---|---|---|---|---|---|---|---|---|---|---|---|
| | 20 | 4.58 | | 20 | 4.17 | | 20 | 4.98 | | 20 | 4.576666667 |
| | 40 | 8.6885 | | 40 | 8.201 | | 40 | 9.01 | | 40 | 8.633166667 |
| | 60 | 13.631 | | 60 | 12.983 | | 60 | 13.234 | | 60 | 13.28266667 |
| | 80 | 18.409 | | 80 | 18.001 | | 80 | 18.432 | | 80 | 18.28066667 |
| | 100 | 23.311 | | 100 | 22.965 | | 100 | 23.084 | | 100 | 23.12 |
| | 120 | 28.127 | | 120 | 28.321 | | 120 | 28.945 | | 120 | 28.46433333 |
| | 140 | 33.006 | | 140 | 33.291 | | 140 | 33.582 | | 140 | 33.293 |
| | 160 | 37.542 | | 160 | 37.111 | | 160 | 38.312 | | 160 | 37.655 |
| | 180 | 42.251 | | 180 | 42.981 | | 180 | 43.308 | | 180 | 42.84666667 |
| | 200 | 46.934 | | 200 | 47.003 | | 200 | 48.134 | | 200 | 47.357 |
| | 220 | 51.563 | | 220 | 52.213 | | 220 | 53.764 | | 220 | 52.51333333 |
| | 240 | 55.874 | | 240 | 56.01 | | 240 | 57.981 | | 240 | 56.62166667 |
| | 260 | 60.556 | | 260 | 61.234 | | 260 | 62.329 | | 260 | 61.373 |
| | 280 | 64.856 | | 280 | 65.871 | | 280 | 66.1 | | 280 | 65.609 |
| | 300 | 69.322 | | 300 | 70.009 | | 300 | 70.991 | | 300 | 70.10733333 |

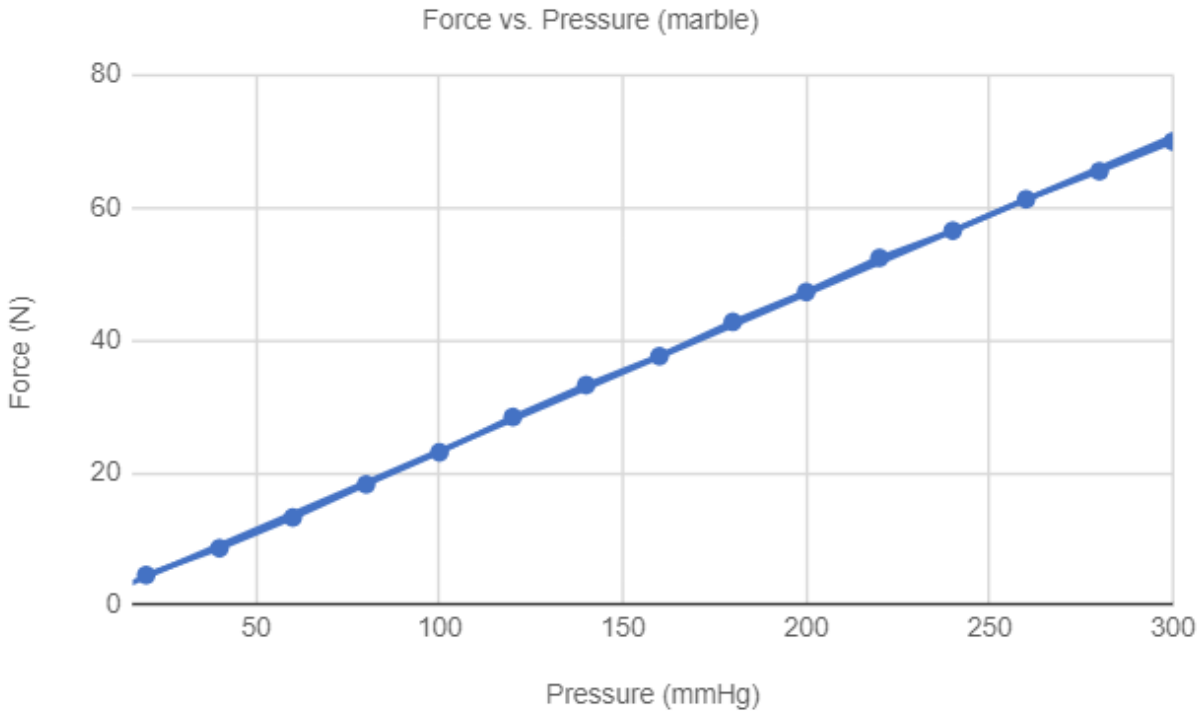


***Figure 43 – Marble Force Test Graph***

***Table 15 – Balloon Force Test***

| **Trial 1** | mmHg | Newtons | **Trial 2** | mmHg | Newtons | **Trial 3** | mmHg | Newtons | | **Avg.** | mmHg | Newtons |
|---|---|---|---|---|---|---|---|---|---|---|---|---|
| | 20 | 5.3235 | | 20 | 5.1962 | | 20 | 3.1674 | | | 20 | 4.562366667 |
| | 40 | 9.6135 | | 40 | 9.2235 | | 40 | 9.116 | | | 40 | 9.317666667 |
| | 60 | 14.501 | | 60 | 14.12 | | 60 | 13.793 | | | 60 | 14.138 |
| | 80 | 19.21 | | 80 | 19.241 | | 80 | 18.436 | | | 80 | 18.96233333 |
| | 100 | 23.903 | | 100 | 23.787 | | 100 | 23.389 | | | 100 | 23.693 |
| | 120 | 28.902 | | 120 | 28.763 | | 120 | 28.278 | | | 120 | 28.64766667 |
| | 140 | 33.753 | | 140 | 33.483 | | 140 | 33.168 | | | 140 | 33.468 |
| | 160 | 38.773 | | 160 | 38.728 | | 160 | 38.054 | | | 160 | 38.51833333 |
| | 180 | 43.368 | | 180 | 42.932 | | 180 | 42.337 | | | 180 | 42.879 |
| | 200 | 48.312 | | 200 | 47.695 | | 200 | 47.358 | | | 200 | 47.78833333 |
| | 220 | 52.885 | | 220 | 52.668 | | 220 | 52.008 | | | 220 | 52.52033333 |
| | 240 | 57.619 | | 240 | 57.476 | | 240 | 56.826 | | | 240 | 57.307 |
| | 260 | 62.552 | | 260 | 62.295 | | 260 | 61.841 | | | 260 | 62.22933333 |
| | 280 | 67.174 | | 280 | 66.939 | | 280 | 66.723 | | | 280 | 66.94533333 |
| | 300 | 71.751 | | 300 | 71.744 | | 300 | 71.209 | | | 300 | 71.568 |

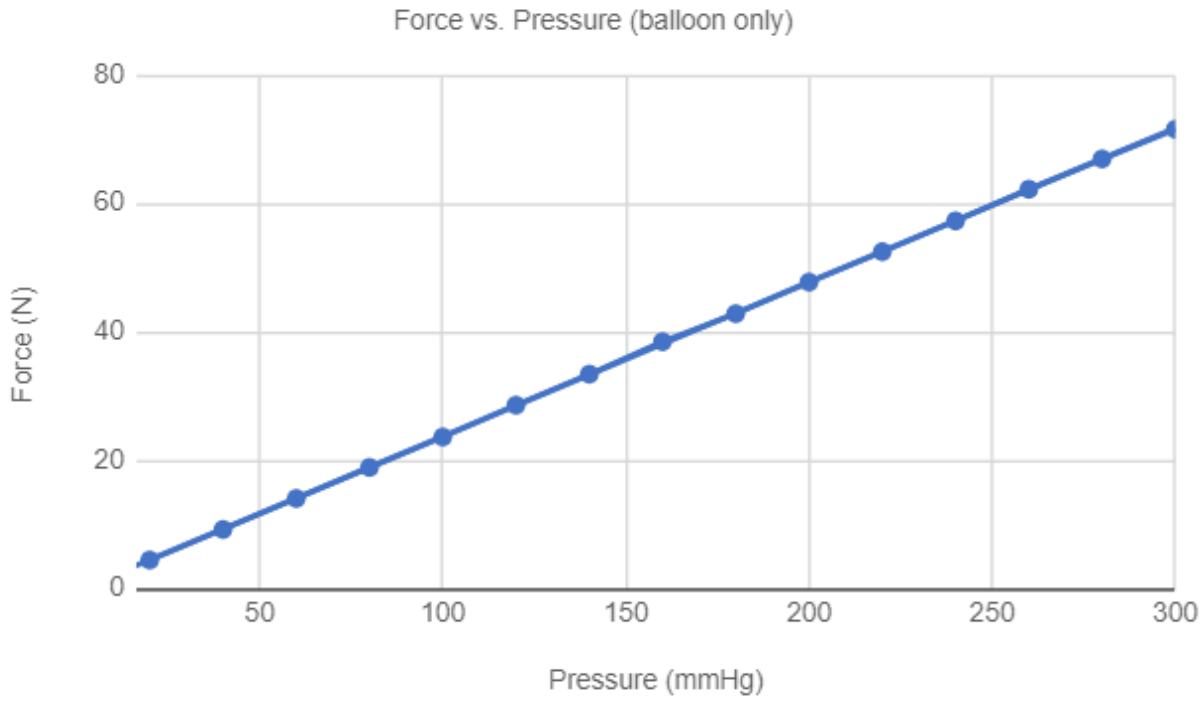


***Figure 44 – Balloon Force Test Graph***

***Table 16 – 6mm Dowel Force Test***

| **Trial 1** | mmHg | Newtons | **Trial 2** | mmHg | Newtons | **Trial 3** | mmHg | Newtons | **Avg.** | mmHg | Newtons |
|---|---|---|---|---|---|---|---|---|---|---|---|
| | 20 | 2.7984 | | 20 | 4.4236 | | 20 | 3.4629 | | 20 | 3.561633333 |
| | 40 | 7.7267 | | 40 | 9.3409 | | 40 | 8.6932 | | 40 | 8.586933333 |
| | 60 | 13.223 | | 60 | 16.195 | | 60 | 14.34 | | 60 | 14.586 |
| | 80 | 18.663 | | 80 | 21.779 | | 80 | 19.775 | | 80 | 20.07233333 |
| | 100 | 23.76 | | 100 | 27.004 | | 100 | 25.003 | | 100 | 25.25566667 |
| | 120 | 28.736 | | 120 | 32.591 | | 120 | 30.292 | | 120 | 30.53966667 |
| | 140 | 33.816 | | 140 | 37.716 | | 140 | 34.944 | | 140 | 35.492 |
| | 160 | 38.474 | | 160 | 42.738 | | 160 | 39.909 | | 160 | 40.37366667 |
| | 180 | 43.608 | | 180 | 48.11 | | 180 | 44.467 | | 180 | 45.395 |
| | 200 | 48.418 | | 200 | 53.411 | | 200 | 49.607 | | 200 | 50.47866667 |
| | 220 | 53.411 | | 220 | 58.103 | | 220 | 54.14 | | 220 | 55.218 |
| | 240 | 57.916 | | 240 | 63.336 | | 240 | 58.756 | | 240 | 60.00266667 |
| | 260 | 62.645 | | 260 | 68.521 | | 260 | 63.59 | | 260 | 64.91866667 |
| | 280 | 67.241 | | 280 | 73.27 | | 280 | 67.767 | | 280 | 69.426 |
| | 300 | 71.883 | | 300 | 77.964 | | 300 | 71.286 | | 300 | 73.711 |

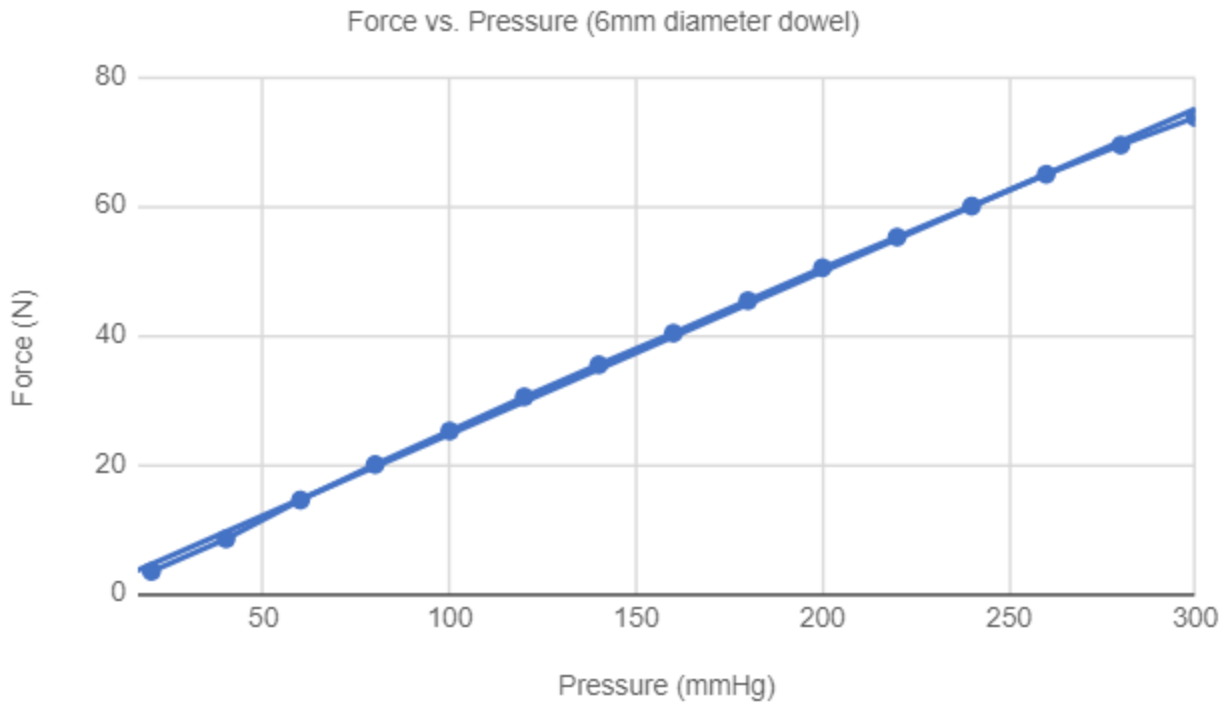


***Figure 45 – 6mm Dowel Force Test Graph***

***Table 17 – 12.5mm Dowel Force Test***

| **Trial 1** | mmHg | Newtons | **Trial 2** | mmHg | Newtons | **Trial 3** | mmHg | Newtons | **Avg.** | mmHg | Newtons |
|---|---|---|---|---|---|---|---|---|---|---|---|
| | 20 | 4.2659 | | 20 | 3.3748 | | 20 | 3.889 | | 20 | 3.843233333 |
| | 40 | 9.9477 | | 40 | 8.7421 | | 40 | 8.6822 | | 40 | 9.124 |
| | 60 | 14.262 | | 60 | 13.988 | | 60 | 13.626 | | 60 | 13.95866667 |
| | 80 | 19.55 | | 80 | 19.339 | | 80 | 18.308 | | 80 | 19.06566667 |
| | 100 | 24.544 | | 100 | 24.4 | | 100 | 23.867 | | 100 | 24.27033333 |
| | 120 | 29.566 | | 120 | 29.746 | | 120 | 28.513 | | 120 | 29.275 |
| | 140 | 34.595 | | 140 | 34.323 | | 140 | 33.518 | | 140 | 34.14533333 |
| | 160 | 39.217 | | 160 | 39.047 | | 160 | 38.471 | | 160 | 38.91166667 |
| | 180 | 44.446 | | 180 | 43.956 | | 180 | 43.456 | | 180 | 43.95266667 |
| | 200 | 49.005 | | 200 | 48.922 | | 200 | 48.083 | | 200 | 48.67 |
| | 220 | 53.706 | | 220 | 53.764 | | 220 | 52.846 | | 220 | 53.43866667 |
| | 240 | 58.65 | | 240 | 58.372 | | 240 | 57.316 | | 240 | 58.11266667 |
| | 260 | 63.589 | | 260 | 62.834 | | 260 | 62.177 | | 260 | 62.86666667 |
| | 280 | 67.838 | | 280 | 67.683 | | 280 | 66.587 | | 280 | 67.36933333 |
| | 300 | 72.52 | | 300 | 71.887 | | 300 | 71.388 | | 300 | 71.93166667 |

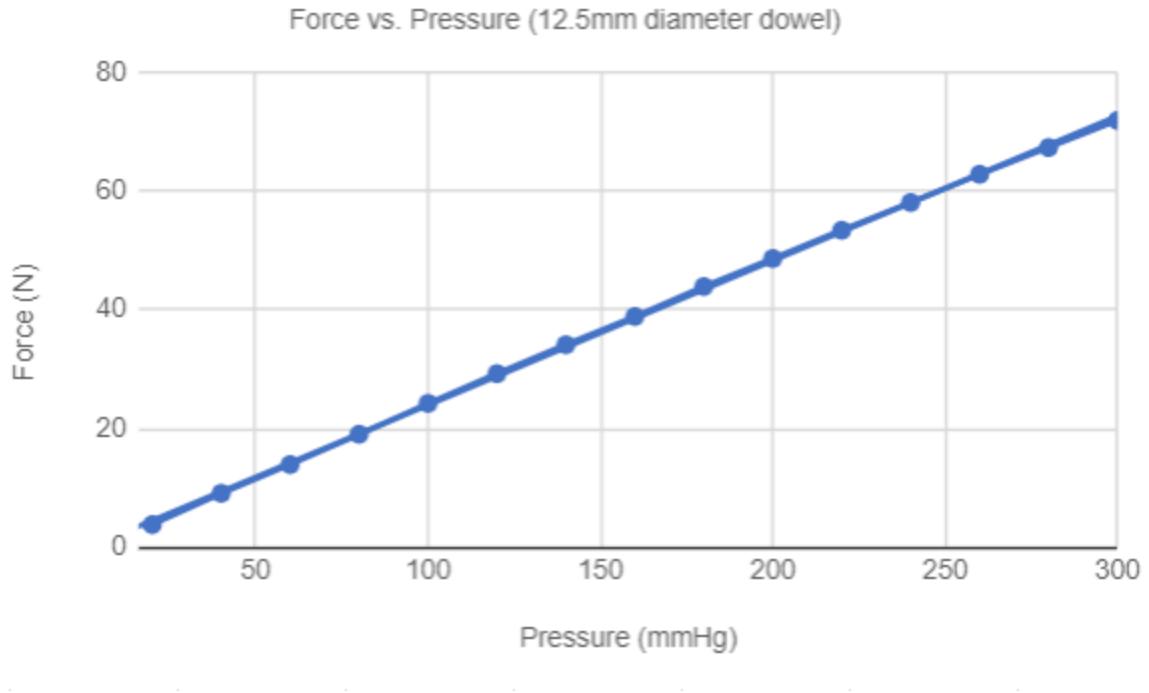


***Figure 46 – 12.5mm Dowel Force Test Graph***

***Table 18 – 12.5mm Neoprene Wrapped Dowel Force Test***

| **Trial 1** | mmHg | Newtons | **Trial 2** | mmHg | Newtons | **Trial 3** | mmHg | Newtons | **Avg.** | mmHg | Newtons |
|---|---|---|---|---|---|---|---|---|---|---|---|
| | 20 | 3.80 | | 20 | 3.5 | | 20 | 3.593 | | 20 | 3.63 |
| | 40 | 8.20 | | 40 | 7.598 | | 40 | 7.824 | | 40 | 7.87 |
| | 60 | 13.16 | | 60 | 13.26 | | 60 | 12.82 | | 60 | 13.08 |
| | 80 | 18.39 | | 80 | 17.97 | | 80 | 18.05 | | 80 | 18.14 |
| | 100 | 23.38 | | 100 | 23.48 | | 100 | 23.11 | | 100 | 23.32 |
| | 120 | 28.18 | | 120 | 28.56 | | 120 | 28.07 | | 120 | 28.27 |
| | 140 | 33.38 | | 140 | 32.92 | | 140 | 32.45 | | 140 | 32.92 |
| | 160 | 38.48 | | 160 | 37.84 | | 160 | 37.54 | | 160 | 37.95 |
| | 180 | 43.43 | | 180 | 42.49 | | 180 | 42.37 | | 180 | 42.76 |
| | 200 | 48.39 | | 200 | 47.17 | | 200 | 46.93 | | 200 | 47.50 |
| | 220 | 53.03 | | 220 | 51.58 | | 220 | 52.09 | | 220 | 52.23 |
| | 240 | 57.35 | | 240 | 56.42 | | 240 | 56.44 | | 240 | 56.74 |
| | 260 | 61.90 | | 260 | 61.36 | | 260 | 61.15 | | 260 | 61.47 |
| | 280 | 66.48 | | 280 | 65.25 | | 280 | 65.46 | | 280 | 65.73 |
| | 300 | 71.18 | | 300 | 70.29 | | 300 | 70.49 | | 300 | 70.65 |

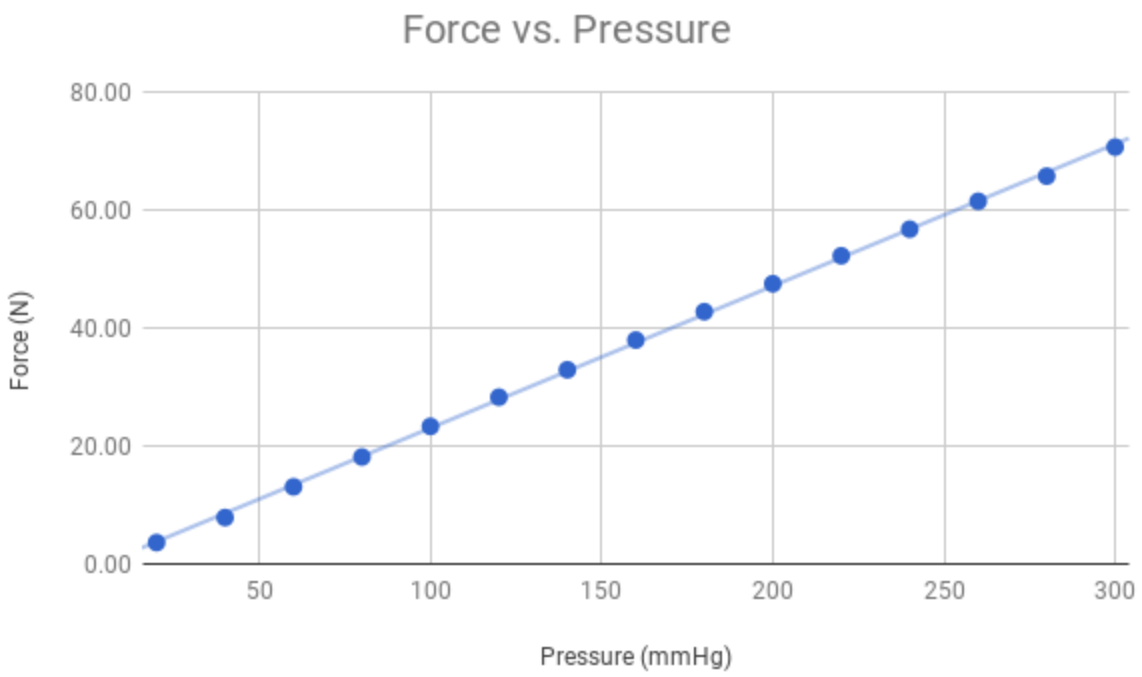


***Figure 475 – 12.5mm Neoprene Wrapped Dowel Force Test Graph***

***Table 19 – Legacy Piece Force Test***

| **Trial 1** | mmHg | Newtons | **Trial 2** | mmHg | Newtons | **Trial 3** | mmHg | Newtons | **Avg.** | mmHg | Newtons |
|---|---|---|---|---|---|---|---|---|---|---|---|
| | 20 | 6.0473 | | 20 | 5.4387 | | 20 | 4.9822 | | 20 | 5.4894 |
| | 40 | 10.372 | | 40 | 9.9518 | | 40 | 9.9122 | | 40 | 10.07866667 |
| | 60 | 15.153 | | 60 | 15.954 | | 60 | 15.647 | | 60 | 15.58466667 |
| | 80 | 20.953 | | 80 | 21.195 | | 80 | 21.272 | | 80 | 21.14 |
| | 100 | 26.265 | | 100 | 26.99 | | 100 | 26.162 | | 100 | 26.47233333 |
| | 120 | 31.184 | | 120 | 32.217 | | 120 | 31.658 | | 120 | 31.68633333 |
| | 140 | 36.528 | | 140 | 37.557 | | 140 | 36.848 | | 140 | 36.97766667 |
| | 160 | 41.824 | | 160 | 42.949 | | 160 | 42.683 | | 160 | 42.48533333 |
| | 180 | 46.365 | | 180 | 48.137 | | 180 | 47.029 | | 180 | 47.177 |
| | 200 | 52.099 | | 200 | 53.417 | | 200 | 51.667 | | 200 | 52.39433333 |
| | 220 | 57.106 | | 220 | 58.191 | | 220 | 56.156 | | 220 | 57.151 |
| | 240 | 61.968 | | 240 | 62.787 | | 240 | 59.973 | | 240 | 61.576 |
| | 260 | 67.383 | | 260 | 67.935 | | 260 | 64.046 | | 260 | 66.45466667 |
| | 280 | 72.505 | | 280 | 72.592 | | 280 | 67.356 | | 280 | 70.81766667 |
| | 300 | 77.171 | | 300 | 76.958 | | 300 | 72.449 | | 300 | 75.526 |

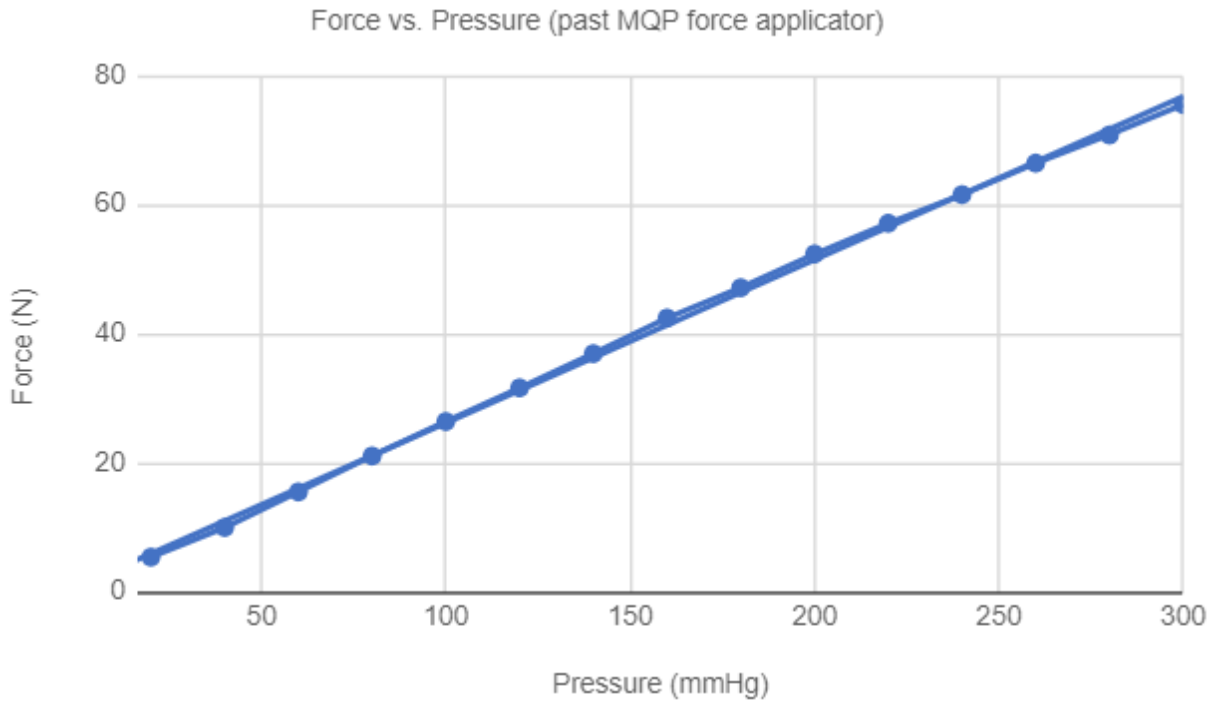


***Figure 48 – Legacy Piece Force Test Graph***

## G. Pressure to Force Conversion – Neoprene Covered Dowel

***Table 20 – Balloon Pressure to Force (Newtons) Conversion***

| mmHg | Newtons |
|---|---|
| 0 | 0 |
| 20 | 3.63 |
| 40 | 7.87 |
| 60 | 13.08 |
| 80 | 18.14 |
| 100 | 23.32 |
| 120 | 28.27 |
| 140 | 32.92 |
| 160 | 37.95 |
| 180 | 42.76 |
| 200 | 47.5 |

| | |
|---|---|
| 220 | 52.23 |
| 240 | 56.74 |
| 260 | 61.47 |
| 280 | 65.73 |
| 300 | 70.65 |

## H. Arduino Code

```
void setup() {
    Serial.begin(9600);
}

void loop(){
int sensorVal=analogRead(A1);
Serial.print("Sensor Value: ");
Serial.print(sensorVal );

  float pressure_pascal = (2.1167*((float)sensorVal)-174.52);
  float pressure_mmHg = pressure_pascal;
    Serial.print(" Pressure = ");
    Serial.print(pressure_mmHg);
    Serial.println(" mmHg");

  float force_newton = (0.2434*((float)pressure_mmHg)-0.3449);
    Serial.print("Force = ");
    Serial.print(force_newton);
    Serial.println(" N");

    delay(100);
}
```

***Figure 49 – Arduino Code***

# References

Bosisio, M., Talmant, M., Skalli, W., Laugier, P., & Mitton, D. (2007). Apparent Youngs modulus of human radius using inverse finite-element method. Journal of Biomechanics, 40(9), 2022-2028. doi:10.1016/j.jbiomech.2006.09.018

Cho, S. H., Sung, Y. M., & Kim, M. S. (2012). Missed rib fractures on evaluation of initial chest CT for trauma patients: pattern analysis and diagnostic value of coronal multiplanar reconstruction images with multidetector row CT. The British Journal of Radiology, 85(1018), e845–e850. http://doi.org/10.1259/bjr/28575455

Claes, L. E., & Cunningham, J. L. (2009). Monitoring the Mechanical Properties of Healing Bone. Clinical Orthopaedics and Related Research, 467(8), 1964–1971. http://doi.org/10.1007/s11999-009-0752-7

Emilio, M. D. (2013). Data acquisition systems: from fundamentals to applied design. New York: Springer.

CFR - Code of Federal Regulations Title 21. (n.d.). Retrieved October 02, 2017, from https://www.accessdata.fda.gov/scripts/cdrh/cfdocs/cfcfr/CFRSearch.cfm?CFRPart=888&showFR=1&subpartNode=21%3A8.0.1.1.31.1

Golden, Jennifer, Ahmed Hakim, Hannah Sattler Golden, J., Hakim, A., Sattler, H. (2017). Design of a Non-Invasive Device to Measure Bone Strength Recovery of Distal Radius Fractures for Use with HR-pQCTImaging (Undergraduate Major Qualifying Project No. E-project-042617-233014). Retrieved from Worcester Polytechnic Institute Electronic Projects Collection: https://web.wpi.edu/Pubs/E-project/Available/E-project-042617-233014/

Hosseini, H. S., Dünki, A., Fabech, J., Stauber, M., Vilayphiou, N., Pahr, D., . . . Zysset, P. K. (2017). Fast estimation of Colles fracture load of the distal section of the radius by homogenized finite element analysis based on HR-pQCT. Bone, 97, 65-75. doi:10.1016/j.bone.2017.01.003

Labarbera, J. (1999). U.S. Patent No. 5991651. Washington, DC: U.S.

Littlewood, R. (n.d.). The Benefits and Risks of The Ilizarov Technique For Limb

Reconstruction. Retrieved April 25, 2018.

Liverneaux, P. A. (2017). The minimally invasive approach for distal radius fractures and malunions. Journal of Hand Surgery (European Volume), doi:10.1177/1753193417745259

Lowth, D. M. (2014, December 05). Complications from Fractures. Information and treatment. Retrieved from https://patient.info/doctor/complications-from-fractures

Meena, S., Sharma, P., Sambharia, A. K., & Dawar, A. (2014). Fractures of Distal Radius: An Overview. Journal of Family Medicine and Primary Care, 3(4), 325–332. http://doi.org/10.4103/2249-4863.148101

Metz, V., & Gilula, L. (1993). Imaging techniques for distal radius fractures and related injuries. The Orthopedic clinics of North America, 24(2), 217-228.

Mills, L. A., & Simpson, A. H. R. W. (2013). The relative incidence of fracture non-union in the Scottish population (5.17 million): a 5-year epidemiological study. BMJ Open, 3(2), e002276. http://doi.org/10.1136/bmjopen-2012-002276

Morshed, Saam. (2014). Current Options for Determining Fracture Union. Advances in Medicine, vol. 2014, Article ID 708574, 12 pages, 2014. doi:10.1155/2014/708574

National Instruments (2017). What Is Data Acquisition? Retrieved September 19 , 2017, from http://www.ni.com/data-acquisition/what-is/

Nellans, K. W., Kowalski, E., & Chung, K. C. (2012). The Epidemiology of Distal Radius Fractures. Hand Clinics, 28(2), 113–125. http://doi.org/10.1016/j.hcl.2012.02.001

Ningbo Yu, Hollnagel, C., Blickenstorfer, A., Kollias, S. and Riener, R. (2008). Comparison of MRI-Compatible Mechatronic Systems With Hydrodynamic and Pneumatic Actuation. IEEE/ASME Transactions on Mechatronics, 13(3), pp.268-277.

Noonan, K. J., & Price, C. T. (1998). Forearm and distal radius fractures in children. Journal of the American Academy of Orthopaedic Surgeons, 6(3), 146-156.

Nunamake, D. . CHAPTER 38 DELAYED UNION, NONUNION, AND MALUNION. Retrieved from http://cal.vet.upenn.edu/projects/saortho/chapter_38/38mast.htm

Payne, D. J. Wrist Fractures. Distal radius, ulna and carpal Fractures. Retrieved

September 17, 2017, from https://patient.info/doctor/wrist-fractures

Poruthur, J. (1999). Three Point Bending of Chicken Bones. Retrieved from http://www.oocities.org/watrlilies/Professional/BEW6E7.pdf

Prommersberger, K., & Fernandez, D. L. (2004). Nonunion of Distal Radius Fractures. Clinical Orthopaedics and Related Research, 419, 51-56. doi:10.1097/00003086-200402000-00009

Real time Vital Signs Monitoring Using NI LabVIEW. (2013, September 24). Retrieved October 02, 2017, from https://talha09bm04.wordpress.com/2013/01/12/real-time-vital-signs-monitorong-using-ni-labview/

Takishi, O. (2014). Analysis of the Arthroscopically Diagnosed Soft-Tissue Injuries Associated With the Distal Radius Fractures. Macedonian Journal of Medical Sciences, 7(2). doi:10.3889/mjms.1857.5773.2014.0415

Wolfe, S. W. (2009). Distal Radius Fractures of the Wrist: Avoiding Complications with Proper Diagnosis and Treatment. Retrieved from https://www.hss.edu/conditions_distal-radius-fractures-of-the-wrist.asp

Zhou, B. (2015). Bone Quality Assessment Using High Resolution Peripheral Quantitative Computed Tomography (HR-pQCT) (Doctoral dissertation, Columbia University).